



Contents lists available at ScienceDirect

## Arabian Journal of Chemistry

journal homepage: [www.ksu.edu.sa](http://www.ksu.edu.sa)

Review article

# An overview on generation and general properties of *N*-heterocyclic carbenes: Applications of 1,2,4-triazolium carbenes as metal free organocatalysts

Raphael Silva Moratório de Moraes, Maria Tereza Miranda Martins, Gabriel Tavares de Almeida Pinto, Searitha Couto Rodrigues, Patrick Antunes do Nascimento, Camille Cardoso Cruz, Karina D'Oliveira Góes, Anna Claudia Cunha \*

Universidade Federal Fluminense, Instituto de Química, Departamento de Química Orgânica, Programa de Pós-Graduação em Química, 24020-141, Niterói, Rio de Janeiro, Brazil

## ARTICLE INFO

## Keywords:

1,2,4-triazolium carbene  
Organocatalysis  
Cascade reaction

## ABSTRACT

*N*-Heterocyclic carbenes (NHCs) have been widely explored in the areas of catalysis, organometallic and medicinal chemistry. In particular, NHCs catalyze the formation of C–C and C-heteroatom bonds with high regioselectivity and stereoselectivity through umpolung and non-umpolung processes for unconventional access to create a vast scope of heterocycle molecules, including  $\beta$ -lactones, tetrahydroquinolines and pyrroloquinolones. Here we summarized the generation and general properties of NHC and important NHC-catalyzed reactions, which typically involve species such as Breslow intermediates, homoenolates, enolates and  $\alpha$ ,  $\beta$ -unsaturated acyl azoliums, among others. Examples of aerobic oxidative/oxygenative carbene catalysis, specifically highlighting NHC-catalyzed reactions involving oxygen and strategies employed for activation of oxygen in NHC-catalytic processes are discussed in detail.

The catalytic use of NHCs has been one of the most powerful tools in the chemist's arsenal, with applications to commercially important protocols. Given this context, the relevance of *N*-heterocyclic carbene chemistry is described in this review.

## 1. Introduction

*N*-Heterocyclic carbenes (NHCs) (Fèvre et al., 2013; Huynh, 2018) represent a class of neutral heterocyclic molecules containing a neutral

carbon species with two coordinately unsaturated electrons, and at least one nitrogen atom is positioned adjacent to the carbene donor within the heterocyclic ring (Shen et al., 2022).

Contrary to classical carbenes, which exist in a triplet state, *N*-

**Abbreviations:** 2,6-DTBP, 2,6-di-*tert*-butylphenol; CAN, acetonitrile; Bn, benzyl; Boc, *tert*-butyloxycarbonyl; BPZ, 4,4'-cyclohexane-1,1-diylidiphenol; CDC, cross dehydrogenative coupling; DABCO, 1,4-diazabicyclo[2.2.2]octane; DBU, 1,8-diazabicyclo[5.4.0]undec-7-ene; DCM, dichloromethane; DIEA, *N,N'*-diisopropylethylamine; DFT, Density Functional Theory; Dipp, 2,6-diisopropylphenyl; DMAC, *N,N*-dimethylacetamide; DMAP, 4-dimethylaminopyridine; DME, dimethyl ether; DMF, dimethylformamide; DMSO, dimethyl sulfoxide; DQ, 3,3',5,5'-tetra-*tert*-butyldiphenylquinone; dr, diastereomeric ratio; ee, enantiomeric excess;  $E_{p_{oxi}}$ , experimental oxidation potential;  $E_{p_{red}}$ , experimental reduction potential; er, enantiomeric ratio; ETM, electron transfer mediator; EWG, electron withdrawing group; FePc, iron(II)phthalocyanine; FG, functional group; HFIP, hexafluoro-2-propanol; HPLC, high-performance liquid chromatography; LG, leaving group; LiHMDS, lithium bis(trimethylsilyl)amide; MCA, methyl cation affinity; Mes, mesityl; NFSI, *N*-fluorobenzenesulfonimide; NHC, *N*-heterocyclic carbene; NMR, nuclear magnetic resonance; *o*-QDM, ortho-quinodimethanes; PA, proton affinity; PA10F, poly(decamethylene 2,5-furandicarboxylamide); PA10T, poly(decamethylene terephthalamide); PA6T, poly(hexamethylene terephthalamide); PAM, polyamide; PETA, poly(*p*-ethylene terephthalamide); *p*-QM, *para*-quinone methide; PIDA, phenyliodine (III) diacetate; Pre-NHC, *N*-heterocyclic carbene precursor; RC, Rauhut-Currier; SCE, saturated calomel electrode; SET, single electron transfer; SFC, supercritical fluid chromatography; TBD, triazabicyclodecene; TBDPS, *tert*-butyldiphenylsilyl; TBHP, *tert*-butyl hydroperoxide; TBS, *tert*-butyldimethylsilyl; TEA, triethylamine; TEMPO, 2,2,6,6-tetramethylpiperidinyloxy; THF, tetrahydrofuran; UV/Vis, ultraviolet/visible.

Peer review under responsibility of King Saud University.

\* Corresponding author.

E-mail address: [annacunha@id.uff.br](mailto:annacunha@id.uff.br) (A. Claudia Cunha).

<https://doi.org/10.1016/j.arabjc.2023.105527>

Received 13 July 2023; Accepted 4 December 2023

Available online 16 December 2023

1878-5352/© 2023 The Author(s). Published by Elsevier B.V. on behalf of King Saud University. This is an open access article under the CC BY-NC-ND license (<http://creativecommons.org/licenses/by-nc-nd/4.0/>).

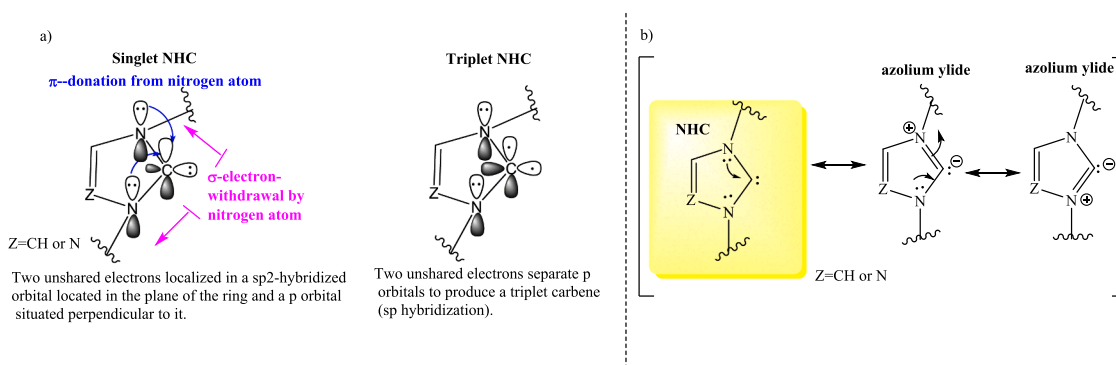


Fig. 1. a) Structures of the singlet and triplet ground states; b) Mesomeric structures of NHCs.

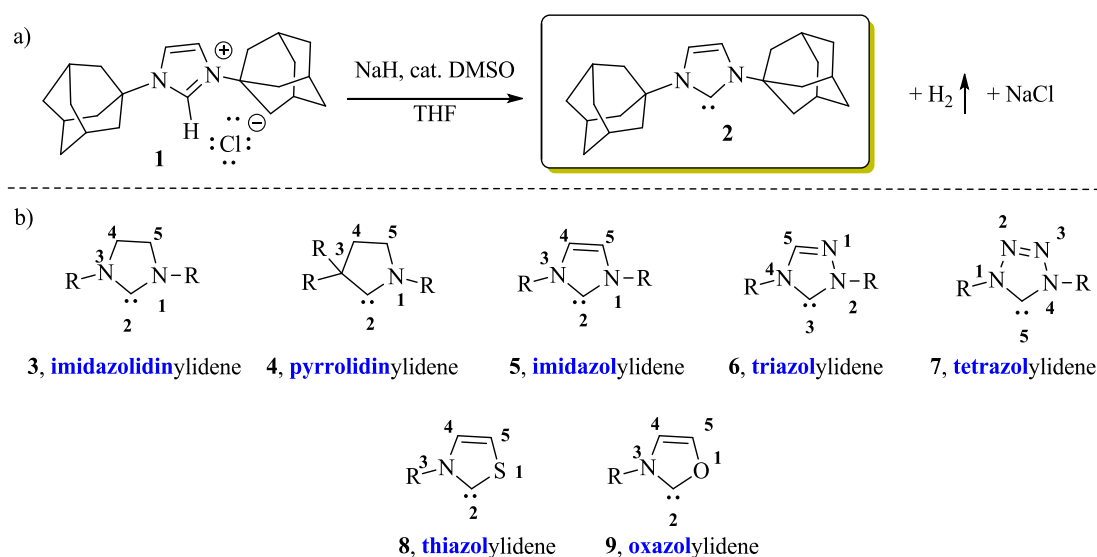


Fig. 2. a) Synthesis of the first crystalline carbene; b) Some examples of five-membered NHCs.

Heterocyclic carbenes (NHCs) exist in a singlet ground state (Fig. 1a). In the cyclic structure, mesomeric effects due to  $\pi$ -electron donation from adjacent heteroatoms into the empty p orbital of the carbene and the inductive effect due to the  $\sigma$ -electron withdrawal of the heteroatoms help to favor the singlet state (Hopkinson et al., 2014). NHCs can be represented as an ylide or as a carbene species, as shown in Fig. 1b (Feroci et al., 2016b; Hopkinson et al., 2014; Okano, 2013).

Because they do not respect the “octet rule”, general alkyl based carbenes have long been recognized as an unstable species; however, in 1991, Arduengo et al. (1991) reported the synthesis and structural characterization of 1,3-di(adamantyl)imidazol-2-ylidene **2** (Fig. 2a), a stable *N*-heterocyclic carbene obtained from deprotonation of the corresponding imidazolium chloride **1**. The nitrogen atoms adjacent to the carbene serves to make the NHCs more stable than the general alkyl based carbene (Arduengo et al., 1991; Feroci et al., 2016b; Hopkinson et al., 2014).

Most of the known NHCs are derived from five-membered rings with additional oxygen, sulfur or phosphorus heteroatoms. Fig. 2b summarizes some of the more common examples of NHCs **3–9** and their associated names (Cavallo and Cazin, 2010; Jahnke and Hahn, 2017).

The origin of the abundance of publications on NHCs lies in the structural diversity of the air-stable azolium salt precursors (Pre-NHCs), as shown in Fig. 3 for the 1,2,4-triazolium salts **10–65** (Flanigan et al., 2015).

The synthesis of Pre-NHCs has been reported in the literature by several research groups (Benhamou et al., 2011; Grieco et al., 2015;

Hutchinson et al., 2019).

### 1.1. Generation of free NHCs

Free NHCs are most frequently generated *in situ* via the deprotonation of the corresponding Pre-NHCs (Scheme 1). Several bases, including NaH, KH, TEA, tBuOK, DBU, NaOH,  $\text{K}_2\text{CO}_3$  and NaOEt, and solvents, such as THF, ACN and DCM, among others, have been used for this purpose (Vetica et al., 2021). Free NHCs (Dong et al., 2022; Mondal et al., 2019; Bhatia et al., 2013) and a wide range of metal-NHCs ( $\text{NHCML}_{n-1}$ ) (Zhao et al., 2020) have been found to be useful as catalysts in various organic reactions. The free form of NHCs **67** can usually be achieved through the reductive desulfurization of imidazol-2-thione derivatives **66** with strong reducing metals (Scheme 2) (Bhatia et al., 2013) or via various thermally labile (Fèvre et al., 2013; Naumann and Buchmeiser, 2014) NHC precursors (Fig. 4), which can be divided into typical categories such as betaine adducts, azolium hydrogen carbonate, azolium carboxylate salts, neutral NHC adducts and NHC-metal adducts. These protected NHCs are versatile tools in organocatalysis and polymerization catalysis (Fèvre et al., 2013; Naumann and Dove, 2016).

According to Scheme 3, another method that can be used to obtain free NHCs is the electron cathodic reduction of the C–H bond between the heteroatoms of Pre-NHCs (Schotten et al., 2021a, 2021b). An electrochemically synthesized NHC is called electrogenerated. In the electrochemical reaction, the Pre-NHC is reduced to a free NHC at the cathode with the evolution of hydrogen. At the anode, the NHC can

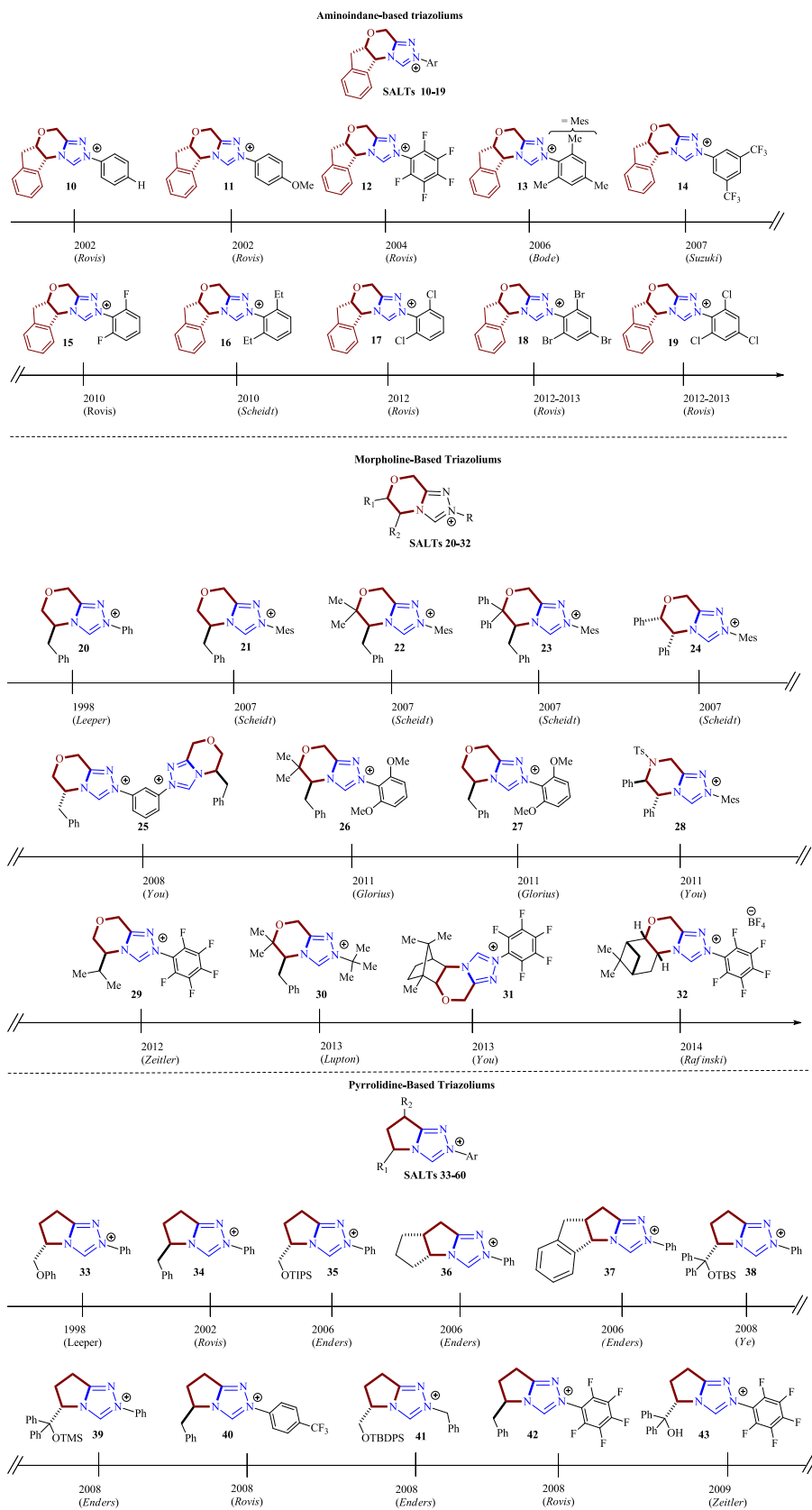


Fig. 3. Some examples of 1,2,4-triazolium salt structures extracted from the literature (Flanigan et al., 2015).

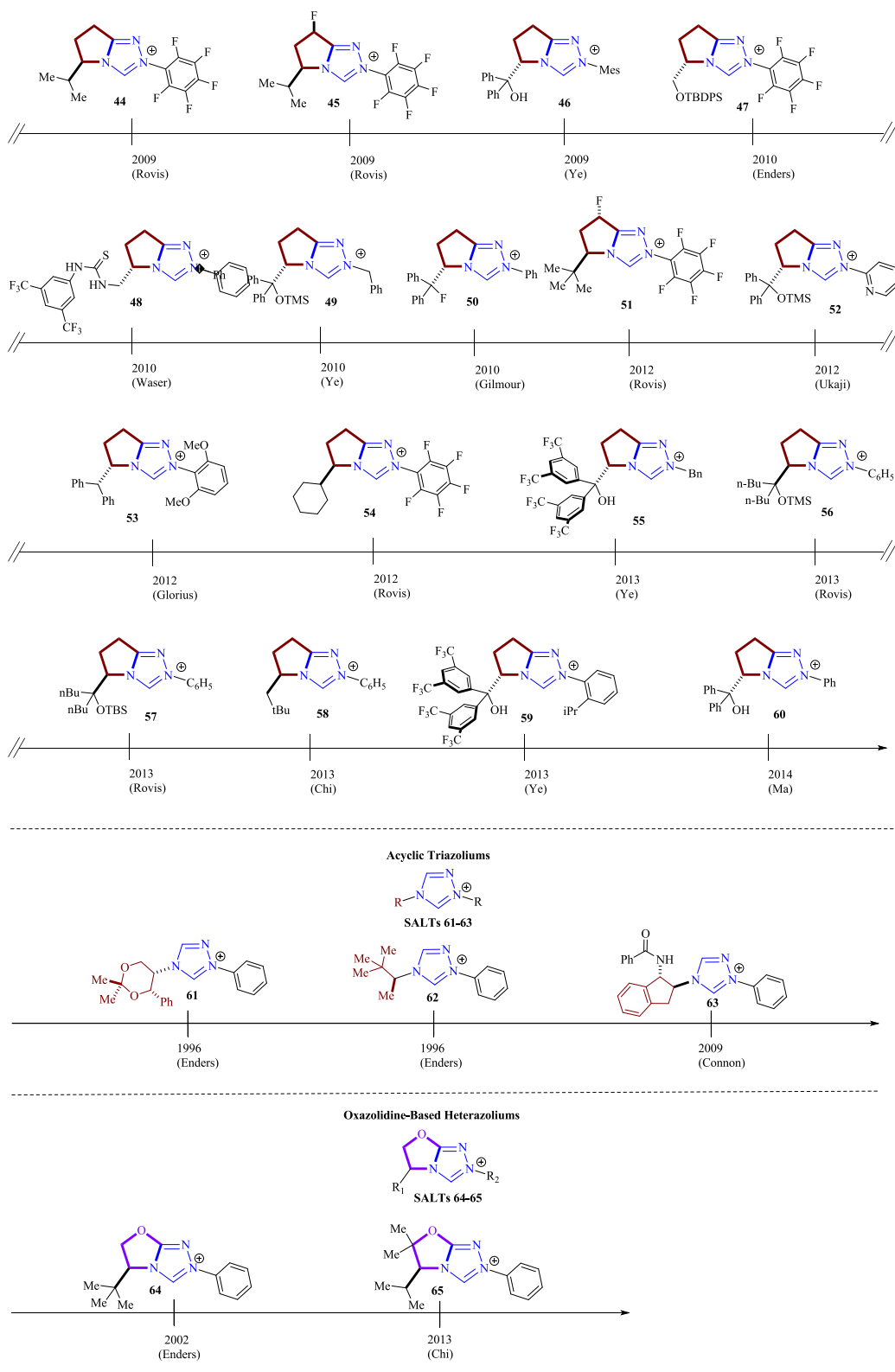
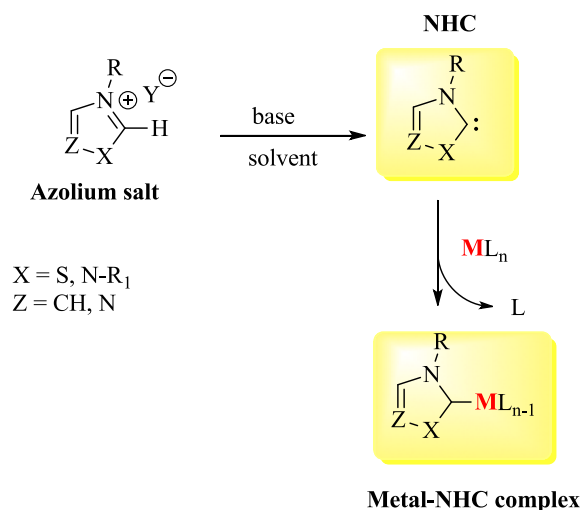


Fig. 3. (continued).

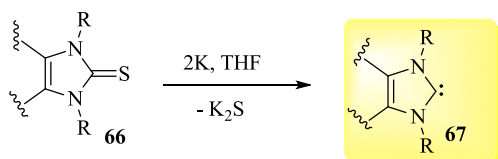
posteriorly react with a substrate (Schotten et al., 2021a) or with a metal cation (Schotten et al., 2021b), which is produced from the sacrificial anode via oxidation, to provide a reaction product or metallo-complex, respectively. Still, other reactions can occur, including solvent decomposition, counterion oxidation or the oxidation of a sacrificial anode to release metal ions. This method represents a green and advantageous

alternative to traditional synthetic methods that often rely on strong bases and air-sensitive materials (Schotten et al., 2021a).

The literature shows that the limited lifetime of various NHCs can be related to the formation of dimeric structures. Steric and electronic effects, among other factors, can affect the dimerization process. For example, saturated NHCs have a stronger tendency to dimer than



Scheme 1. Chemical generation of NHCs and metal-NHC complex.



Scheme 2. Reduction of imidazole-2-thiones to obtain NHCs.

unsaturated NHCs (Feroci et al., 2016b). The irreversible capture of the NHC by the metallic cation prevents its oxidation and degradation (Schotten et al., 2021a).

As previously shown, free NHCs are most often prepared via the deprotonation of Pre-NHCs, and knowing the  $pK_a$  values of these species is an important factor, mainly in reactions involving NHCs as Brønsted base catalysts (N. Wang et al., 2018).

## 1.2. Quantifying the electronic properties of NHCs

### 1.2.1. $pK_a$ measurements of Pre-NHCs

The  $pK_a$  values reflect how easily Pre-NHC can form an NHC precursor (Hopkinson et al., 2014; Konstandaras et al., 2020; Quinn et al., 2021; Zhu et al., 2022). The  $-NC(H)N-$  proton in Pre-NHCs is acidic due to its connection to the carbon atom bonded to the two adjacent electron-withdrawing nitrogen atoms. The reactivity of the NHCs is highly sensitive to the azolium nucleus and structural changes in their cyclic carbon skeletons (Zhu et al., 2022), but the nature of the solvent and the counter-ion  $Y^-$  also plays a significant role (Feroci et al., 2016b). The Brønsted basicity of NHCs has been investigated by combining computational and experimental methodologies to determine the  $pK_a$  values of the Pre-NHCs, both in solution and in the gas phase, and the relative proton affinities (PAs) of the NHCs (Fèvre et al., 2013). For example, the equilibrium acidities of the most commonly used NHC were measured in DMSO using an overlapping indicator method via UV/vis spectra. The  $pK_a$  values range from 12.8 to 23.4 (Fig. 5a) (Li et al., 2017). Triazolium salts 68a–71 are generally more acidic, with  $pK_a$  values ranging from 12.8 to 14.7, than thiazolydene 72 and imidazolydene 73–75 salts due the inclusion of a third electronegative nitrogen atom in their azole ring, leading to a lowering of the  $pK_a$  value. In the

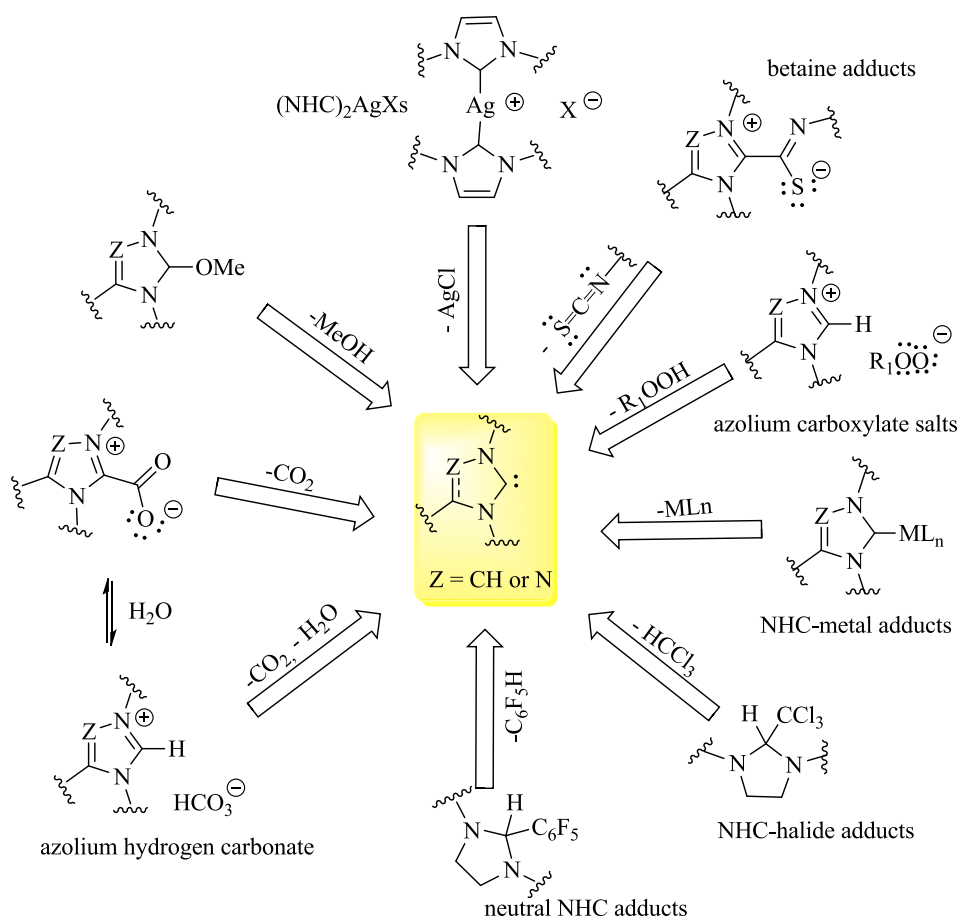
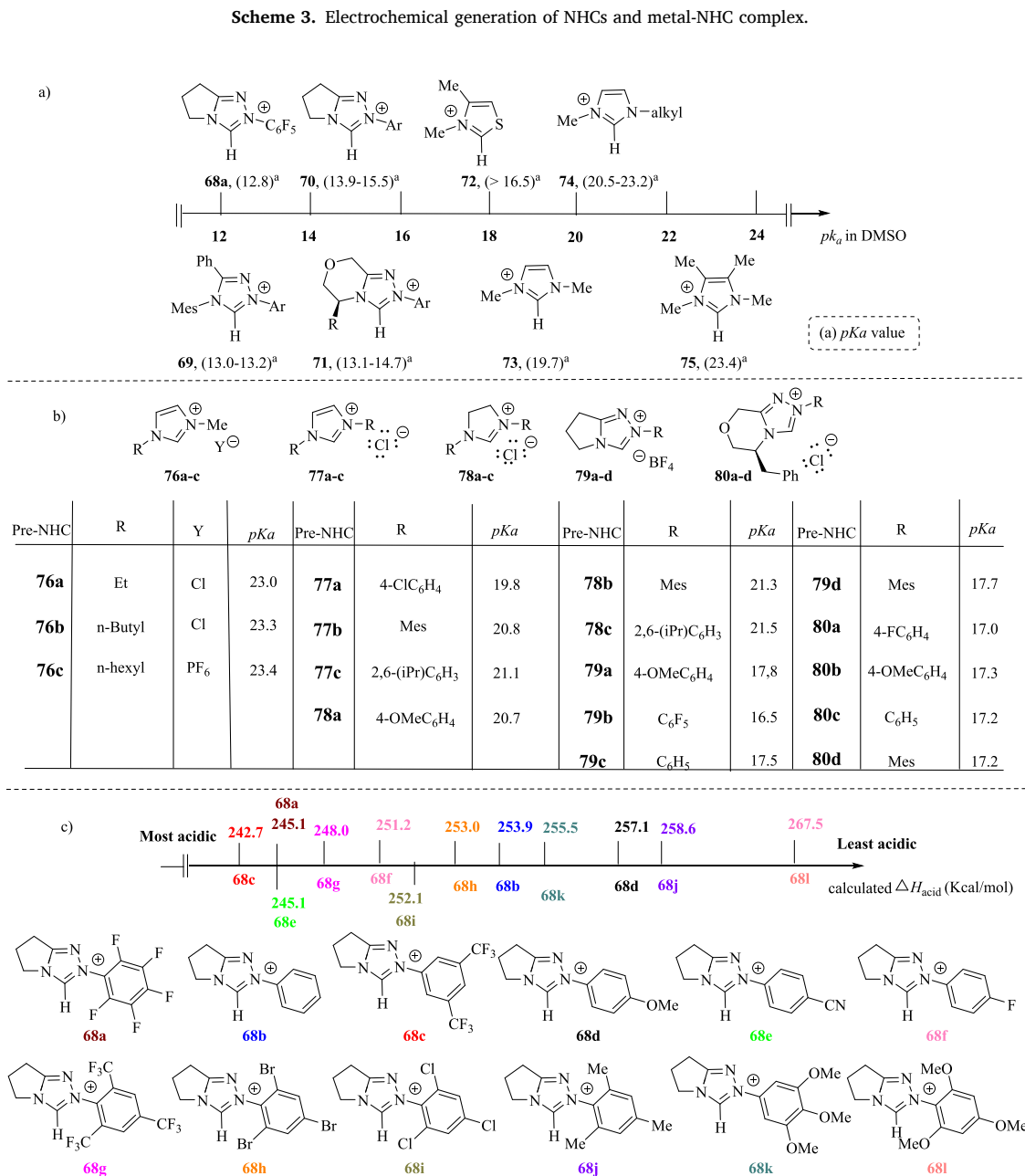
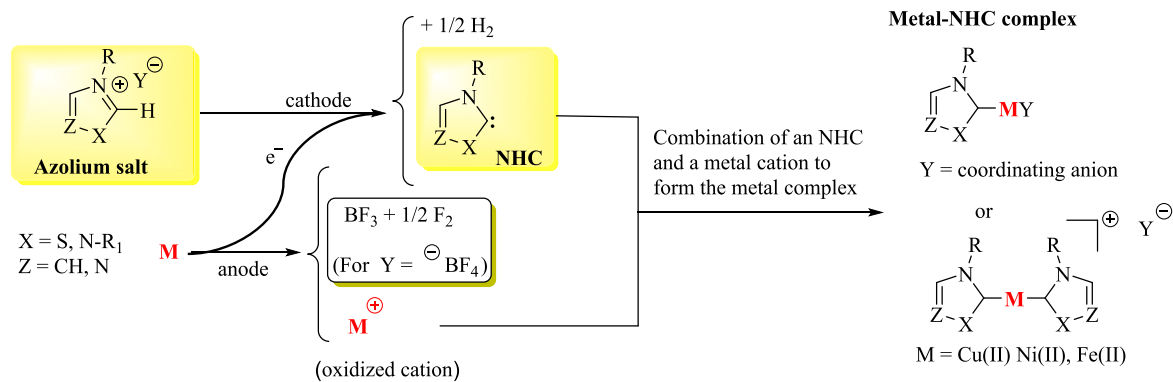
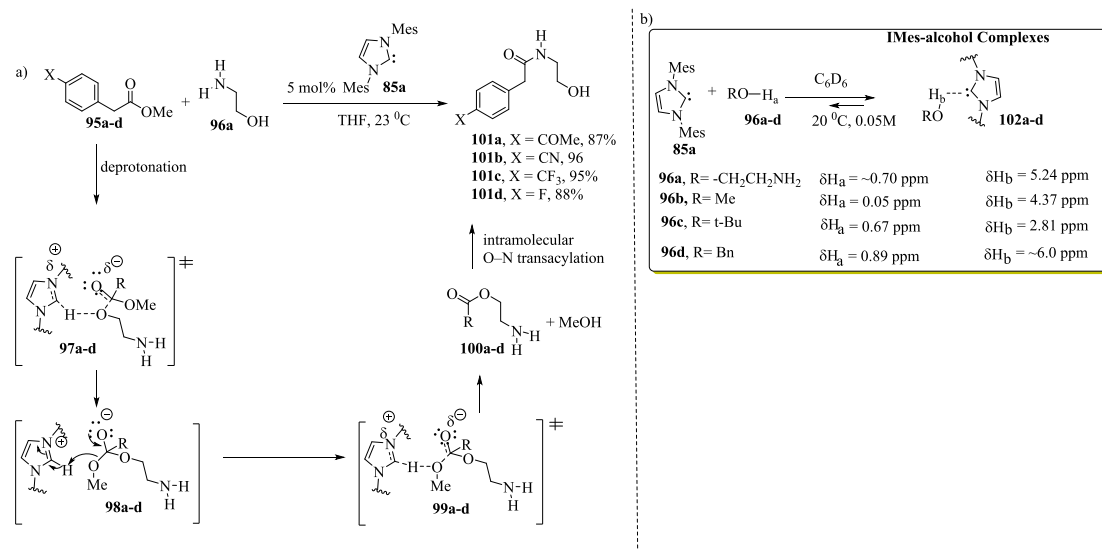


Fig. 4. Some examples of thermo-latent NHC progenitors.





**Scheme 4.** a) NHC-catalyzed amidation of esters; b) Evidence by NMR of the involvement of Brønsted base catalysis.

Compounds	81a	77b	82	83a	83b	83c
Reduction potential ( $E_{pred}$ ) [V]	- 3.00	- 2.87	- 2.76	- 2.47	- 2.11	- 2.09
Oxidation potential ( $E_{pox}$ ) [V]	0.00	+ 0.22	+ 0.60	+ 0.75	+ 0.58	+ 0.64

**Fig. 6.** Reduction and oxidation potentials of the Pre-NHCs and NHC parents, respectively, (0.10 M in DMF), in V vs saturated calomel electrode (SCE) according to data from the literature (Feroci et al., 2016a).

triazolylidene series, the change from a pentafluorophenyl group (electron-withdrawing substituent) **68a** to a mesityl group **70** (Ar = Mes, electron-donating substituent) results in an increased  $pK_a$  (15.52) (Li et al., 2017). Fig. 5b shows  $pK_a$  values determined in water for some select Pre-NHCs **76–80**. In general, imidazolium and imidazolium salts are less acidic ( $pK_a \approx 19.8–23.4$ ) in aqueous solution than 1,2,4-triazoliums ( $pK_a \approx 17.2–21.5$ ) (Flanigan et al., 2015; Higgins et al., 2011; Massey et al., 2012). The  $pK_a$  value of a Pre-NHC **73** in DMSO is lower than the  $pK_a$  value determined in aqueous media (compound **76a**), because neutral carbene is insensitive to solvent stabilization, while the azolium cation can be stabilized by hydrogen bonding in water to a greater extent than in an aprotic solvent (Konstandaras et al., 2020).

The experimental and computational gas-phase acidities of triazolylidene salts **68a–1** (Fig. 5c) in the gas phase were investigated by Niu et al. (2017). The calculated acidities ( $\Delta H_{acid}$ ) of the triazolium salts, which correspond to the proton affinity of their corresponding carbene species, were determined using the B3LYP method at a 6–31 + G\* basis (Niu et al., 2017). The higher the value of the proton affinity, the stronger the base and the weaker the conjugate acid in the gas phase. In general, the electron-withdrawing *N*-aryl substituent favors the destabilization of the cationic triazolium carbon acid in relation to the neutral NHC conjugate base, thus favoring the deprotonation process, while the electron-donating *N*-aryl substituent has the opposite effect on the acidity ( $pK_a$  increase), which will stabilize the cation and shift the equilibrium towards the protonated form. Comparing **68c** with **68g**, the

*ortho*-substituted *N*-aryl triazolium salt forces the phenyl ring out of planarity relative to the azolium nucleus. This steric restriction present in salt **68g** does not allow the conjugation between the electron withdrawing phenyl ring and the azole ring, resulting in the stabilization of the acidic proton and, consequently, reducing the acidity of the *ortho*-substituted triazolium salt.

The basicity and nucleophilicity of NHCs have also been reported using the electrochemical reduction potential of the corresponding Pre-NHCs in different solvents by several research groups (Feroci et al., 2016a, 2016b; Green et al., 2015; Ogawa and Boydston, 2014; Petersen et al., 2022; Rocco et al., 2022; Schotten et al., 2021a; Zhou et al., 2022). The researchers identified a linear relationship between the  $pK_a$  value and the experimental reduction potential ( $E_{pred}$ ) of Pre-NHCs, while the oxidation potential ( $E_{pox}$ ) of NHCs is closely related to their nucleophilicity. The cathodic process is concerned with breaking the C–H bond between the heteroatoms of the Pre-NHCs to form the corresponding azolium-based NHCs (reduction of the NHCH<sup>+</sup> azolium cations to NHCs) and H<sub>2</sub> (Scheme 4), while the anodic pathway is related to the oxidation of the electrogenerated NHCs. NHC formation is usually connected with the acidity of the corresponding Pre-NHC, while the carbene reactivity is usually connected with its lone-pair availability (Feroci et al., 2016b). The reduction potential of Pre-NHCs correlates with their acidity. Larger positive values of the reduction potential are indicative of a greater tendency to be reduced. According to Fig. 6, thiazolium salts **83a–c** are easier to reduce to the corresponding NHCs than triazolium salt **82**

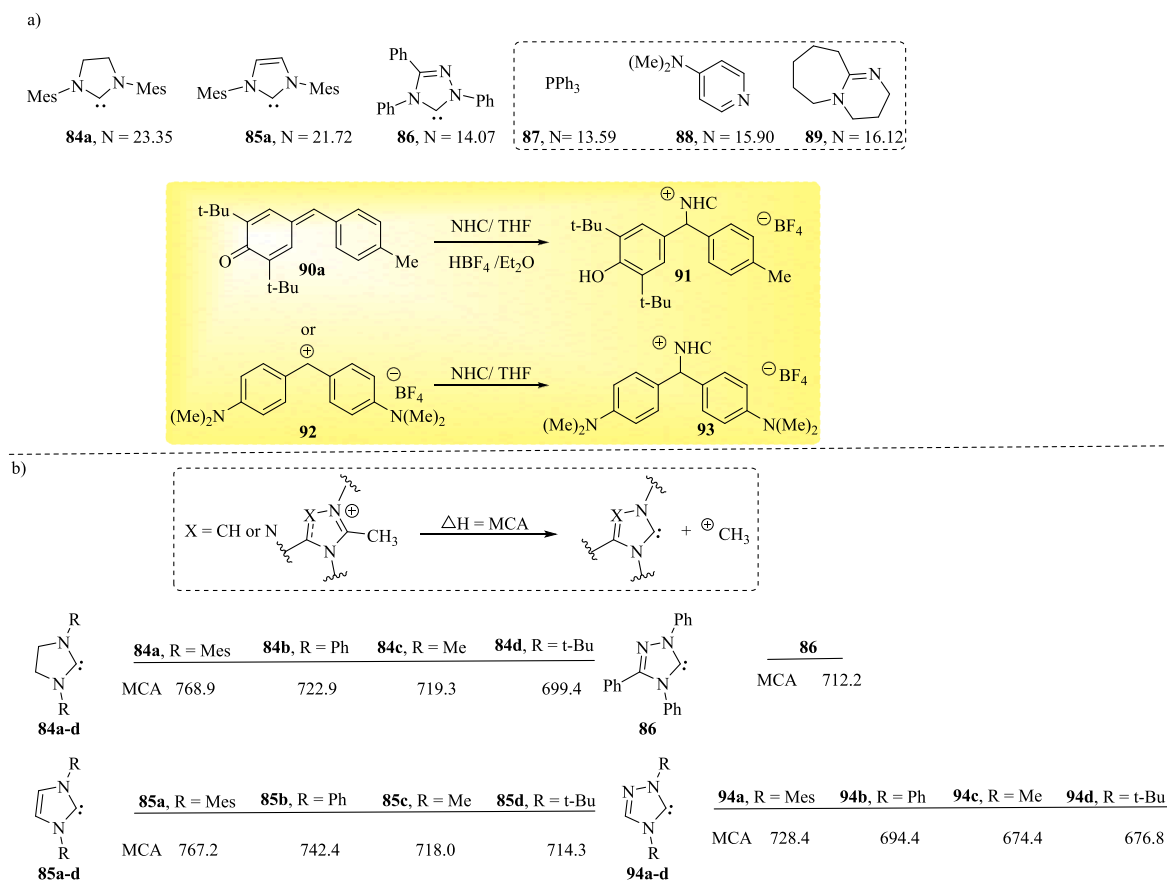


Fig. 7. a) Nucleophilicity parameters for NHCs in THF; b) MCAs (kJ/mol) [MP2/6-31 + G(2d,p)//B98/6-31G(d)].

(lower reduction potential), which in turn has a more positive  $E_{1/2}$  (-2.76 V) compared to imidazolium-based cations **81a** ( $E_{1/2}$  (-3.0 V) and **77b** ( $E_{1/2}$  (-2.87 V)). Data from the literature show that imidazolium salts are less acidic ( $pK_a = 22-24$  in water and 22 in DMSO) than thiazolium and triazolium cations ( $pK_a = 16-19$  in water and 14 in DMSO) (Feroci et al., 2016a). There is an essential difference between the  $pK_a$  values for the triazolium and imidazolium salts, as the presence of an additional electronegative nitrogen atom in the triazolium ring destabilizes the Pre-NHC with respect to the corresponding NHC, thus increasing its acidity.

The anodic process is related to the electroactivity of the electro-generated carbene. From electrochemical studies, the authors suggest that  $E_{pox}$  values decrease with increasing NHC nucleophilicity, which reflects its ability to attack an electrophilic reactant. Imidazolium salts **81a** and **77b** ( $E_{pox} = 0.00$  and + 0.22) are three orders of magnitude more nucleophilic than the triazolium salt **82** ( $E_{pox} = +0.60$ ) (Fig. 6).

### 1.2.2. Nucleophilicity and Lewis basicity of NHCs

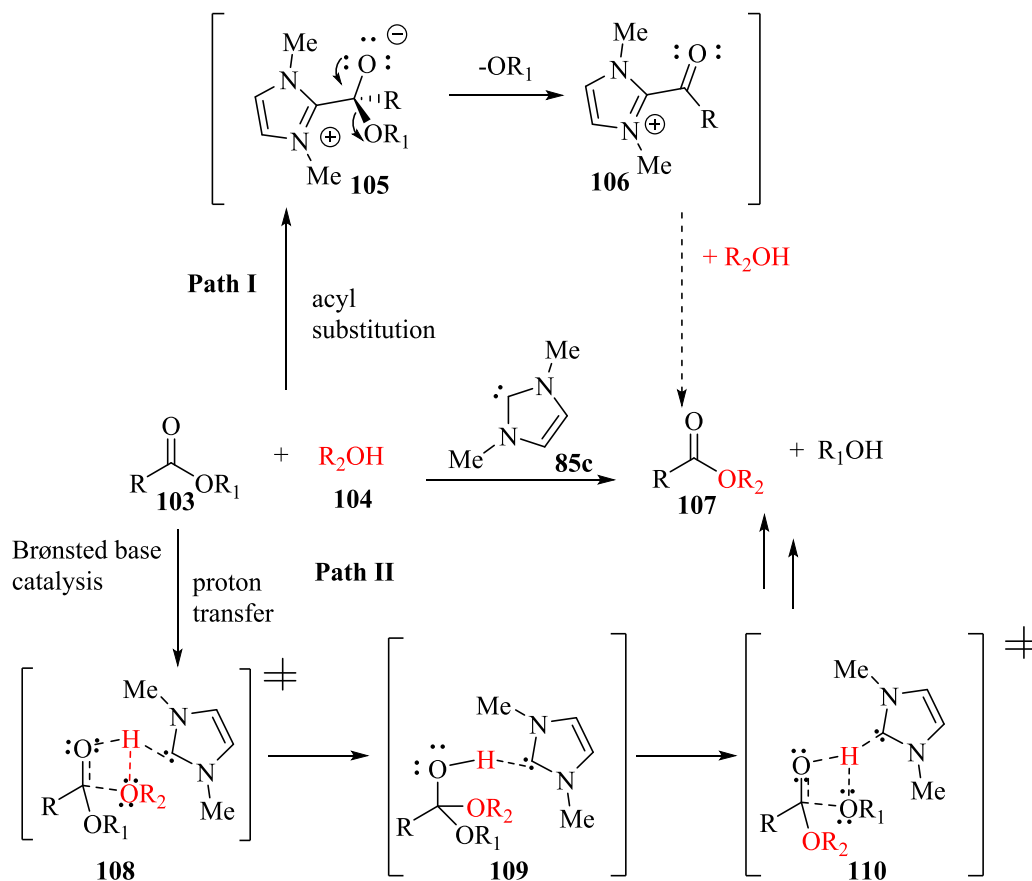
In addition to the use of NHCs as Lewis base catalysts, they are also nucleophiles. In general, NHCs are of moderate nucleophilicity but high Lewis basicity. However, most of the organocatalytic transformation NHCs act as nucleophilic species attacking an electrophilic reactant to form umpolung species, such as Breslow intermediates, this being the first and crucial step (Gudimetla et al., 2022). Nucleophilicity is also a crucial factor for the coordination of NHCs to transition metal complexes (Nesterov et al., 2018). The nature of the azolium ring and *N*-substituent plays an important role in defining the nucleophilicity of the NHC as a catalyst. The nucleophilicity of several NHCs has been quantified according to the Mayr-Patz equation,  $\log k_{(20\text{C})} = s_N(N + E)$  (Eq. 1), which is described by three parameters: the electrophile-dependent reactivity parameter  $E$  (electrophilicity), nucleophilicity parameter (solvent dependent) and nucleophile-specific sensitivity parameter ( $s_N$ ), which is

sensitive to changes in the electrophilicity of the reaction partner (solvent dependent). From the above equation, Maji et al. (2011) determined the nucleophilicity parameters ( $N$ ) of NHCs **84-86** and other nucleophiles **87-89** (Fig. 7a) through reaction, with structurally related quinone methide **90a** or benzhydrylium ion **92** used as reference electrophiles (Fèvre et al., 2013; Levens et al., 2016; Maji et al., 2012, 2011; Mayr et al., 2012; Wei et al., 2008) to form adducts **91** and **93**.

The results of these studies showed that imidazolidinylidene **84a** and imidazolyliidene **85a** carbenes were significantly more nucleophilic than Enders carbene (TPP, **86**) (Fig. 7a). This fact can be explained on the basis of the inductive electron withdrawal exerted by the extra nitrogen in the triazolium carbene. In general, the number, identity and position of ring heteroatoms and backbone substitution play a role in influencing the NHC stability and reactivity. In addition to these considerations, compounds with unsaturated backbones such as imidazolyliidene **85a** and triazolyliidene **86** benefit from increased stability because of their partial aromatic character. The saturated imidazolinylidene **84a** reacted at a slightly faster rate than the unsaturated analog **85a**. The less nucleophilic triazolium carbene **86** is moderately more nucleophilic than  $\text{PPh}_3$  **87**, 4-(dimethylamino)pyridine (**88**, DMAP) and 1,8-diazabicyclo[5.4.0]undec-7-ene (**89**, DBU) (Maji et al., 2011).

Maji et al. (2011) also determined the Lewis basicity of the NHCs **84a**, **85a** and **86** and of their related azolium carbenes **84b-d**, **85b-d** and **94a-d** (Fig. 7b) by using the methyl cation affinity (MCA), which corresponds to  $\Delta H_{298}$  to generate the naked NHC and  $^+\text{CH}_3$  from the covalent adduct  $\text{NHC-CH}_3^+$  (Maji et al., 2011).

The five-membered ring is of a planar nature for most NHCs; the *tert*-butyl imidazoline carbene **84d** adopts a twist conformation with an N-C-C-N interplanar angle of  $18^\circ$ . In the NHCs **84b**, **85b** and **94b**, the phenyl groups are coplanar with the heterocycle ring or only slightly distorted out of the plane, while the mesityl groups in **84a**, **85a** and **94a**



Scheme 5. Proposed mechanism of NHC-catalyzed transesterification.

are almost perpendicular to the plane of the aza-heterocycle moiety. Phenyl groups can stabilize the NHCs by  $\pi$ -conjugation, unlike 2,6-(OMe)<sub>2</sub>C<sub>6</sub>H<sub>3</sub>-group, which cannot operate through mesomeric effect. Regarding the products (NHCs-CH<sub>3</sub><sup>+</sup>) obtained through the methylation of *N*-mesityl-substituted NHCs **84a**, **85a** and **94a** and *N*-phenyl-substituted NHCs **84b**, **85b** and **94b**, in both series, the aryl groups are distorted out of the plane to minimize the steric hindrance effect, with the methyl group at the former carbene center. This means that the phenyl-substituted series are weaker Lewis bases than mesityl analogues, because the phenyl group can stabilize the NHCs by  $\pi$ -conjugation but not their corresponding adducts NHCs-CH<sub>3</sub><sup>+</sup>. The electron-withdrawing effect of the additional nitrogen in series **94a-d** makes these NHCs less basic than other NHCs. The NHC **86** is more basic than **94b** due to the mesomeric effect of the additional phenyl group. Imidazole **84a** (768.9 kJ mol<sup>-1</sup>) and imidazole-type **85a** (767.2 kJ mol<sup>-1</sup>) NHCs, respectively, are thus stronger Lewis bases than the triazolium carbene **94a** (728.4 kJ mol<sup>-1</sup>); the latter is stronger than other neutral Lewis bases that have been studied with PPh<sub>3</sub> (618.4 kJ mol<sup>-1</sup>) and DMAP (581.2 kJ mol<sup>-1</sup>).

Other methods for quantifying the properties of NHCs using a variety of different parameters have been described (Ando et al., 2020; Dröge and Glorius, 2010; Falivene and Cavallo, 2017; Gómez-Suárez et al., 2017; Huynh, 2018; Nelson et al., 2013).

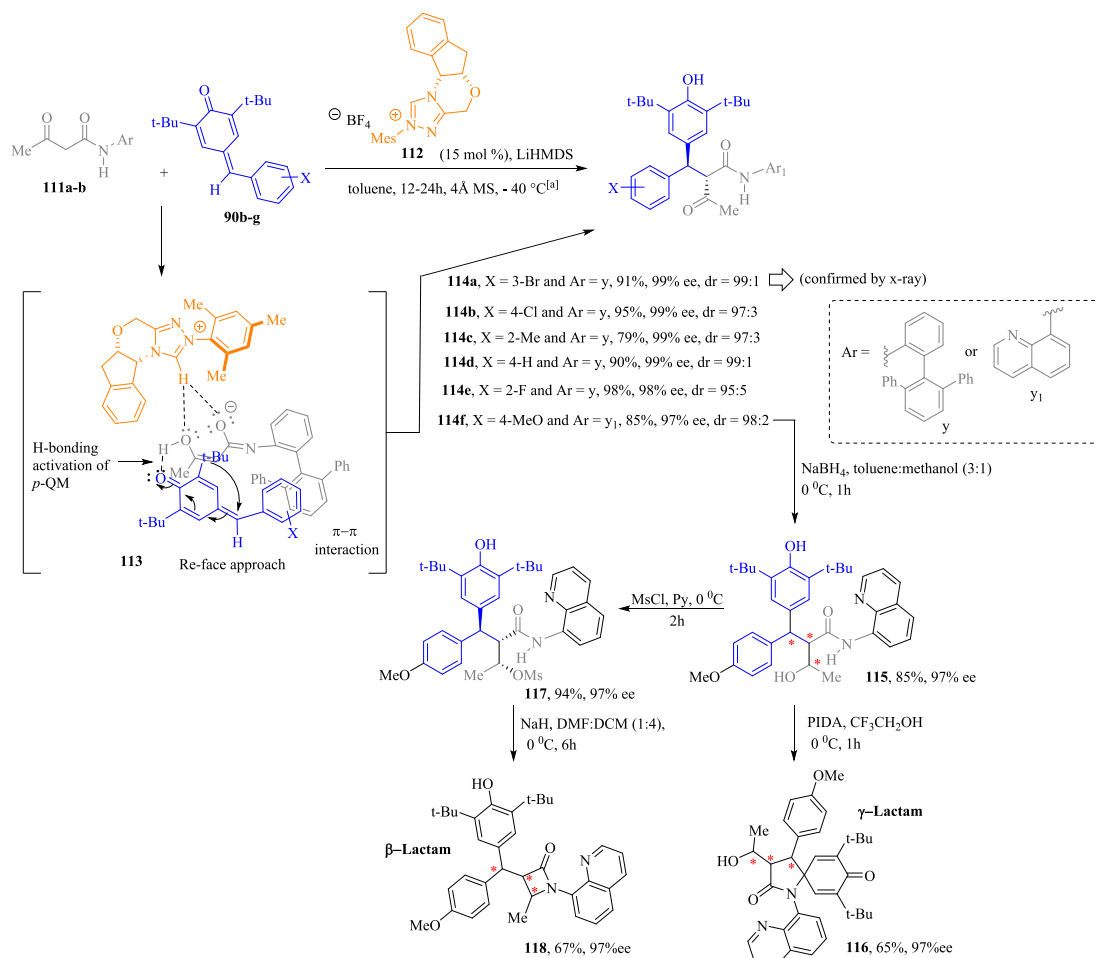
### 1.3. Some examples of NHC-Brønsted base-catalyzed reactions

In 2005, Movassaghi and Schmidt (2005) described the NHC Brønsted base-catalyzed amidation of esters **95a-d** with amino alcohol **96a** (Scheme 4a). They proposed that NHC **85a** acts as a Brønsted base catalyst based on evidence of hydrogen-bonding interactions between NHC **85a** and alcohols **96a-d** (Scheme 4b) supported by <sup>1</sup>H NMR, <sup>13</sup>C

NMR and a single-crystal X-ray of **102b** (Chen and Huang, 2019; Movassaghi and Schmidt, 2005; N. Wang et al., 2018). Initially, the carbene **85a** acts as a Brønsted base interacting with the alcohol **96a** through hydrogen bonding. Upon the activation of the hydroxyl group of the amino alcohol by the NHC catalyst, the oxygen atom is nucleophilic enough to attack the carbon carbonyl of the esters (transition states **97a-d**), followed by the liberation of the alcohol (transition states **99a-d**). Movassaghi and Schmidt (2005) observed that the products **101a-d** were obtained from **100a-d** through an intramolecular O-N acyl transfer (Movassaghi and Schmidt, 2005).

In the NMR analysis, it was observed that the proton of the hydroxyl group in the complexes **102a-d** (Scheme 4b) becomes more deshielded than alcohols **96a-d** (Movassaghi and Schmidt, 2005). The X-ray structure of a stable hydrogen-bonded carbene-alcohol complex **102b** and NMR study support a carbene-base nucleophile activation mechanism.

Another example that involved an NHC acting as a Brønsted base catalyst was reported by Lai et al. (2005) (Fèvre et al., 2013; Lai et al., 2005; Ryan et al., 2013) in their theoretical studies on the mechanism of transesterification reactions. They investigated two types of mechanisms: an NHC acting as a nucleophilic catalyst (Path I) (Scheme 5) and an NHC acting as a Brønsted base catalyst (Path II). In the first case, the nucleophilic attack of the NHC **85c** on carbonyl ester **103** leads to the formation of a tetrahedral zwitterion **105**, which releases an alkoxide anion, transforming into acylazolium intermediate **106**. In the second case, NHC **85c** assists in the proton transfer from alcohol **104** to the carbonyl group of ester **103**, forming a concerted four-member-ring transition state **108**, followed by a stable tetrahedral intermediate **109**, which transfers a proton to the  $-OR_1$  group via transition state **110**, increasing its ability to act as a leaving group. Reforming the carbonyl double bond causes the elimination of an alcohol ( $HOR_1$ ) and the



<sup>[a]</sup>Reaction conditions: **90b-g** (0.1 mmol), amides **111a-b** (0.1 mmol), Pre-NHC **112** 3g (15 mol%), LiHMDS (12 mol%), 4Å MS (70 mg) in toluene (2.0 mL); isolated yields. Diastereoisomeric ratio (dr) determined by <sup>1</sup>H NMR and HPLC analysis. Enantiomeric excess (ee) determined by HPLC analysis on a chiral stationary phase

**Scheme 6.** Synthesis of chiral amides **114a-f** and  $\gamma$ - and  $\beta$ -lactams **116** and **118**, respectively, mediated by NHCs acting as chiral Brønsted base catalysts.

formation of the desired product. In the study, it was observed that neutral intermediate **109** (Path II) was significantly more stable than tetrahedral zwitterionic intermediate **105** and the acyl azolium **106** (Path I), suggesting that the mechanism involved an NHC acting as a Brønsted base and not as a nucleophilic catalyst.

A highly stereoselective 1,6-addition reaction of 1,3-ketoamides **111a-b** with acidic N-H to *p*-quinone methides (*p*-QMs) **90b-g** using an NHC as a Brønsted base catalyst was reported by Santra et al. (2018) to obtain the compounds **114a-f** with excellent stereoselectivity (ee and dr) and yields. Among these compounds, the substance **114f** stands out; it was used as a synthetic precursor in the design and synthesis of chiral  $\gamma$ -lactam **116** and  $\beta$ -lactam **118**, bearing three stereocenters in good yields with excellent stereocontrol (Scheme 6). Based on mechanistic studies, the authors suggest that, after the deprotonation of the N-H acid of the amides by the NHC Brønsted base, the reaction proceeds through an intermediate pair composed of the enolate ion and the azolium cation **113**. The chemistry reduction of **114f** led to the attainment of **115** as the major product in good yield and with excellent ee; it can subsequently be transformed into spirocyclic  $\gamma$ -lactam **116** via oxidation with phenyliodine(III) diacetate (PIDA). Substance **115** was also subjected to the mesylation reaction to form compound **117**, which later, under basic conditions, can be converted into the enantioenriched  $\beta$ -lactam **118** in good yield with excellent stereocontrol. The absolute configuration of the stereocenters of compound **114a** was unambiguously determined by single-crystal X-ray analysis. (Santra et al., 2018).

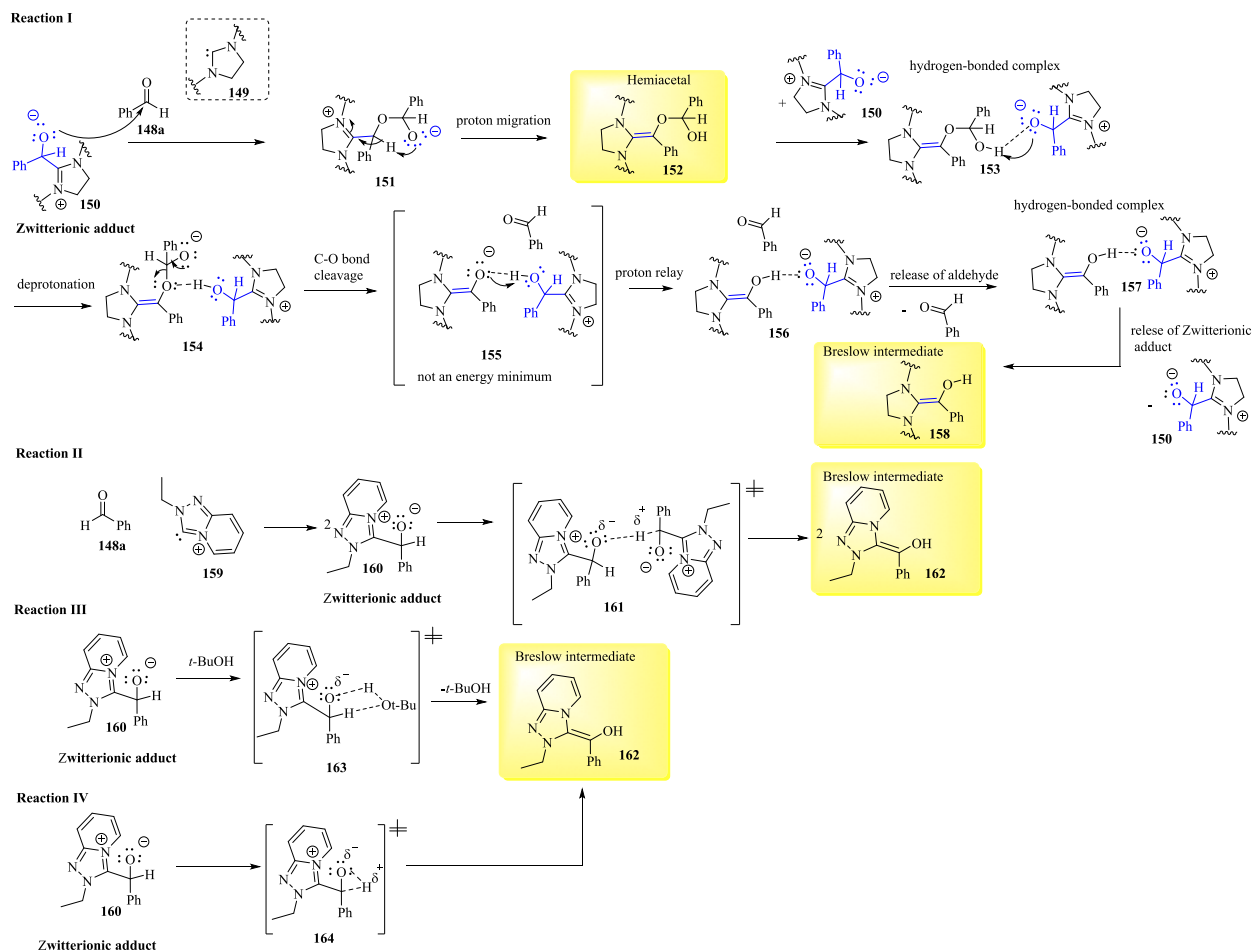
#### 1.4. Application of 1,2,4-triazolium carbenes as nucleophilic organocatalysts

Since vitamin B1, a naturally occurring thiazolium salt, was utilized by Ukai et al. (Ukai et al., 1943) as an organic catalyst to promote a class of umpulung reactions that induce aldehydes to undergo nucleophilic addition reactions, a wide range of related chemical transformations catalyzed by different Pre-NHCs has been investigated intensively (Zhu et al., 2022).

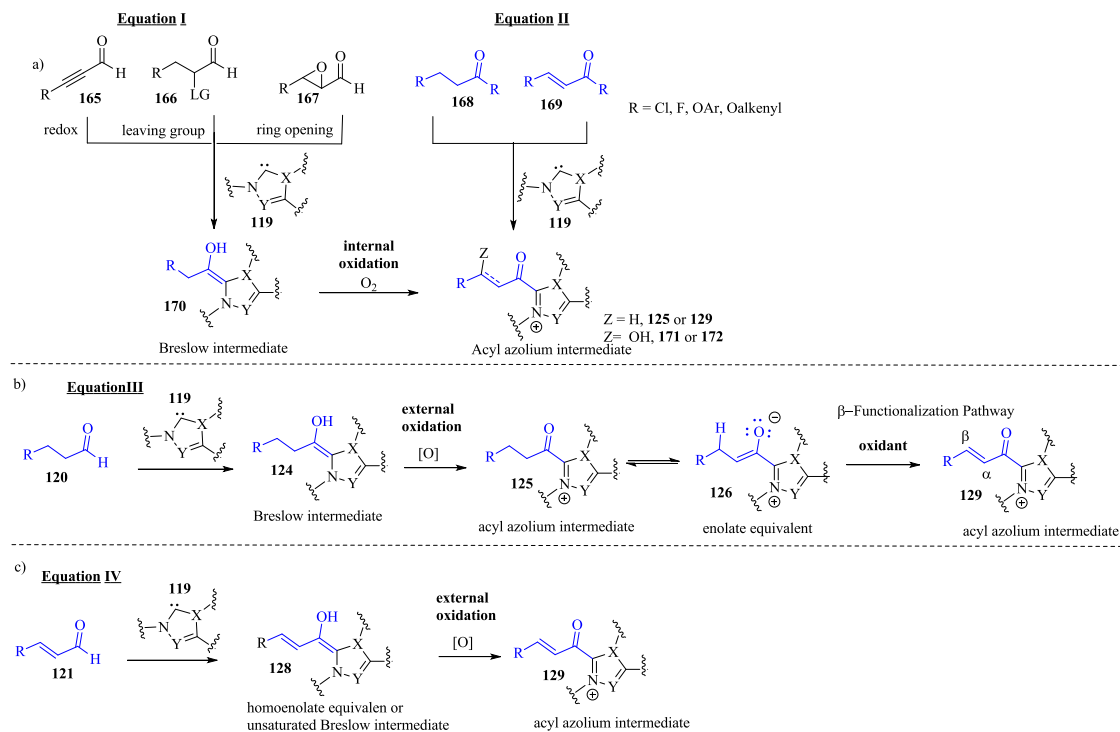
Free NHCs, as nucleophilic species, have shown significant importance as organocatalysts and ligands for transition metals (Riederer et al., 2011), and they have been used in metal-free polymer synthesis (Fèvre et al., 2013; Kohsaka et al., 2021), ionic liquids (Alpers et al., 2018) and metallodrugs (Vellé et al., 2017). Particularly in the field of organocatalysis, chiral NHC-catalyzed reactions have been a powerful strategy for the stereoselective formation of C-C and C-heteroatom bonds, leading to the construction of interesting cyclic systems (Ni et al., 2015). Specifically, 1,2,4-triazolium carbene catalysts have proved to be more effective at inducing enantioselectivity with systems that have asymmetric centers incorporated into a rigid structure (Mahatthanachai and Bode, 2014; Zhu et al., 2022). Other examples of chemical transformations involving 1,2,4-triazolylidenes include the oxidative formation of esters and carboxylic acids from aldehydes and the oxidation of alcohols, among others (Harnying et al., 2021).

In order to understand the reactions mediated by NHCs acting as nucleophilic catalysts, this review will initially present the different

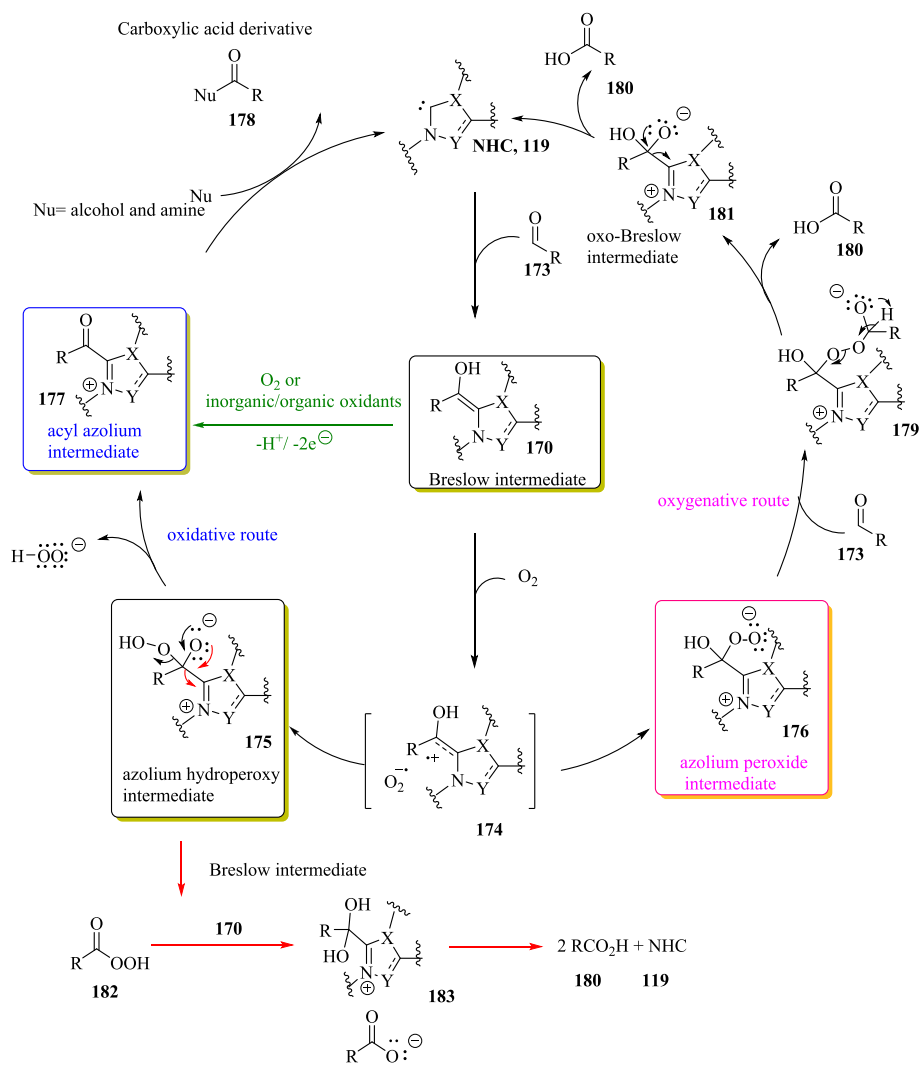




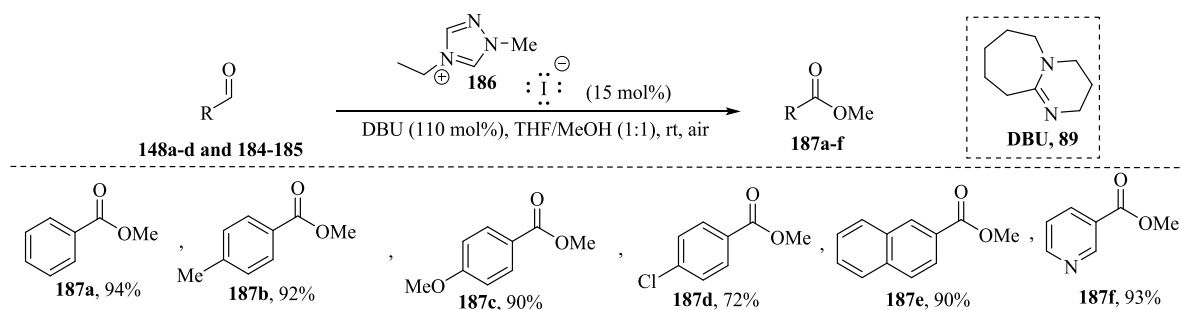
Scheme 9. Proton transfer mechanisms to provide Breslow intermediate.



Scheme 10. Oxidative pathways towards acylazolium intermediates.



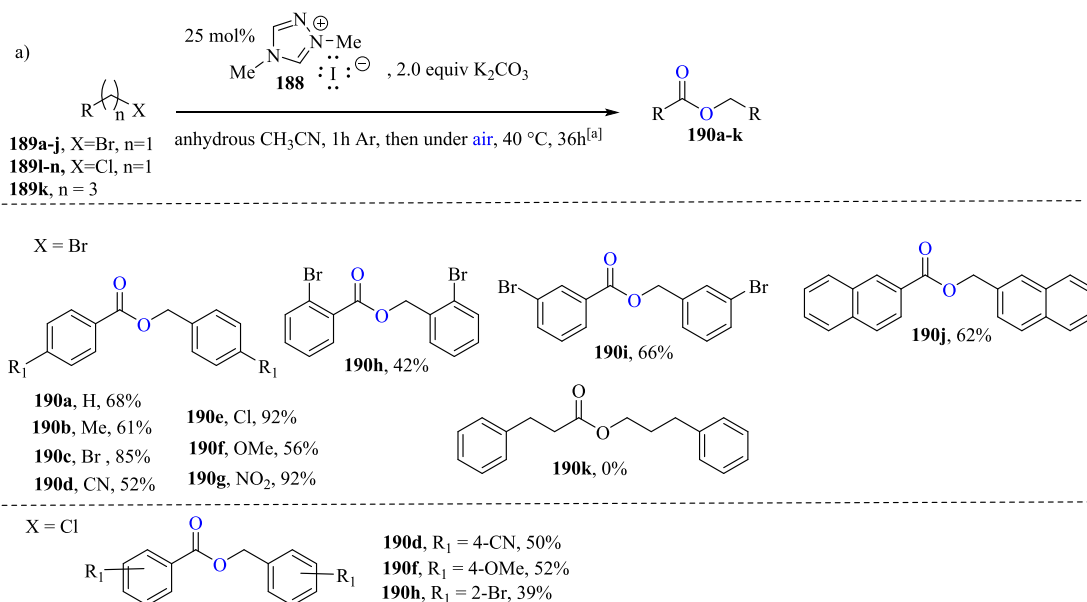
**Scheme 11.** Possible mechanisms for the aerobic oxidation of aldehydes to carboxylic acid derivatives (oxidative path) and carboxylic acid (oxygenative path).



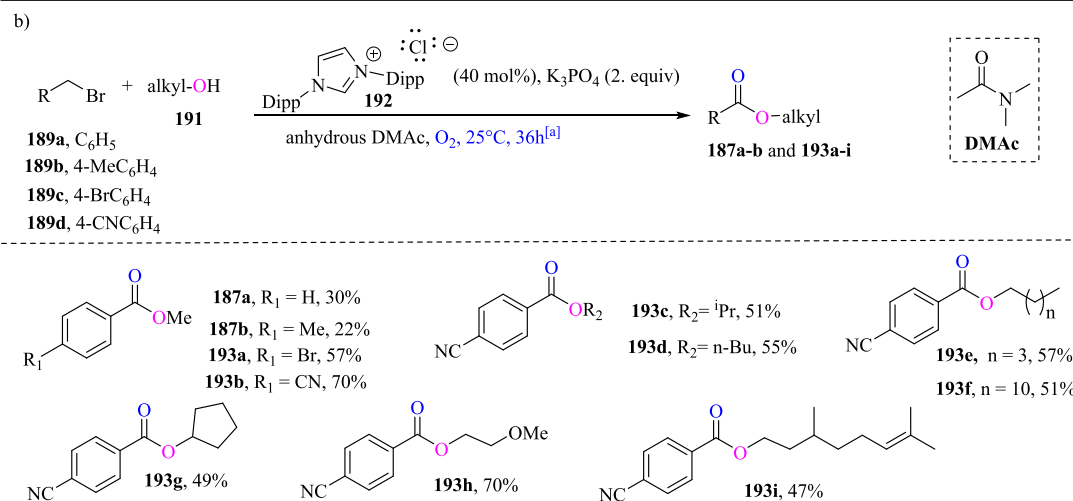
**Scheme 12.** Oxidative carbene-catalyzed esterification of aldehydes.

and Bode, 2014; Pareek et al., 2021; Que and He, 2020; Zhao et al., 2021) (Scheme 7a–b) such as Breslow intermediates **124**, acyl azoliums **125**, azolium enolates **126**, homoenolate equivalents **127**, unsaturated Breslow intermediates **128**,  $\gamma$ -unsaturated acyl azolium intermediates **129** and azolium dienolates **130**. The *in situ* activation of carboxylic acid derivatives **131** and **132**, followed by the addition of NHC **119**, provides the acyl azoliums **125** and **129**, respectively, which have been used for the preparation of esters **133** and amides **134**. At this point, the azolium dienolate intermediates **130** (Scheme 7b) can be generated through the addition of NHC **119** to a carbonyl compound with an acidic

$\alpha,\beta$ -hydrogen atom **139–141**. The most commonly used methods for obtaining NHC-derived azolium dienolate intermediates rely on the redox activation of  $\alpha,\beta$ -unsaturated aldehydes **139** and **140**,  $\alpha,\beta$ -unsaturated acid derivatives **141** and cyclobutenones **142** (Chen et al., 2020, 2018a). The reactivity of the aforementioned intermediates has been extensively exploited in various chemical synthetic methods, including annulation, benzoin, Stetter, Claisen rearrangement, cycloaddition, and C–C and C–heteroatom bond functionalization reactions (Mahatthananchai and Bode, 2014), to obtain different classes of organic compounds **133–138** (Scheme 7a) and **143–145** (Scheme 7b).



<sup>[a]</sup> Conditions: the solution of organic halides (0.1 mmol), Pre-NHC (25 mol%), and  $K_2CO_3$  (0.2 mmol) in anhydrous  $CH_3CN$  (2.0 mL) was stirred at 40 °C under argon (Ar) atmosphere for 1 hour, and then under dry air for 36 hours. Isolated yields



<sup>[a]</sup> Conditions: the solution of benzylic halides (0.1 mmol), alcohols (0.3 mmol), Pre-NHC (40 mol%), and  $K_3PO_4$  (0.2 mmol) in anhydrous DMAc (0.5 mL) was stirred at 25 °C under O<sub>2</sub> atmosphere for 36 hours. Isolated yields.

**Scheme 13.** a) Esterification of organic halides **189a-j**; **189l-n** and **189k** b) Cross-esterification of organic halides **189a-d** with aliphatic alcohols **191**.

Examples of these reactions are shown throughout this review.

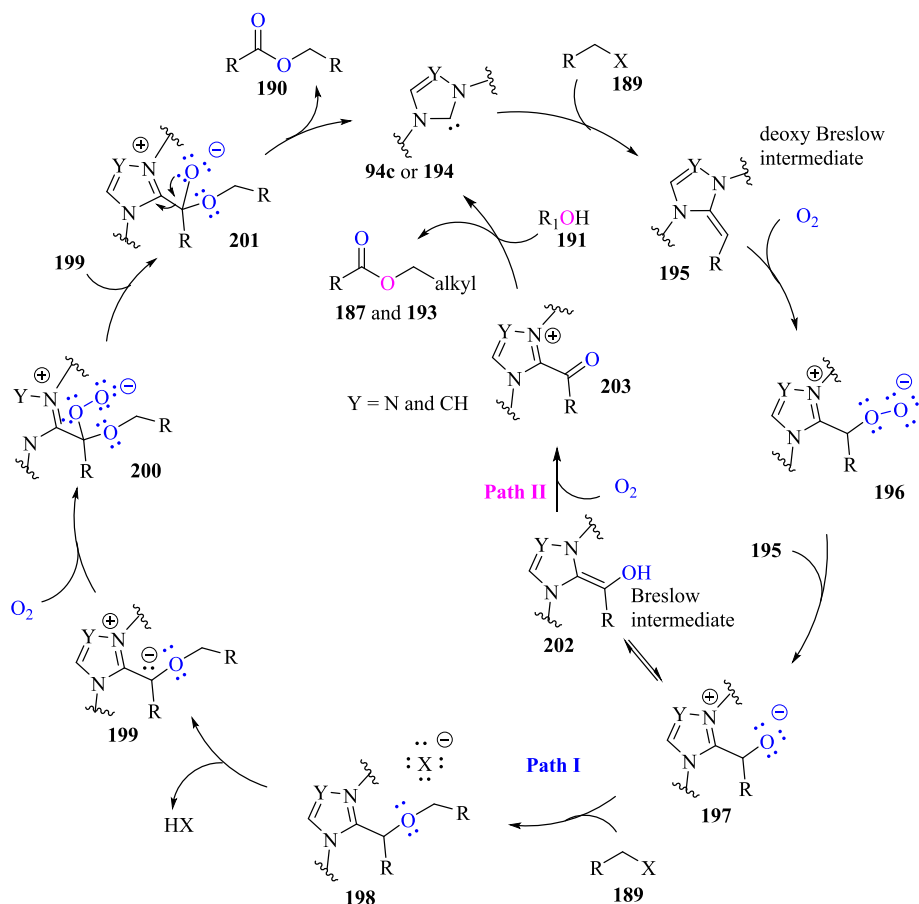
In addition to NHCs, metallophosphites and phosphines are organocatalysts that can provide access to the umpolung of organic compounds (Bugaut and Glorius, 2012). The concept of umpolung, or reversed polarity, introduced by D. Seebach and E. J. Corey (Rezayee et al., 2022), can be better understood by considering Scheme 7. The carbon atom (C-3 or C<sub>β</sub>) of the  $\alpha,\beta$ -unsaturated aldehyde **121**, a potential electrophilic Michael acceptor, undergoes a polarity inversion and becomes a nucleophilic site in an a<sup>3</sup> to d<sup>3</sup> umpolung (also called a conjugate umpolung) when the nucleophilic catalyst transiently transforms it into homoenolate equivalent **127** through an addition – proton transfer sequence (Scheme 8a). If the carbon atom (C-3) is a positively polarized synthon (acceptor synthon), it is denoted by the symbol a<sup>3</sup>, while if the carbon atom (C-3) is a negatively polarized synthon (donor synthon), it is denoted by the symbol d<sup>3</sup>. Synthons a and d are numbered with respect to the relative positions of a functional group (FG) and the reaction site. Activation of the carbonyl group of an electrophilic aldehyde

**120** via the umpolung strategy to form a nucleophilic Breslow intermediate is shown in Scheme 8b (Bugaut and Glorius, 2012; Vetica et al., 2021).

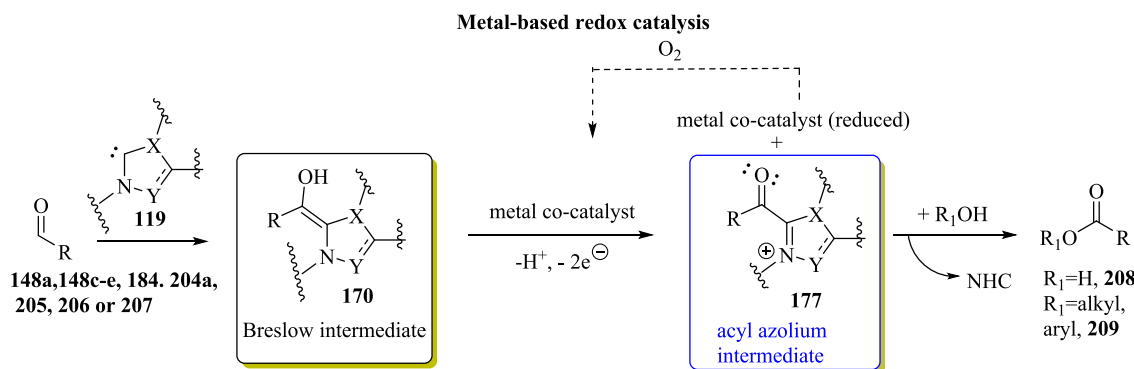
This polarity inversion makes it possible to explore new synthetic possibilities that cannot be realized from the normal reactivity of functional groups. From the reactive species (Scheme 7), depending on the reaction conditions and catalyst choice, different pathways can be taken, resulting in a diverse array of products that can be formed under NHC catalysis.

#### 1.4.2. Proposed mechanisms for the transformation of a zwitterionic adduct into a Breslow intermediate

In NHC-catalyzed reactions, the most crucial step in the formation of the Breslow intermediate is the deprotonation of the carbon attached to the negatively charged oxygen atom in the zwitterionic adducts **122** and **123** (Scheme 7a) (Reddi and Sunoj, 2017). The pathway to the formation of the Breslow intermediates **124** and **128** from zwitterionic



**Scheme 14.** Proposed mechanism for NHC-catalyzed esterification of organic halides (Path I) and cross-esterification of organic halides with aliphatic alcohols (Path II).



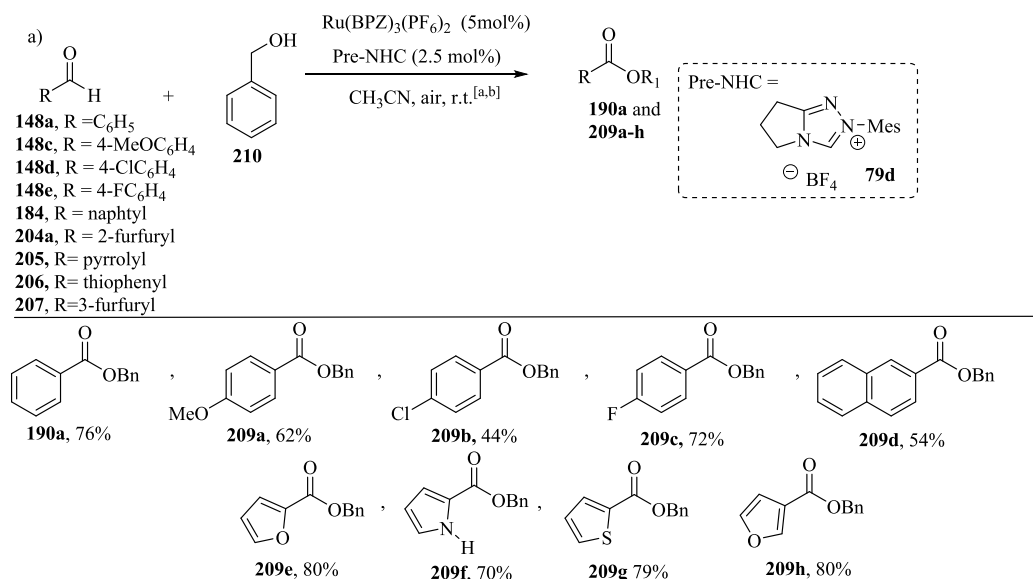
**Scheme 15.** NHC-catalyzed oxidative esterification of aldehydes via cooperative NHC/metal-based catalysis.

adducts **122** and **123**, respectively, has been explicated computationally and experimentally under different conditions, including direct [1,2] proton shift, acid/base catalysis and the assistance of protic media (Huang et al., 2022; Nandi et al., 2021; Pareek et al., 2021; Wessels et al., 2022).

Recently, based on quantum chemistry calculations using density-functional theory (DFT), Huang et al. (2022) proposed a bimolecular mechanism to explain the formation of the Breslow intermediates **158** from the zwitterionic adducts **150** under aprotic conditions. These last intermediates were obtained via the reaction between benzaldehyde **148a** and an imidazolinyldene **149** (Scheme 9). According to researchers, the conversion of the zwitterionic adducts **150** into the Breslow intermediates **158** takes place via hemiacetals **152**. This step

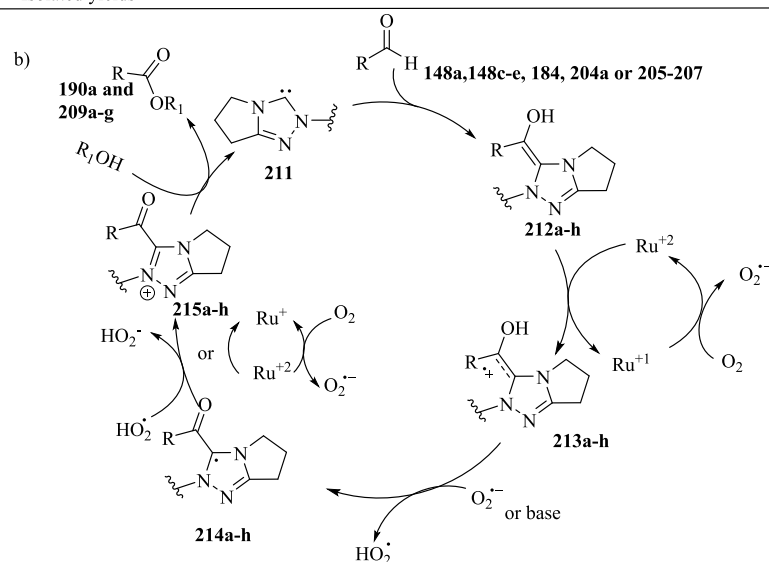
involved the oxy-addition of the zwitterionic adduct **150** to another benzaldehyde molecule **148a**, followed by the proton migration of **151** to form hemiacetal **152**. The hydrogen bond interaction between the zwitterionic adducts **150** and **152** results in the complex **153**, which advances the hemiacetal decomposition to form Breslow intermediate **158** with the assistance of the zwitterionic adduct **150**. The hydrogen bond interaction between the zwitterionic adduct and the hemiacetal (complex **153**) / Breslow intermediate (complex **157**) plays an important role (Huang et al., 2022; Wessels et al., 2022).

Theoretical investigations of the mechanism of formation of Breslow intermediates were also proposed (He and Xue, 2011). In Scheme 9 (Equation II), the Breslow intermediate **162** is formed via two sequent intermolecular proton transfers between two NHC/benzaldehyde



<sup>[a]</sup> Reactions were carried out on a 0.25 mmol scale of aldehyde with 0.25 mL alcohol **210** (2.5 mmol) in 1 mL acetonitrile at room temperature.

<sup>[b]</sup> Isolated yields



**Scheme 16.** a) Cooperative NHC- and ruthenium-based redox catalysis for oxidative esterification of aldehyde; b) Proposed mechanism for oxidative esterification.

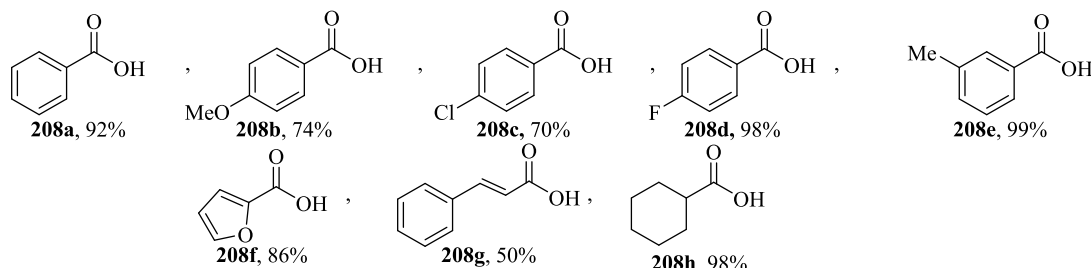
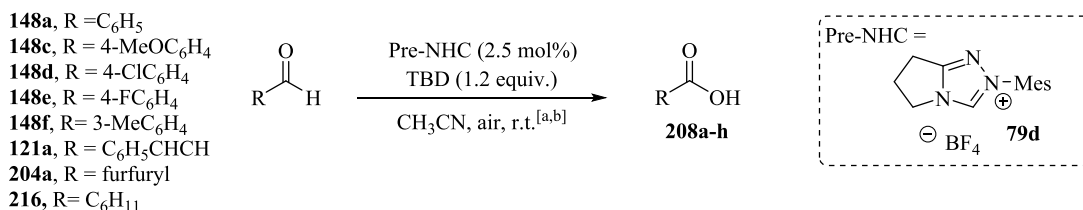
coupled intermediates. The theoretical results show that this intermolecular proton transfer to form a tertiary alcohol and enolate anion is rate-determining, with a barrier of 30.93 kcal/mol. In **Scheme 9** (Equation III), the protic solvent-assisted hydrogen transfer furnishing Breslow intermediate **162** is rate-determining, with a barrier of 28.84 kcal/mol. These studies and other research reports suggest that both pathways (**Scheme 9**, Equations II and III) are competitive for their similar barriers. Furthermore, it was reported that the great tension associated with the three-membered transition state (**Scheme 9**, Equation IV) results in the high intramolecular barrier (45.23 kcal/mol) that leads to the formation of Breslow intermediate **162**, which is an unfavorable process.

#### 1.4.3. Generation of acylazoliums by internal and external oxidation of Breslow intermediates

The scope of NHC chemistry can be expanded with protocols for the oxidative transformations of Breslow intermediates into electrophilic acyl azolium intermediates via an internal redox process or through the addition of an external oxidant. Electrophilic acyl azolium has been generated from internal redox processes, such as redox isomerization,

the loss of a leaving group or ring-opening, with several  $\alpha$ -oxidizable aldehydes (e.g., ynals **165**,  $\alpha$ -haloaldehydes **166** and epoxyaldehydes **167**) (Dzieszkowski et al., 2020; Flanigan et al., 2015; Ni et al., 2015) (**Scheme 10**, Equation I). Carboxylic acid derivatives (**Biswas et al., 2021**) **168** and **169** (**Scheme 10**, Equation II) are other examples of compounds that lead to the formation of the acylazolium intermediates without the use of an external oxidant agent.

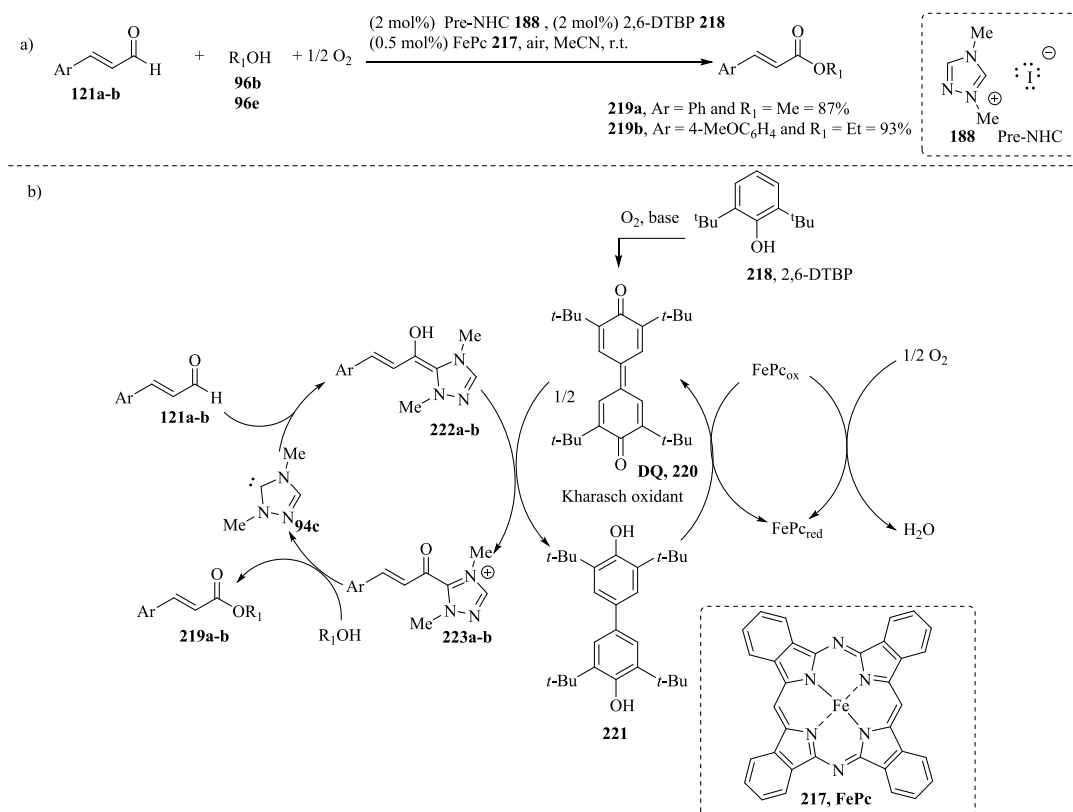
The addition of an external oxidant for the oxidation of the Breslow intermediates **124** and **128** into the corresponding acyl azolium intermediates **125** and **129** paves the way for the use of other raw materials, including saturated **120** and  $\alpha,\beta$ -unsaturated **121** aldehydes (**Scheme 10**, Equations III–IV). Some examples of external inorganic/organic oxidants that can be used for the oxidation of the Breslow intermediate to the corresponding reactive acylazolium ion intermediate include 3,3',5,5'-tetra-*tert*-butyldiphenylquinone (Kharasch-reagent, DQ), nitrobenzene, MnO<sub>2</sub>, ferricyanide, 2,2,6,6-Tetramethylpiperidinyloxy (TEMPO), *N*-fluorobenzenesulfonimide (NFSI), riboflavin, phenazine, azabenzene, polyhalides and electrochemical (Finney et al., 2012; Ishii et al., 2020; Wu et al., 2017). It should be noted that normally, the use of substrates capable of undergoing redox processes using external



[a] Reactions were carried out on a 0.25 mmol scale of aldehyde in 1 mL acetonitrile at room temperature.

[b] Isolated yields

**Scheme 17.** NHC-catalyzed aerobic oxidation of aldehydes.



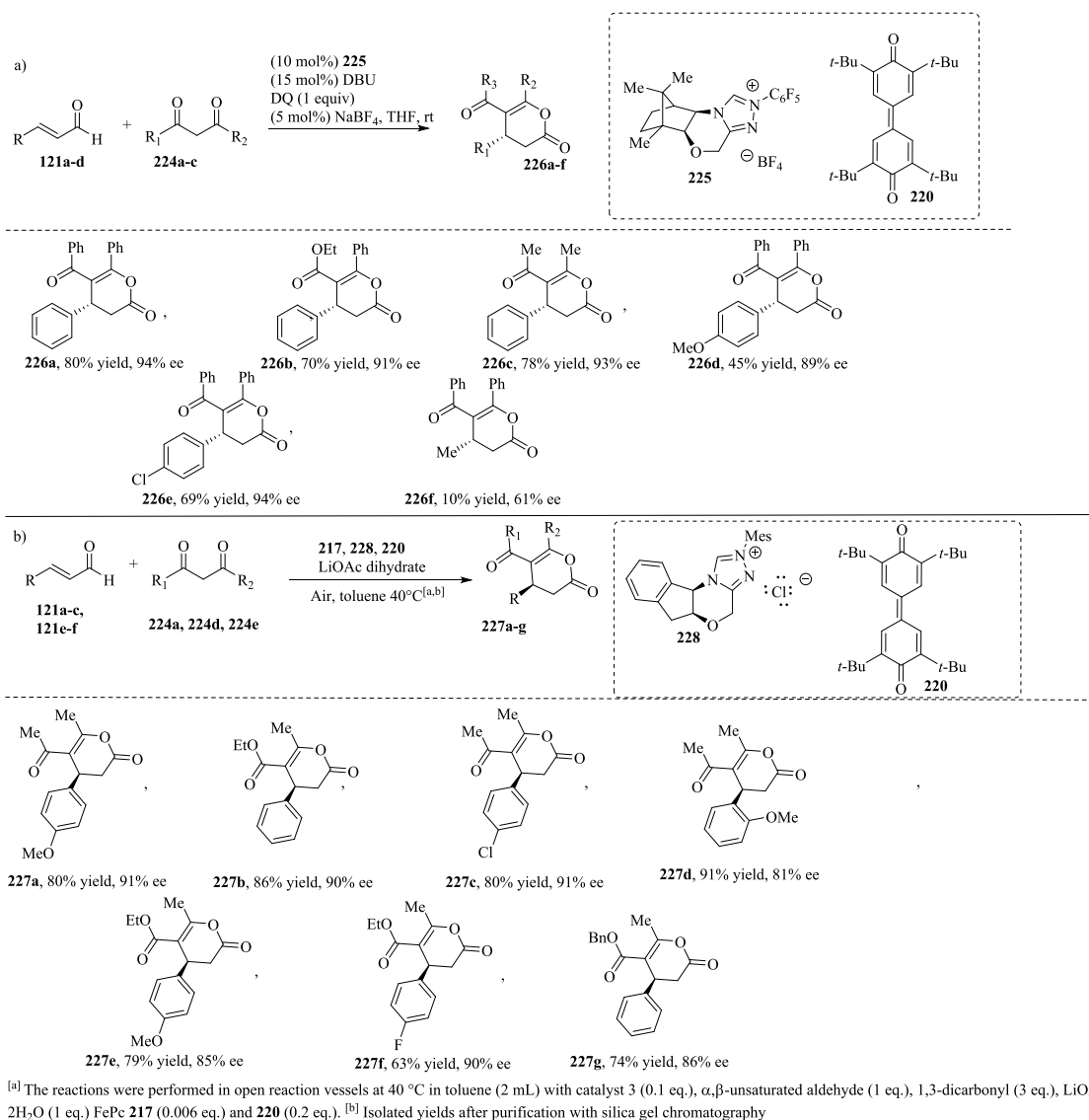
**Scheme 18.** NHC-catalyzed ester synthesis; b) Proposed mechanism of aerobic oxidation via multistep electron transfer.

oxidants requires a stoichiometric amount and has cost, toxicity and sustainability problems (Wu et al., 2019). Cooperative systems that employ atmospheric oxygen as a terminal oxidant, such as organocatalysis with NHCs and a transition metal-based catalyst in combination with O<sub>2</sub>, would be more desirable (Zhao et al., 2013). Molecular oxygen (O<sub>2</sub>) has been considered as an ideal oxidant due to its natural, inexpensive, and environmentally friendly characters. (Stenkvist et al., 2023).

Some examples of NHC-catalyzed reactions are shown below.

#### 1.5. Oxidative/oxygenative pathways for the aerobic oxidation of aldehydes through NHC catalysis

The aerobic oxidation of the Breslow intermediate **170** generated *in situ* from NHC **119** and aldehyde **173** can occur through two different pathways (Scheme 11): two-electron transfer to the oxidant species (O<sub>2</sub> or inorganic/organic oxidants in stoichiometric quantities) (oxidative route) and/or oxygen atom transfer from the oxidant (O<sub>2</sub>) (oxygenative route). In most cases, the Breslow intermediate is transformed into an



**Scheme 19.** NHC-catalyzed enantioselective annulation of enals with 1,3-dicarbonyls (Shen et al., 2011).

electrophilic acylazolium ion, which may be attacked by nucleophiles, but not all oxidations necessarily occur in this direction. For example, when oxygen is used as the oxidant agent, a complex ion between the Breslow-derived radical cation **174** and superoxide radical anion [O<sub>2</sub>]<sup>•-</sup> is formed via single electron transfer (SET) from the Breslow intermediate to the molecular oxygen.

Subsequently, the complex **174** recombines to provide the hydroperoxy derivative **175** and the peroxide anion. Zwitterionic hydroperoxy **175** forms the acyl azolium ion **177** after the liberation of the hydroperoxy anion in the oxidative pathway, which can then react with further nucleophiles according to a nucleophilic acyl substitution mechanism, with the regeneration of the NHC catalyst (oxidative route, Scheme 11). Alternatively, the peroxide **176** reacts with a second molecule of aldehyde **173** to form intermediate **179** (oxygenative route, Scheme 11), which, through a process reminiscent of Baeyer-Villiger oxidation, forms the first molecule of acid **180**. The final step is the release of an additional molecule of acid **180** from intermediate **181**, with the regeneration of the catalyst. As reported by Bortolini et al., (2014) all intermediates of both catalytic pathways were identified under mass spectrometry conditions (Bortolini et al., 2017, 2014; De Risi et al., 2023). It has also been reported in the literature (Zhao et al., 2013) that azolium hydroperoxy intermediate **175** can undergo fragmentation,

with the release of the peracid compound **182**. This later, in turn, reacts with aldehyde **173** to provide two equivalents of the carboxylic acid **180**. According to Studer, another possible way of generating the carboxylic acid **180** involves the fragmentation of the salt **183** obtained from the reaction between the Breslow intermediate **170** and the peracid **182** (Zhao et al., 2013).

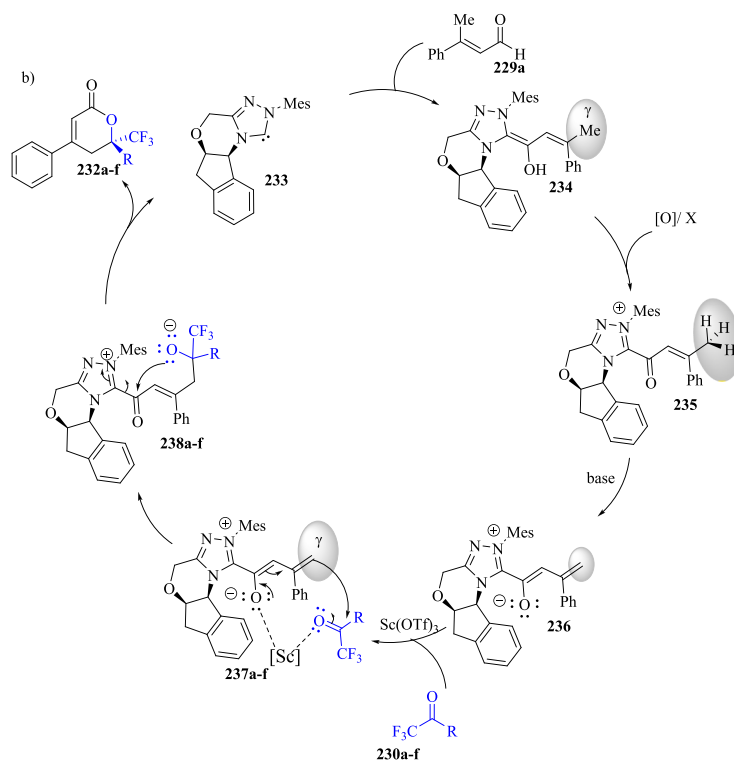
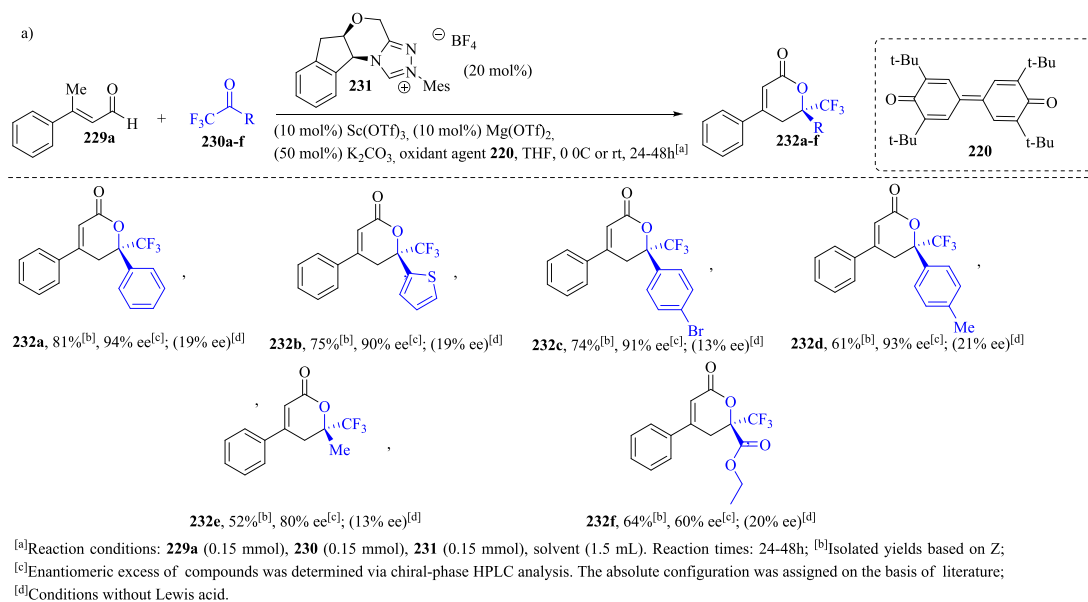
## 1.6. Aerobic oxidative NHC-catalysis

### 1.6.1. Oxidative NHC-catalyzed esterification of aldehydes

Within the previously discussed concept, Delany et al. (2013) described NHC-catalyzed aerobic aldehyde-esterifications with methanol without additives or cocatalysts. Benzaldehyde **148a** and several aromatic aldehydes **148b-d** and **184-185** containing electronically different substituents were converted into the corresponding methyl esters **187a-f** in excellent yields in the presence of DBU, methanol and air (Scheme 12). (Delany et al., 2013).

### 1.6.2. NHC-catalyzed ester synthesis from organic halides

Tan et al. (2021) described the NHC-catalyzed synthesis of esters in moderate to excellent yields via the incorporation of oxygen atoms from O<sub>2</sub> into organic halides (Scheme 13a). Aliphatic bromide **189 k** (n = 3),

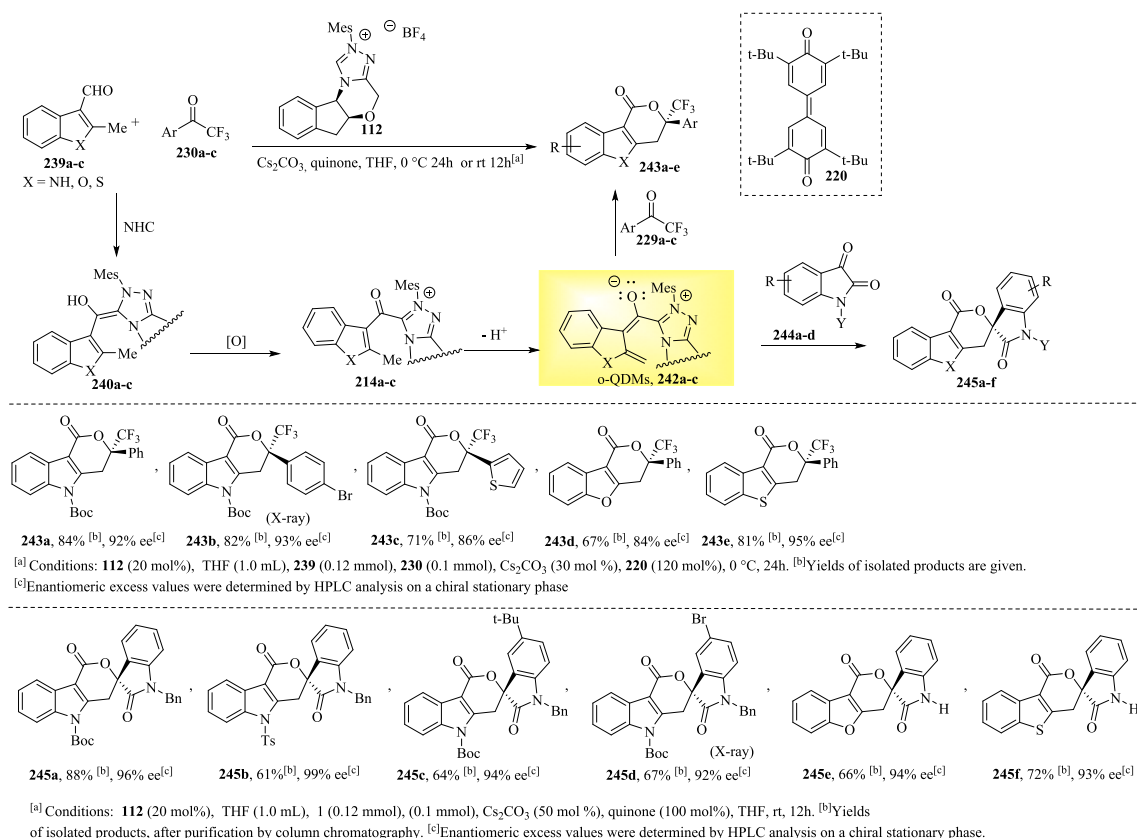


**Scheme 20.** 1,2,4-triazolium-catalyzed oxidative [4 + 2] cycloaddition of an enal with trifluoromethyl ketones; b) Proposed mechanism.

compared to benzylic halides **189a–n**, failed to provide the compound **190 k**. It should be noted that halides can be transformed into aldehydes and ketones under several conditions, with the need for excessive additives and stoichiometric strong oxidant agents, including  $\text{NaIO}_4$ ,  $\text{H}_5\text{IO}_6/\text{V}_2\text{O}_5$ , pyridine *N*-oxide in  $\text{Ag}_2\text{O}$ , *o*-iodoxybenzoic acid and *tert*-butyl hydroperoxide (TBHP), while the NHC-catalyzed oxidation of organic halides provides a green strategy for ester synthesis. In **Scheme 13b**, the NHC-catalyzed oxygenation cross-esterification of benzyl bromides **189a–d** with aliphatic alcohols **191** produced the desired esters **187a–b** and **193a–i** in lower to good yields (Tan et al., 2021).

The proposed mechanism for ester synthesis illustrated in **Scheme 14** was based on  $^{18}\text{O}$  labeling experiments, such as the cross-esterification of 4-nitrobenzyl bromide and hexyl bromide performed under  $^{18}\text{O}$ -labeled  $\text{O}_2$ . From this study, it was established that the two oxygen

atoms of the ester originated from  $^{18}\text{O}_2$ . In **Scheme 14**, the deoxy Breslow intermediate **195** generated *in situ* from NHC **94c** or **194** and organic halide **189** undergoes an oxidative reaction with  $\text{O}_2$ , transforming into peroxide anion **196**. The reaction of this latter compound with **195** leads to the formation of intermediate **197**, which subsequently reacts with an electrophilic halide **189** to form **198** (Path I). The release of a hydrogen halide from **198** culminates in the formation of **199**, which then provides **200** via an oxidative process with molecular oxygen. Finally, the reaction between species **199** and **200** produces intermediate **201**, which is converted into an ester product **190**, with the release of the NHC. In Path II, when an alcohol **191** is employed as one of the starting materials, the Breslow intermediate **202** is oxidized by  $\text{O}_2$  to form acyl azolium compound **203**, which is subsequently attacked by the nucleophilic oxygenated compound to provide esters **187a–b** and



**Scheme 21.** NHC-catalyzed oxidative cycloaddition via *ortho*-quinodimethane intermediate.

**193a-i** and the NHC.

## 1.7. Examples of NHC-catalyzed reactions using external oxidizing agents

### 1.7.1. Aldehyde esterification in the presence of an external oxidant and with molecular oxygen as the terminal oxidant

Based on the mechanistic study of the NHC-catalyzed aerobic oxidation of aldehydes to esters, as demonstrated in [Scheme 11](#), Bortolini et al. (2023) found that the oxidation of a Breslow intermediate with O<sub>2</sub> in the presence of alcohol led to the formation of the carboxylic acid **208** and esters **190a** and **209** as a side product ([Schemes 15 and 16a](#)). According to researchers, the ratio of the compounds **208** and **190a** and **209** is related to the substitution pattern of the R-group ([De Risi et al., 2023; Zhao et al., 2013](#)). An alternative method for the preparation of esters **190a** and **209** with good yields involves an efficient cooperative NHC- and metal-based redox catalysis of aldehydes **148a**, **148c-e**, **184**, **204a**, **205-206** or **207** in the presence of alcohols ([Schemes 16a-b](#)) using aerobic oxygen as the terminal oxidant for the regeneration of the metal cocatalyst ([Zhao et al., 2013](#)).

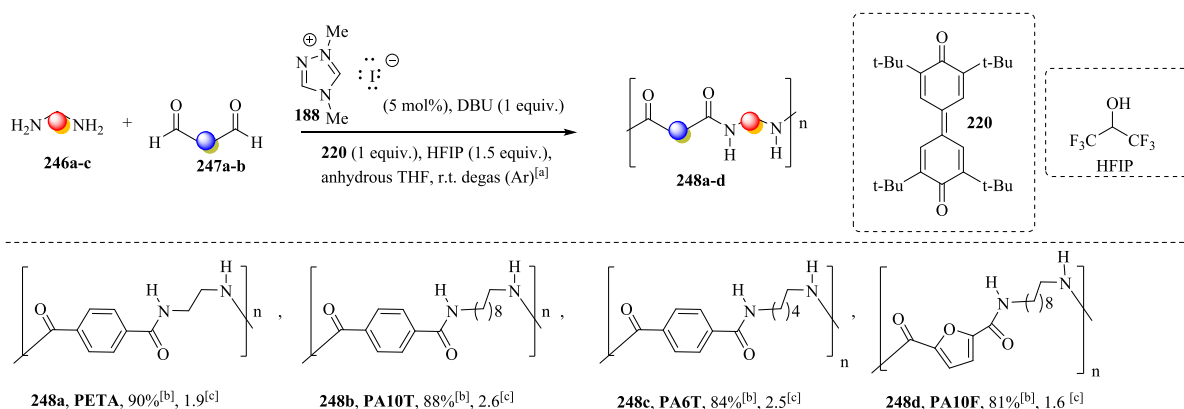
In this regard, several aromatic and heteroaromatic aldehydes **148a**, **148c-e**, **184**, **204a**, **205-206** or **207** could be esterified in moderate to good yields through cooperative NHC and Ru(II)-based redox catalysis, with aerobic oxygen being used as the terminal oxidant ([Scheme 16a](#)) ([Zhao et al., 2013](#)).

In the proposed mechanism ([Scheme 16b](#)), the Breslow intermediates **212a-h** are oxidized by Ru(BPZ)<sub>3</sub>(PF<sub>6</sub>)<sub>2</sub> through a single electron transfer (SET) process to obtain the radical cations **213a-h**. Molecular oxygen acts as the terminal oxidant, restoring the catalytic activity of the catalyst through the oxidation of the intermediate Ru(I) complex to provide the Ru(BPZ)<sub>3</sub><sup>2+</sup> complex, along with the superoxide radical anion (O<sub>2</sub><sup>-</sup>). Subsequently, the deprotonation reaction of **213a-h** with a base or with a superoxide radical anion leads to the formation of tertiary radicals **214a-h**, which then undergo oxidation, yielding the

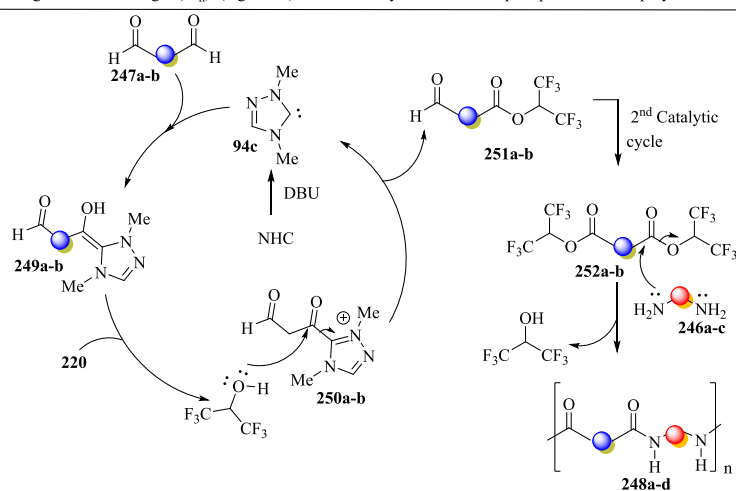
acylazolium ions **215a-h**. This oxidation step can be carried out with Ru (BPZ)<sub>3</sub><sup>2+</sup> or with the hydroperoxyl radical (HO<sub>2</sub>). The attack of the nucleophile on the electrophilic center of acylazolium intermediate culminates in the formation of the esters **190a** and **209a-g** and the release of the NHC. Zhao et al. report ([Zhao et al., 2013](#)) that the major side product identified in this esterification reaction was the carboxylic acid resulting from the oxidation of the Breslow intermediate with O<sub>2</sub>, without the involvement of Ru catalysis. [Zhao et al. \(2013\)](#) studies also show that in the absence of the Ru(II) complex and alcohol, aldehydes were oxidized under aerobic conditions to the corresponding acids in good to excellent yields ([Scheme 17](#), and see [Scheme 11](#)—oxygenative route). ([Zhao et al., 2013](#)).

### 1.7.2. NHC-catalyzed aerobic oxidation coupled to ETM system for ester synthesis

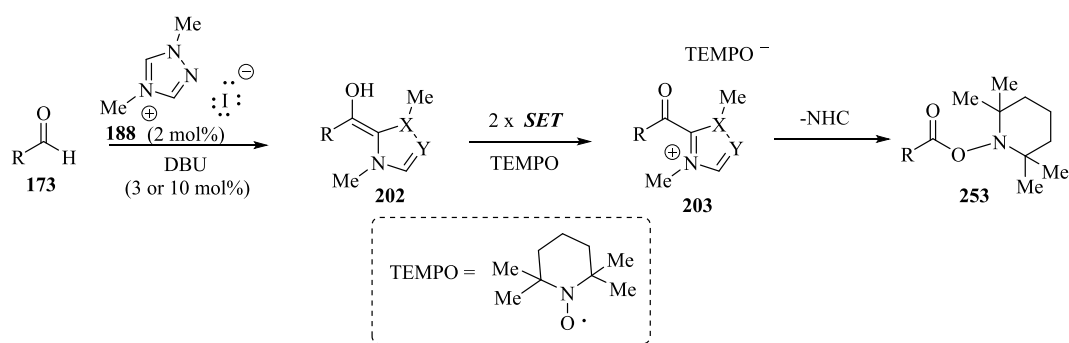
The oxidative NHC-catalyzed aerobic esterification of  $\alpha$ ,  $\beta$ -unsaturated aldehydes **121a-b** with alcohols **96b** and **96e** in the presence of a coupled system of electron transfer mediators (ETMs/ETMs<sup>-</sup>) 2,6-di-*tert*-butylphenol (2,6-DTBP, **218**) and iron(II)phthalocyanine (FePc, **217**) in a basic medium provided ester derivatives in excellent yields ([Scheme 18a](#)). In the proposed mechanism, the 2,6-DTBP catalyst **218** could be introduced as a precursor of DQ **220** through *in situ* chemical oxidation with molecular oxygen. Posteriorly, the electron-transfer process between Breslow intermediates **222a-b** and DQ **220** leads to the formation of the acyl azolium ions **223a-b** and the reduced diol DQH **221**, which is posteriorly re-oxidized by FePc and air (O<sub>2</sub>) acting as the terminal oxidant ([Scheme 18b](#)) ([De Risi et al., 2023; Liu et al., 2021; Ta et al., 2016](#)). It should be noted that ETMs provide a low-energy path that the electrons can use to flow from the Breslow intermediates **222a-b** to a suitable terminal oxidant such as O<sub>2</sub> ([Axelsson et al., 2016; Ta et al., 2016](#)). In the last step of the catalytic cycle, the esters **219a-b** are formed through the nucleophilic attack of alcohol on the electrophilic carbonyl carbon of **223a-b**, regenerating the catalyst.



<sup>[a]</sup>Conditions: **246** (0.88 mmol), **247** (0.80 mmol), **188** (0.08 mmol), DBU (0.20 mmol), **220** (1.60 mmol), HFIP (2.40 mmol), THF (6.0 mL). <sup>[b]</sup>Isolated yield. <sup>[c]</sup>number-average molecular weight ( $M_n$ ) ( $\text{Kg/mol}^{-1}$ ): Calculated by  $^1\text{H NMR}$  after precipitation of the polymer.



**Scheme 22.** a) Synthesis of polyamide oligomers via oxidative nhc catalysis; b) Proposed mechanism.

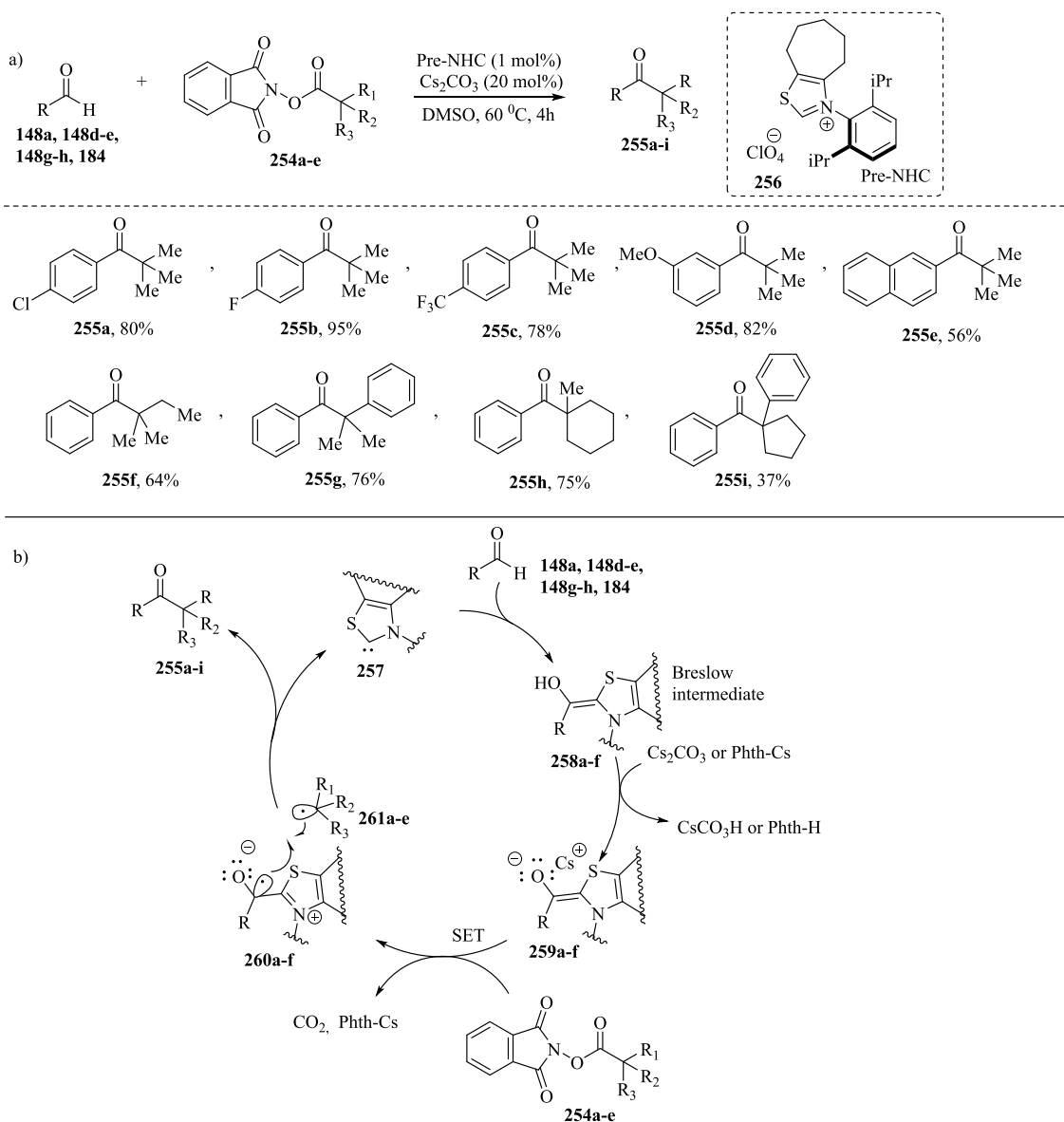


**Scheme 23.** NHC-catalyzed SET reaction.

The oxidative coupling of 2-chlorobenzaldehyde with methanol for the preparation of methyl ester promoted by polystyrene-supported 1,2,4-triazolium carbene offers practical advantages in terms of purification and reusability compared with the homogeneous catalytic process. However, NMR relaxation studies of the solvent effect in the oxidation reaction of 2-chlorobenzaldehyde into the methyl ester promoted by heterogeneous NHC catalysis in the presence of a quinone-based redox mediator such as 2,6-di-*tert*-butylphenol show that the solvent interaction with the surface of the organocatalyst immobilized over a solid support (polystyrene) plays a key role in determining the catalyst activity. Solvents with a high surface affinity lead to a decrease in catalyst activity, possibly by hindering the access of reactant molecules to the catalytic sites over the surface (Di Carmine et al., 2020).

### 1.7.3. NHC-catalyzed synthesis of dihydropyranones utilizing ETMs

Asymmetric aerobic oxidative NHC-catalyzed annulation between enals and 1,3-dicarbonyl compounds was investigated using Kharasch-reagent **220** with a catalytic amount of  $\text{NaBF}_4$  (Scheme 19a) or in combination with another redox mediator such as the phthalocyanine of iron (II) (FePc, **217**) (Scheme 19b). In the first case, the desired dihydropyranones **226a-f** were provided in modest to good yields and with moderate to excellent enantioselectivities (Flanigan et al., 2015). In Scheme 19b, the combination of two electron transfer mediators (DT/FePc) led to the formation of dihydropyranones **227a-g** in good to high yields with ee values of 81–91 % (Axelsson et al., 2016).



**Scheme 24.** a) NHC-catalyzed decarboxylative alkylation of aldehydes; b) Proposed mechanism.

#### 1.7.4. NHC-catalyzed [4 + 2] annulation of $\alpha,\beta$ -disubstituted enals with trifluoromethyl ketones

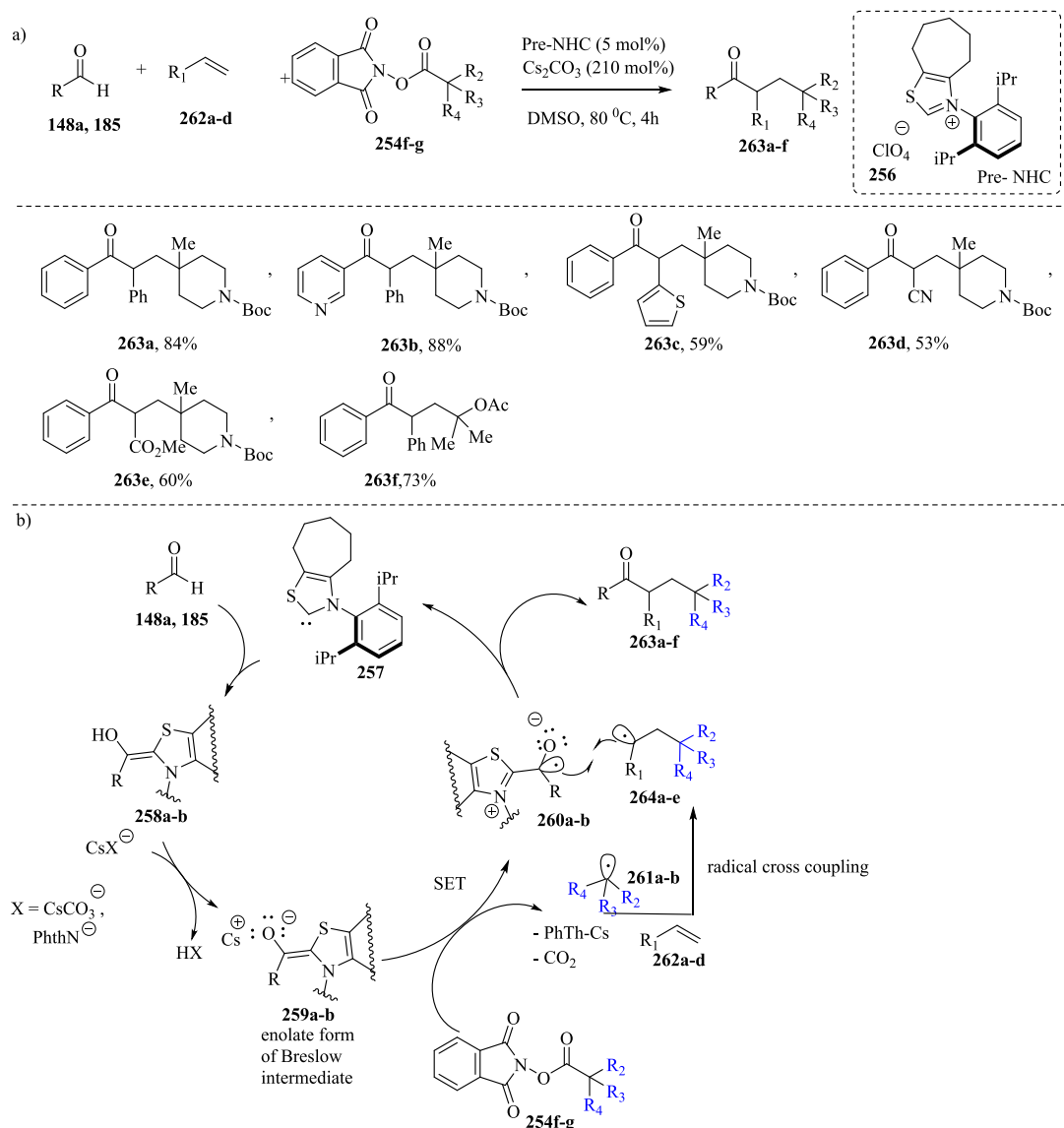
*In situ*-generated 1,2,4-azolium dienolate intermediates **236** (Scheme 20) from  $\alpha,\beta$ -unsaturated aldehyde **229a** were used by Chen et al. (2013) for the synthesis of  $\gamma$ -lactones **232a-f** via the enantioselective  $\gamma$ -addition of enals to activated ketones under oxidative conditions using an NHC / Lewis acid cocatalysts [Sc(OTf)<sub>3</sub> and Mg(OTf)<sub>2</sub>] / quinone as an external oxidant agent (Chen et al., 2018b; Curti et al., 2020; Mo et al., 2012). In the proposed mechanism (Scheme 20b), the  $\alpha,\beta$ -unsaturated-Breslow intermediates **234** are oxidized by quinone, generating the unsaturated acyl azolium intermediate **235**, which subsequently undergoes  $\gamma$ -deprotonation in the presence of a base, transforming into reactive vinyl enolate intermediate **236**. The coordination of the Lewis acid Sc (III) or combined Sc(OTf)<sub>3</sub>/Mg(OTf)<sub>2</sub> with trifluoromethyl ketones **230a-f** and azolium dienolate **236** produces the complexes **237a-f**. The Lewis acid easily coordinates with the carbonyl oxygen of trifluoromethyl ketone, increasing its electrophilicity. In addition, the oxidative  $\gamma$ -functionalization of the enal under NHC catalysis exhibits lower enantioselectivity (Scheme 20b), and the Lewis acid is necessary for obtaining the desired lactones **232a-f** with good to high enantioselectivities. The chelating ketone-azolium dienolate complexes **237a-f**

amplify chiral induction by the chiral NHC catalyst because the Lewis acid brings the ketone into proximity with the azolium dienolate-containing chiral NHC catalyst. Furthermore, in this reaction, an enal containing steric hindrance at the  $\beta$ -position was utilized as a substrate, so that its reactivity was smoothly switched from the  $\beta$ -carbon to the  $\gamma$ -position upon oxidation (X. Chen et al., 2013b).

#### 1.7.5. NHC-catalyzed oxidative [4 + 2] cycloaddition via *ortho*-quinodimethane intermediate

The asymmetric functionalization of the benzylic C – H bonds of heteroaryl aldehydes via NHC organocatalysis has been developed by Chen et al. (2020). This strategy involves the *in situ* generation of heterocyclic *ortho*-quinodimethanes (*o*-QDM, **242**), which undergo highly enantioselective formal [4 + 2] cycloaddition with trifluoromethyl ketones **230a-c** or isatins **244a-d** to form polycyclic lactones **243** and **245a-f**, which contain a quaternary carbon center, in good to excellent yields and with over 90 % ee (Scheme 21) (Chen et al., 2020; X. Chen et al., 2013b).

Other examples of the annulation of *o*-quinodimethanes through NHC catalysis are reported in the literature (Janssen-muller et al., 2016).



### 1.7.6. Synthesis of oligomeric polyamides mediated by NHC catalysis

The synthesis of oligomeric polyamides (PAs) **248a–d** (Scheme 22) via the polycondensation of diamines **246a–c** and dialdehydes **247a–b** mediated by a 1,2,4-triazolium carbene catalyst in the presence of a quinone oxidant and hexafluoro-2-propanol (HFIP), a nucleophilic additive that guarantees oligomer growth, was proposed by Ragno et al. (2021) (Ragno et al., 2021). The polyamides were obtained with a number-average molecular weight ( $M_n$ ) in the range from 1.7 to 3.6 kg mol<sup>-1</sup>, as determined by NMR experiments. In the catalytic process, the deprotonation reaction of the 1,2,4-triazolium salt with DBU, followed by the nucleophilic attack of the carbene **94c** on dialdehydes **247a–b**, provides the Breslow intermediates **249a–b**, which undergo oxidation with quinone, transforming into the corresponding acyl azolium intermediates **250a–b**. Posteriorly, the nucleophilic attack of hexafluoro-2-propanol (HFIP) on the carbonyl carbon of **250a–b** results in the formation of the hexafluoroisopropyl monoester **251a–b** and the release of the NHC catalyst. According to the authors, the hexafluoroisopropyl diester **252a–b** can be obtained via the functionalization of monoesters **251a–b** in a second catalytic cycle. They suggest that the concurrent oxidative esterification of the carbonyl function of dialdehyde **247a–b** seems to be less likely; however, it cannot be ruled out. The reaction of diesters **252a–b** with diamine culminates in the formation of the amide

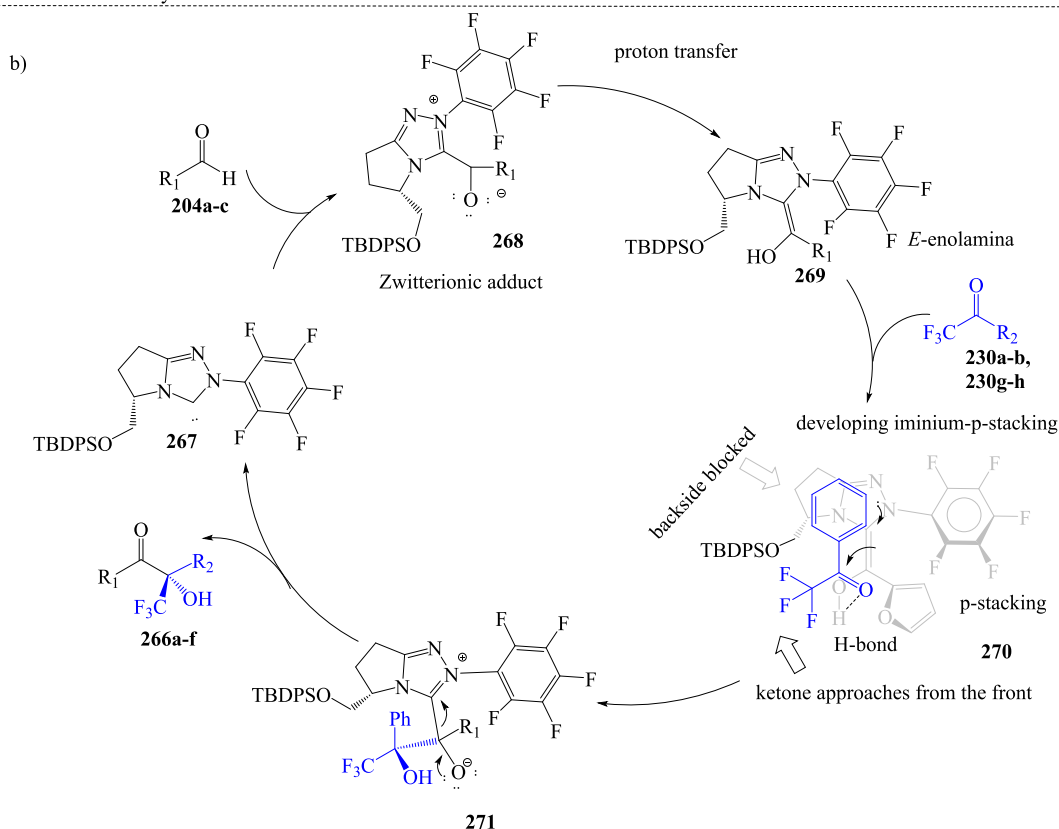
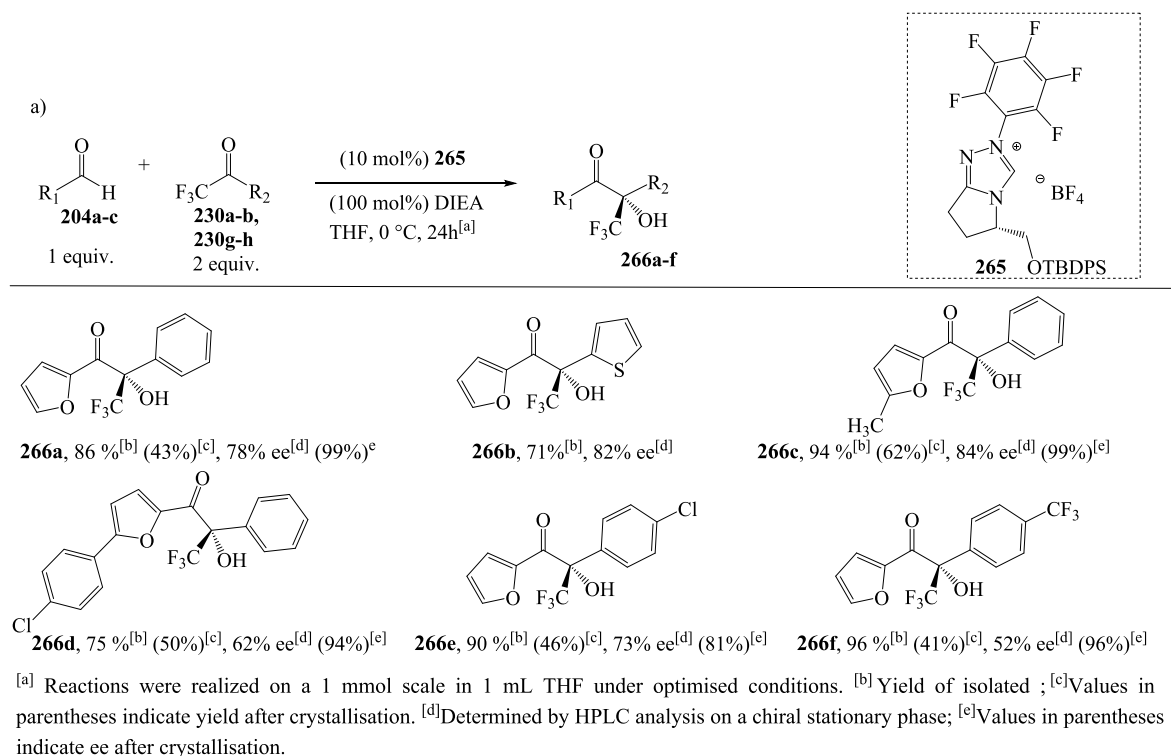
and the release of HFIP. (Ragno et al., 2021).

Several reviews of polymers obtained from NHC-mediated polymerization reactions are reported in the literature (Fèvre et al., 2013; Naik et al., 2012; Ou et al., 2022; Wei et al., 2022).

### 1.7.7. NHC-catalyzed reactions via single electron transfer (SET) process

In 2008, Studer et al reported (Guin et al., 2008; Ishii et al., 2019a; Song and Chi, 2019) the pioneering example of NHC-catalyzed conversion of aldehydes **173** to carboxylic esters **253** through two single-electron oxidation steps in the presence 2,2,6,6-tetramethylpiperidine N-oxyl radical (TEMPO) as the oxidizing agent (Scheme 23). For this methodology, cinnamaldehyde, benzaldehyde and electron-donating and -withdrawing *para*-substituted benzaldehyde derivatives provided the corresponding ester products in excellent yields (Guin et al., 2008). Mechanistically, the process involves two continuous single-electron oxidations of the Breslow intermediates by TEMPO to form the azolium ketones **203**, which react with TEMPO to give the desired TEMPO-ester derivatives **253** and regenerate the *N*-heterocyclic carbene.

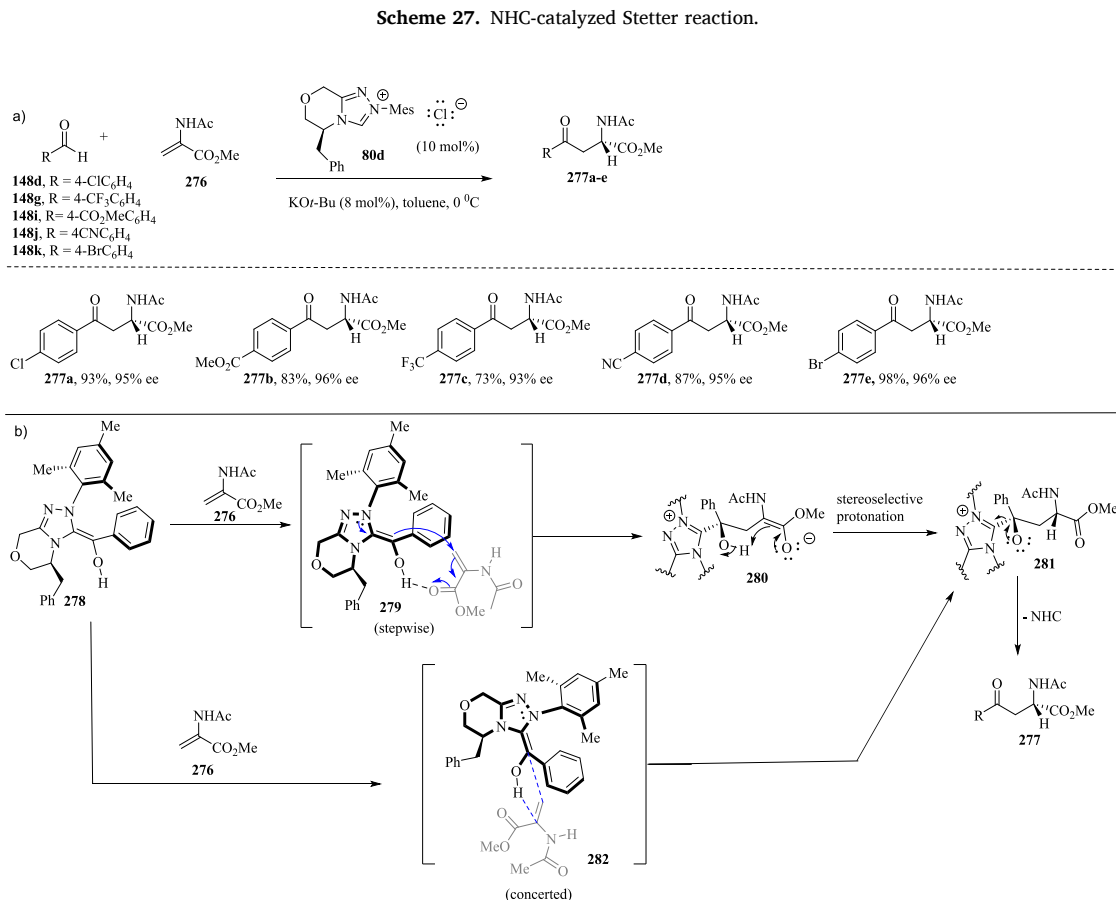
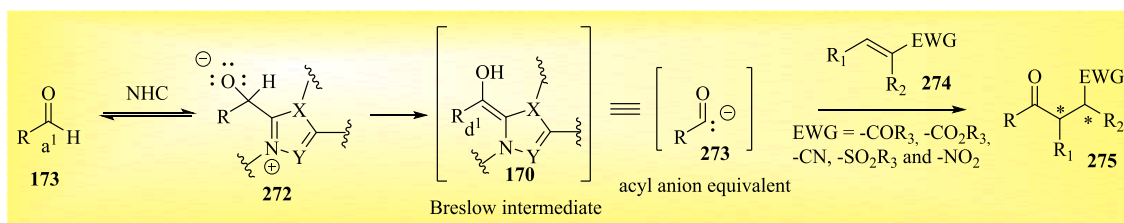
*N*-Heterocyclic carbene-catalyzed decarboxylative alkylation between aldehydes **148a**, **148d–e**, **148 g–h**, **184** and redox ester **254a–e** (Scheme 24a) was reported by Ohmiya et al. (Ishii et al., 2019a, 2020; Song and Chi, 2019). This work constitutes an important example for



**Scheme 26.** a) Asymmetric cross-benzoin-type reaction of heteroaromatic aldehydes and various trifluoromethyl ketones; b) Proposed mechanism.

generating reactive radical intermediates in NHC catalysis. In proposed mechanism, the reaction of **148a**, **148d-e**, **148 g-h**, **184** with NHC **257** produces a neutral Breslow intermediate **258a-f**, which undergoes a deprotonation reaction generating the reducing enolate form of the Breslow intermediate **259a-f**. The SET event between enolate **259a-f** and **254a-e** gives Breslow intermediate type radical **260a-g** and alkyl

radical **261a-e**, respectively, (Scheme 24b). This oxidation involves a decarboxylation step to release CO<sub>2</sub> and form two radical species. The authors suggested that Lewis acidic activation of the phthalimide moiety with the counterion (Cs<sup>+</sup>) favored the oxidation of the enolate **259a-f** to the radical adduct **260a-f**. Radical-radical recombination between **260a-f** and **261a-e** followed by elimination of NHC **257** led to the



formation of the ketone compound **255a-i**.

*N*-Heterocyclic carbene-catalyzed radical cross-coupling between aldehydes and  $\alpha$ -bromoesters or  $\alpha$ -bromoamides was also reported in the literature by Ohmiya and colleagues in 2021 (Ishii et al., 2020).

NHC-catalyzed radical reaction relay facilitates the vicinal alkylation of styrenes, acrylates and acrylonitriles by employing aldehydes and redox-active esters derived from tertiary alkyl carbonic acids (Scheme 25) (Dai and Ye, 2021; Ishii et al., 2019b). The following chemical transformation has a similar mechanism to that illustrated in Scheme 24b up to the stage of formation of the enolate ion **259**. The SET process between enolate **259a-b** and redox ester **254f-g** gives a ketyl radical **260a-b** and tertiary alkyl radical **261a-b**, respectively. This last radical species reacts with alkene **262a-d** to form the secondary radical **264a-e**. Radical-radical combination between **260a-b** and **264a-e** followed by elimination of the NHC catalyst **257** produces the alkylation compound **263a-f**.

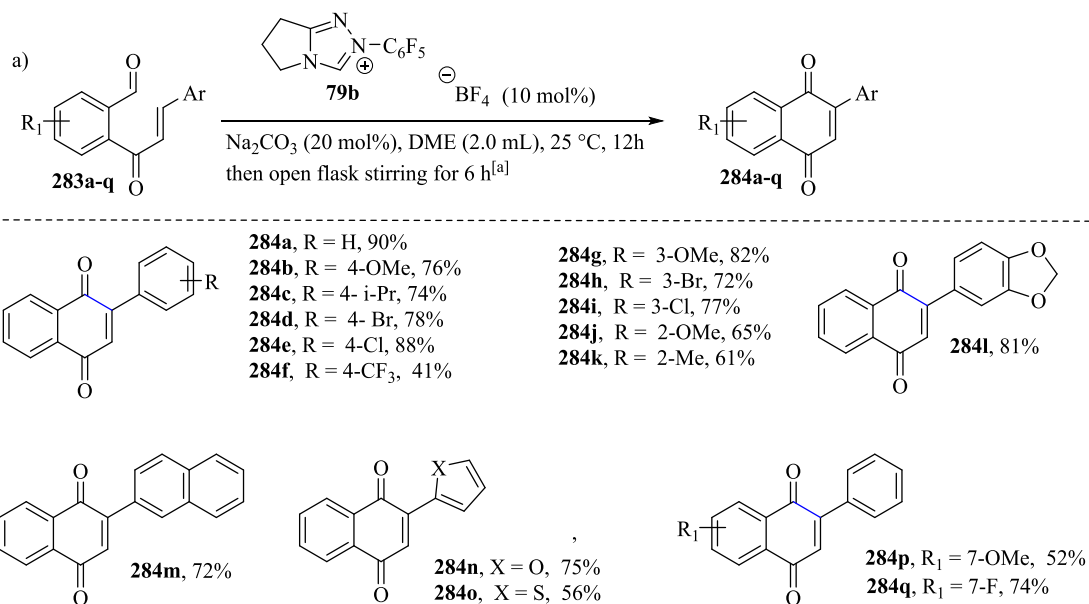
Other examples of reactions based on NHC-catalyzed radical pathways can be found in the literature (Dai and Ye, 2021; Dong et al., 2020; Ishii et al., 2020; Li et al., 2022, 2021; K. Liu et al., 2022; Liu and Chen, 2020; Man et al., 2023; Matsuki et al., 2021; Mulks et al., 2023).

## 1.8. Other examples of NHC mediated reactions

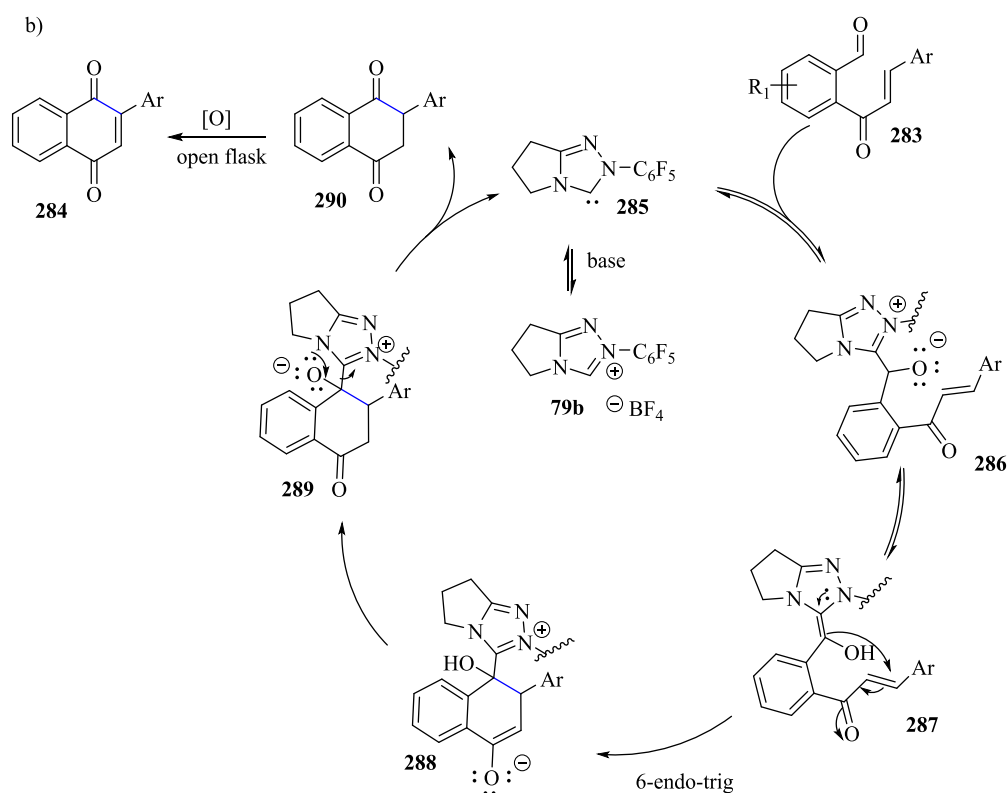
### 1.8.1. NHCs as organocatalysts for cross-benzoin condensation

Benzoin and cross-benzoin condensations represent an important strategy for creating new C–C bonds, leading to the formation of  $\alpha$ -functionalized carbonyl compounds (Menon et al., 2016). In the following example, 1,2,4-triazolium carbene-catalyzed asymmetric cross-benzoin reactions of heteroaromatic aldehydes **204a-c** with trifluoromethyl ketone **230a-b** and **230 g-h** led to the formation of  $\alpha$ -hydroxy ketones **266a-f** in good to excellent yields (71–96 %) and moderate to good enantioselectivities (ee = 52–84 %) (Scheme 26a). After recrystallization, these compounds were obtained with an enantiomeric excess of up to 99 % (Enders et al., 2010).

In the proposed mechanism, the nucleophilic addition of the NHC **267** to aldehydes **204a-c** generates a zwitterionic intermediate **268**, which subsequently undergoes a critical proton transfer through some of the pathways described in Scheme 26b, furnishing Breslow intermediate **269** (Enders et al., 2010). DFT studies have suggested the (*E*) stereochemistry to be favored in Breslow intermediates due to steric and stereoelectronic interaction (Hawkes and Yates, 2008). Leeper (1997) postulated that restricting the rotation of a chiral NHC through the formation of a conformationally restricted chiral *N*-substituted bicyclic



<sup>[a]</sup>General reaction conditions: **283** (0.50 mmol), **79b** (10 mol %), Na<sub>2</sub>CO<sub>3</sub> (20 mol %), DME (2.0 mL), 30 °C, and 12 h. Yields of isolated products are given.

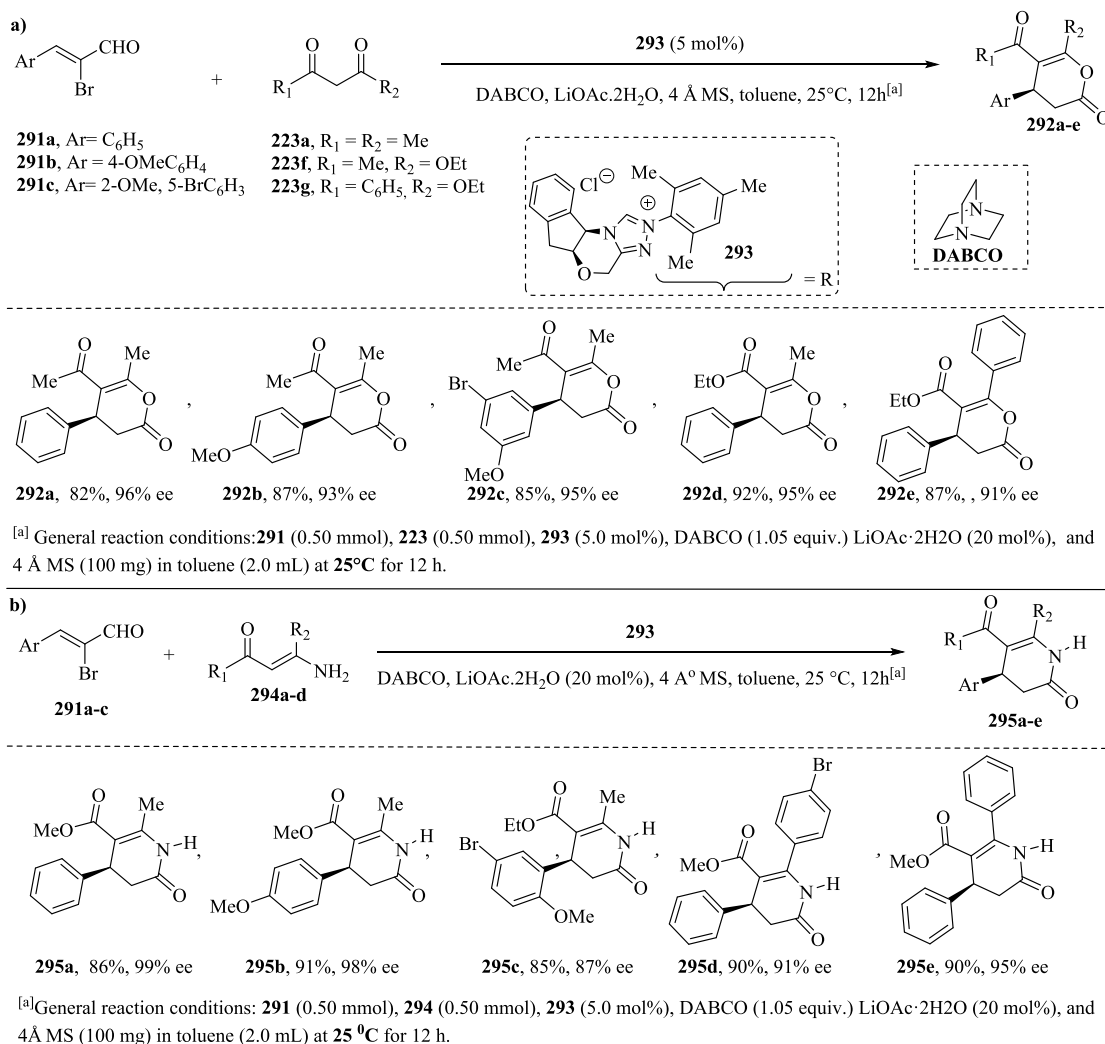


**Scheme 29.** a) Synthesis of 2-aryl-naphthoquinone through NHC-catalyzed intramolecular Stetter reaction; b) Proposed mechanism.

structure would more effectively block only one face of the triazolide-derived acyl anion equivalent (Breslow intermediate) and therefore improve the enantioselectivity of the nucleophilic addition step (Enders and Kallfass, 2002). In the catalytic cycle illustrated in Scheme 26b, other factors may contribute to the selectivity results for the formation of an excess of one enantiomer over the other from a chiral Breslow-intermediate-derived zwitterionic adduct and trifluoromethyl ketone. The sterically demanding silyl protecting group attached to the bicyclic 1,2,4-triazolium catalyst plays an important role in the stereochemistry

of the product. Ketone should approach from the side opposite to the relief of steric interactions with the silyl protecting group attached to the Breslow intermediate (**270**) formed in a catalyzed reaction of the NHC and aldehyde. Other additional factors for enantioselectivity involve a hydrogen bond between the Breslow intermediate and the ketone and a  $\pi$ - $\pi$  interaction between the triazolium ring and the aromatic substituent of the ketone. The release of catalytically active NHC from **271** provides the desired product **266a-f**.

Other examples of benzoin reactions are reported in the literature



**Scheme 30.** NHC-catalyzed reaction of  $\alpha$ -bromo- $\alpha, \beta$ -unsaturated aldehydes with a)  $\beta$ -keto enols compounds and b) enamines.

(Menon et al., 2016).

### 1.8.2. Chiral NHC-catalyzed Stetter reaction

The Stetter reaction is a 1,4-addition of an aldehyde **173** to an  $\alpha, \beta$ -unsaturated compound **274**, catalyzed by cyanide or a Pre-NHC (Heravi et al., 2020). In this case, the NHC reaction involves a Michael acceptor **274** as the electrophile for the Breslow intermediate **170**, resulting in 1,4-bifunctional compounds **275** bearing quaternary centers (Scheme 27).

In the chiral 1,2,4-triazolium-catalyzed Stetter reaction between a variety of aldehydes **148d**, **148 g**, **148i-k** and *N*-acylamido acrylates acting as the Michael acceptor  $\alpha$ -amino acid derivatives **276** (Scheme 28a), compounds **277a-e** were obtained in good yields and with excellent stereoselectivity (Biju et al., 2011; Jousseume et al., 2011). On the basis of computational calculations, Dudding and Houk (2004) suggested that Breslow intermediate **278** derived from aldehyde and triazolylidene Pre-NHC **80d** are electronically suited to preferentially form the *E*-isomer. (Dudding and Houk, 2004) In the catalytic asymmetric intermolecular Stetter reaction, Jousseume et al. (2011) suggest that the stepwise addition of chiral Breslow intermediate **278** to the Michael acceptor **276** from the Si face is supported by an intramolecular protonation involving a hydrogen bond between the enol hydrogen atom and the carbonyl oxygen of the Michael acceptor **279** (Scheme 28b). The protonation of **280** and subsequent regeneration of the carbonyl group of **281** provides  $\alpha$ -amino acid derivative **277a-e**.

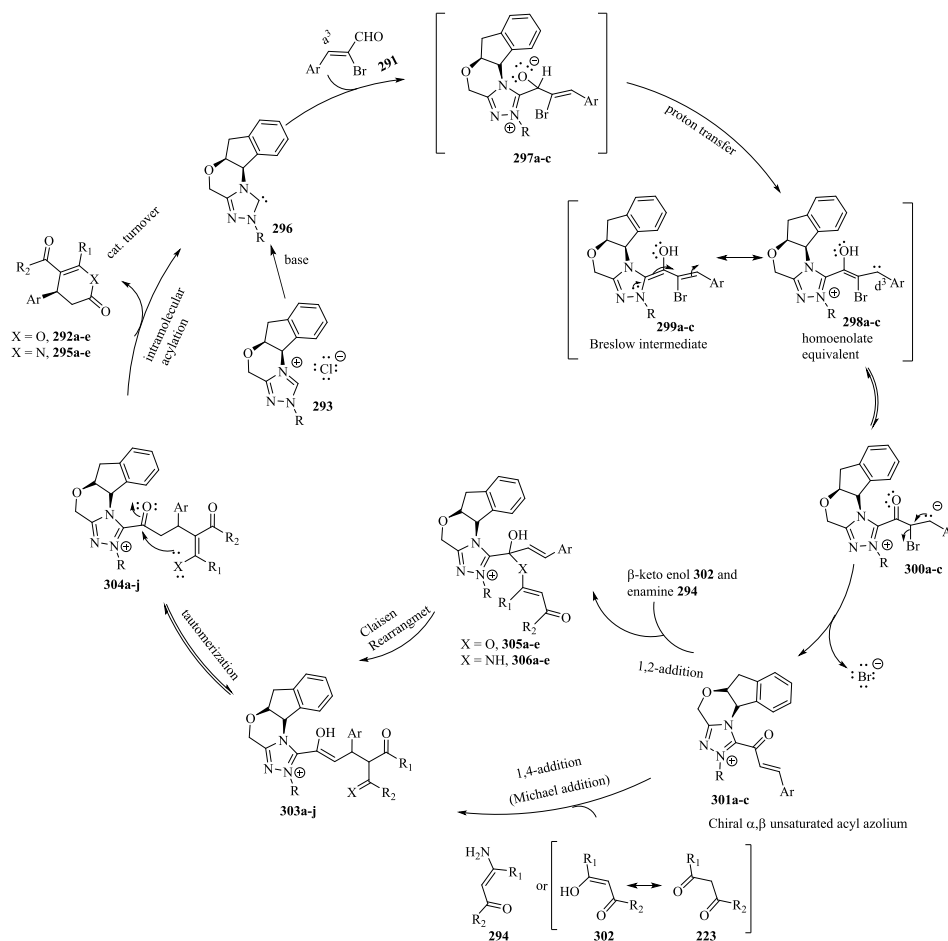
Jousseume et al. (2011) also proposed the synthesis of **277a-e** through an alternative concerted mechanism, which proceeds via cyclic five-membered transition state **282** (Biju et al., 2011; Jousseume et al., 2011; Mondal et al., 2014).

### 1.8.3. Intramolecular Stetter reaction

Ghosh et al. (2019) described a method of preparation of 2-aryl-naphthoquinone derivatives **284a-q** in good yields via cross dehydrogenative coupling (CDC) involving an NHC-catalyzed endo Stetter reaction (Scheme 29a) (Ghosh et al., 2019). The 1,2-addition of free carbene **285** to carbonyl compounds **283a-q** leads to the formation of intermediate **286**, which then undergoes a proton transfer to produce the Breslow intermediate **287** (Scheme 29b). The intramolecular addition of the nucleophilic acyl anion equivalent to the Michael acceptor/electron-poor double bond of **287** occurs through the 6-*endo*-trig pathway (Gilmore and Alabugin, 2011) to provide enolate intermediate **288**, which subsequently undergoes proton exchange, leading to alkoxide intermediate **289**. This alkoxide intermediate eliminates free carbene to produce the dihydronaphthoquinone derivative **290**, which through atmospheric oxidation is converted into the desired product **284**.

### 1.8.4. Chiral NHC-catalyzed annulations of $\alpha, \beta$ -unsaturated aldehydes (enal) with enols and enamines

The NHC-catalyzed [3 + 3] annulation of  $\alpha$ -bromo- $\alpha, \beta$ -unsaturated



**Scheme 31.** Proposed mechanism of the NHC-catalyzed reaction of  $\alpha$ -bromo- $\alpha,\beta$ -unsaturated aldehydes with the  $\beta$ -keto enol forms of 1,3-dicarbonyl compounds and enamines.

aldehydes **291a–c** with  $\beta$ -keto enol forms of 1,3-dicarbonyl compounds **223a**, **223f–g** and enamines **294a–d** provides functionalized 3,4-dihydropyranones **292a–e** (Scheme 30a) and dihydropyridinones **295a–e**, respectively, in good yields and with a high enantiomeric excess (Scheme 30b) (Mondal et al., 2019; Yetra et al., 2013).

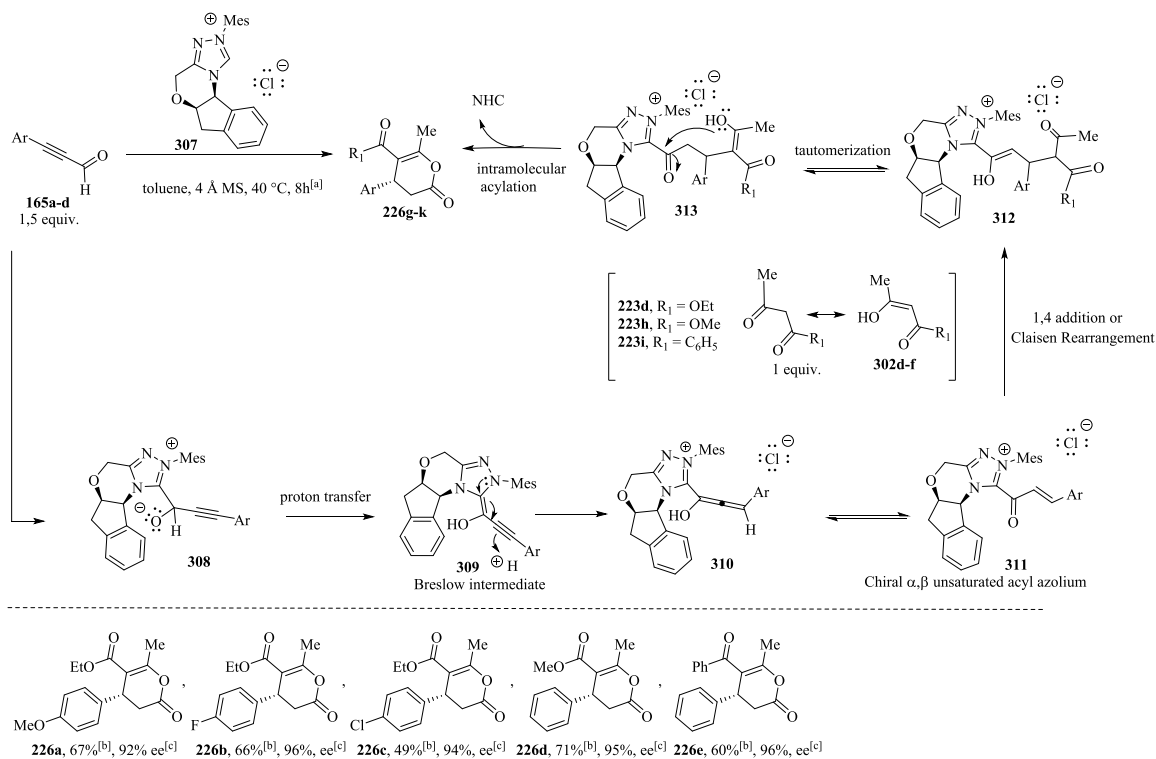
In the proposed mechanism (Scheme 31), Breslow intermediates **299** were generated *in situ* from the reaction of  $\alpha$ -Bromo- $\beta$ -unsaturated aldehydes **291** with the 1,2,4-triazolylidene-derived carbene **296**; then, they were converted into acylazolium ions **301** through  $a^3 \rightarrow d^3$  umpolung and debromination. The acylazolium ions **301** reacted with the  $\beta$ -keto enol forms of **223** and **302** and enamines **294** in a Michael addition reaction, with subsequent tautomerization and intramolecular nucleophilic acyl substitution to provide the corresponding dihydropyranones **292** and dihydropyridinones **295** and to regenerate the NHC catalyst. Alternatively, the intermediates **301** can undergo 1,2-addition with  $\beta$ -keto enols **302** and enamines **294**, followed by a Claisen rearrangement, a [3,3] sigmatropic rearrangement of an allyl vinyl ether **305** ( $X = O$ ) and allyl vinyl enamine **306** ( $X = NH$ ), respectively, and intramolecular nucleophilic acyl substitution to provide the corresponding products **292** and **295**, respectively, and regenerate the NHC catalyst (Mahatthananchai et al., 2012; Mahatthananchai and Bode, 2014; Mondal et al., 2019; Samanta et al., 2012; Yao et al., 2012; Yetra et al., 2013).

Based on kinetic experiments and theoretical data on the mode of addition of nucleophiles ( $\beta$ -keto enols) to the  $\alpha,\beta$ -unsaturated acyl azolium ions, Samantha et al. (2012) suggest that 1,4-addition is more preferable than 1,2-addition (Samanta et al., 2012). In contrast, Kaeobamrung et al. (2010) proposed that the annulation step-mechanism

occurs via a Claisen-type rearrangement rather than via the 1,4-addition of the enol and enamines to the catalytically generated  $\alpha,\beta$ -unsaturated acyl azolium (Kaeobamrung et al., 2010; Lyngvi et al., 2012; Mahatthananchai et al., 2012; Samanta et al., 2012).

#### 1.8.5. Chiral NHC-catalyzed annulations of ynals with enols

Zhu et al. (2010) reported the use of ynals **164a–d** as precursors for the NHC-catalyzed generation of  $\alpha,\beta$ -unsaturated acyl azoliums **311** for the preparation of functionalized dihydropyranones **226 g–k** (Scheme 32) in moderate yields and with a high enantiomeric excess (Mahatthananchai et al., 2012; Zeitler, 2006; Zhu et al., 2011; Zhu and Xiao, 2010). The use of sterically chiral carbene generated from the 1,2,4-triazolium salt **307** was an important factor for the stereoselectivity of the annulation reaction. The 1,2-addition of the NHC catalyst to ynals **165a–d** forms tetrahedral intermediates **308**, which undergo proton transfer to provide Breslow intermediates **309**. The latter can then generate the  $\alpha,\beta$ -unsaturated acyl azoliums **311** through  $\beta$ -protonation, followed by the tautomerization reaction of the allenol intermediates **310**. The generated acyl azoliums **311** are captured by enol derivatives **302d–f** to provide dihydropyranone compounds **226 g–k** and regenerate the catalyst. As previously reported in Scheme 31, two different mechanisms have been suggested to transform acyl azoliums into dihydropyranones and dihydropyridinones. Zhu and Xiao (2010) (Zhu and Xiao, 2010) and (2012) Samantha (Samanta et al., 2012) suggest that the acylazolium salt reacts with various nucleophiles via the 1,4-addition pathway. The proposal by Kaeobamrung et al. (2010) (Kaeobamrung et al., 2010; Lyngvi et al., 2012) based on kinetic investigations shows that the annulation process does not proceed via the 1,4-addition



<sup>[a]</sup>General reaction conditions: 1.5 equiv. of **165**, 1 equiv. of **307**, 10 mol% of **C3**, and 200 mg of 4Å MS in 0.1 M in toluene at 40 °C for 8 h

<sup>[b]</sup>Isolated yield after chromatography. <sup>[c]</sup>Determined by HPLC analysis on a chiral column

**Scheme 32.** NHC-catalyzed annulations of ynals **165a-d** with enols to obtain dihydropyranone derivatives **226a-e**.

of the enol to the catalytically generated  $\alpha$ ,  $\beta$ -unsaturated acyl azolium; instead, a Claisen-type rearrangement is the key catalytic step.

A literature review (Dong et al., 2022) also focuses on the generation and reactivity of NHC-linked alkynyl acyl azolium intermediates from ynals.

#### 1.8.6. Synthesis of pyrrolo[3,2-*c*]quinolines via NHC-catalyzed enantioselective addition of benzylic carbon to unsaturated acyl azolium

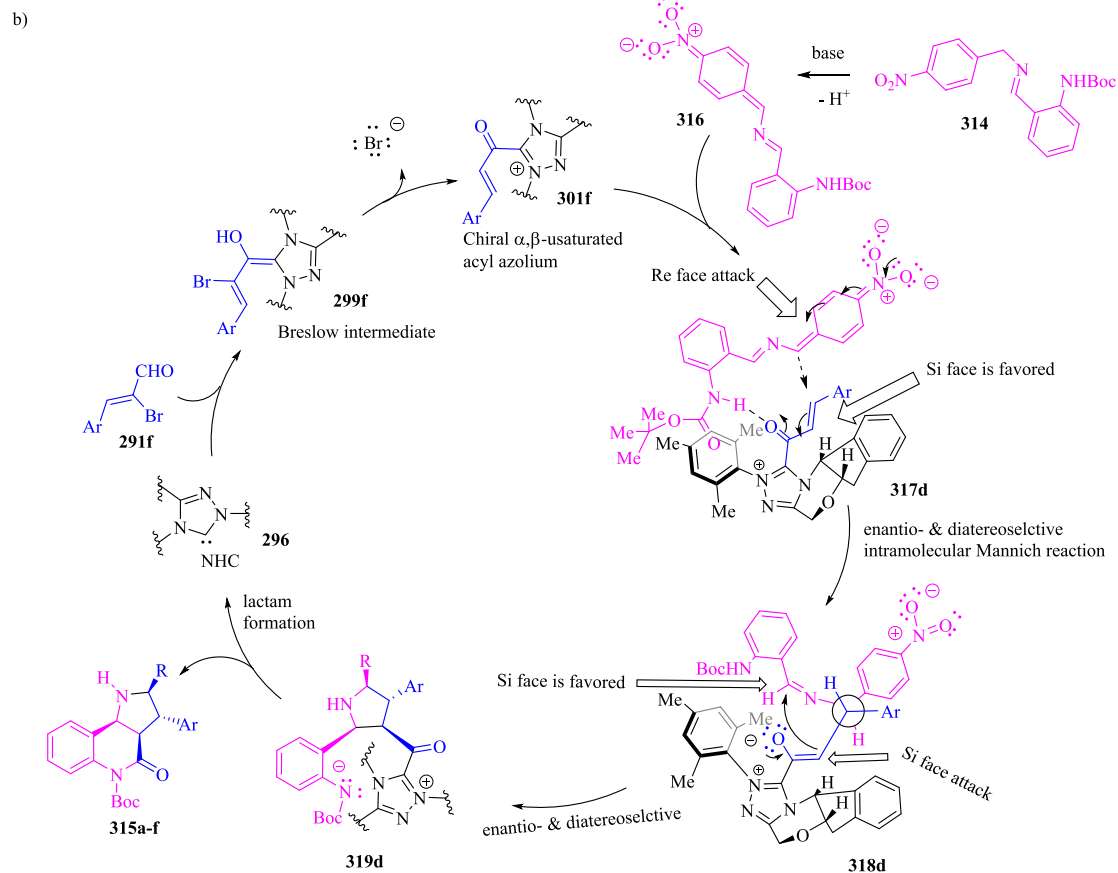
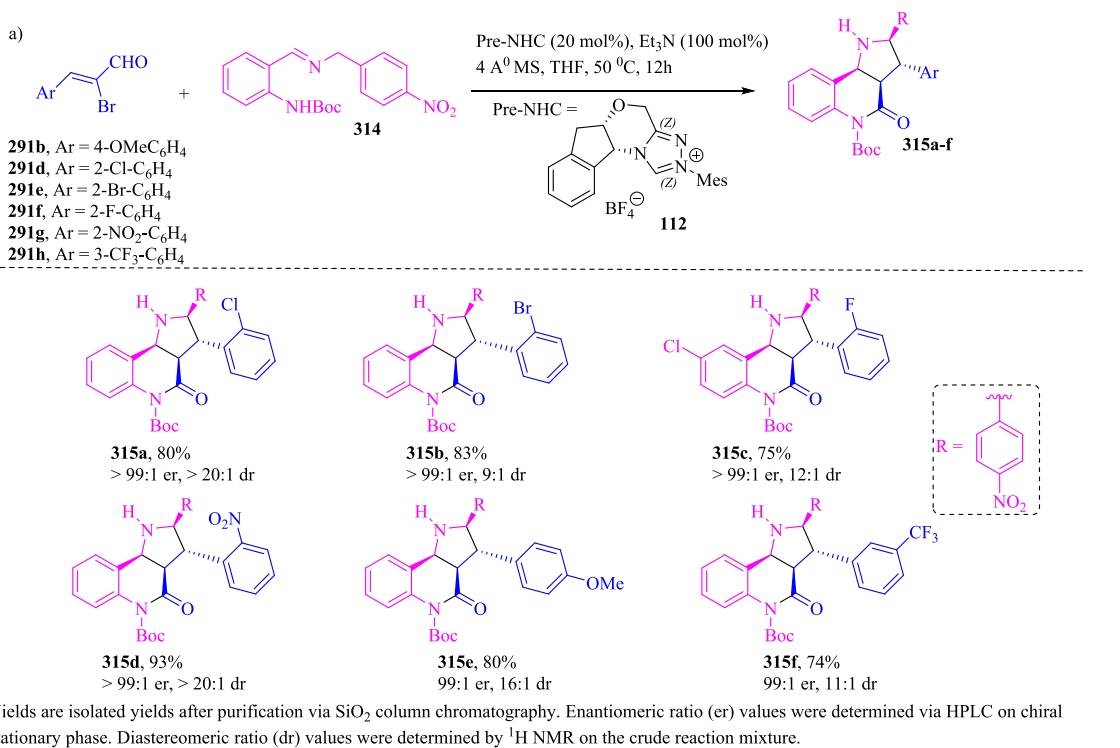
Wang et al. (2018) (J. Wang et al., 2018) related the synthesis of pyrrolo[3,2-*c*] quinolines **315a-f** (Scheme 33a) via the catalyzed enantioselective addition of benzylic carbon to  $\alpha,\beta$ -unsaturated acyl 1,2,4-triazolium intermediates **301b** and **301d-h** generated *in situ* from  $\alpha$ -bromo enals **291b** and **291d-h** and a chiral triazolium carbene precursor. In the proposed simplified mechanism (Scheme 33b), the reaction proceeds via the formation of Breslow intermediates **299f** through the addition of NHC **296** generated *in situ* from chiral 1,2,4-triazolium salt **112** to  $\alpha$ -bromo enal **291f** under basic conditions. Subsequently, the intermediate **299f** undergoes bromide elimination to provide the  $\alpha$ ,  $\beta$ -unsaturated acyl azolium intermediate **301f**, which then reacts with the nucleophilic intermediate **316** generated by a deprotonation reaction of imine derivative **314**. The authors suggest that due to the formation of an intramolecular hydrogen bond and the steric effect provided by the chiral portion of the NHC-based acyl azolium intermediate in complex **317d**, the Re face of NHC-bound  $\alpha$ ,  $\beta$ -unsaturated acyl azolium is blocked by the catalyst, while the Si face is attacked by the Re face of the nucleophilic  $sp^2$  carbon of intermediate **316**. In complex **317d**, the NHC-catalyzed Michael addition between species **301f** and **316** provides the chiral adduct **318d**, which then undergoes intramolecular cyclization, providing chiral pyrrolidine intermediate **319**. The intramolecular nucleophilic acyl substitution of **319** provides the desired pyrrolo[3,2-*c*]quinoline product **315** and releases the NHC catalyst.

#### 1.8.7. Synthesis of functionalized tetrahydroquinolines through NHC-catalyzed cascade reaction

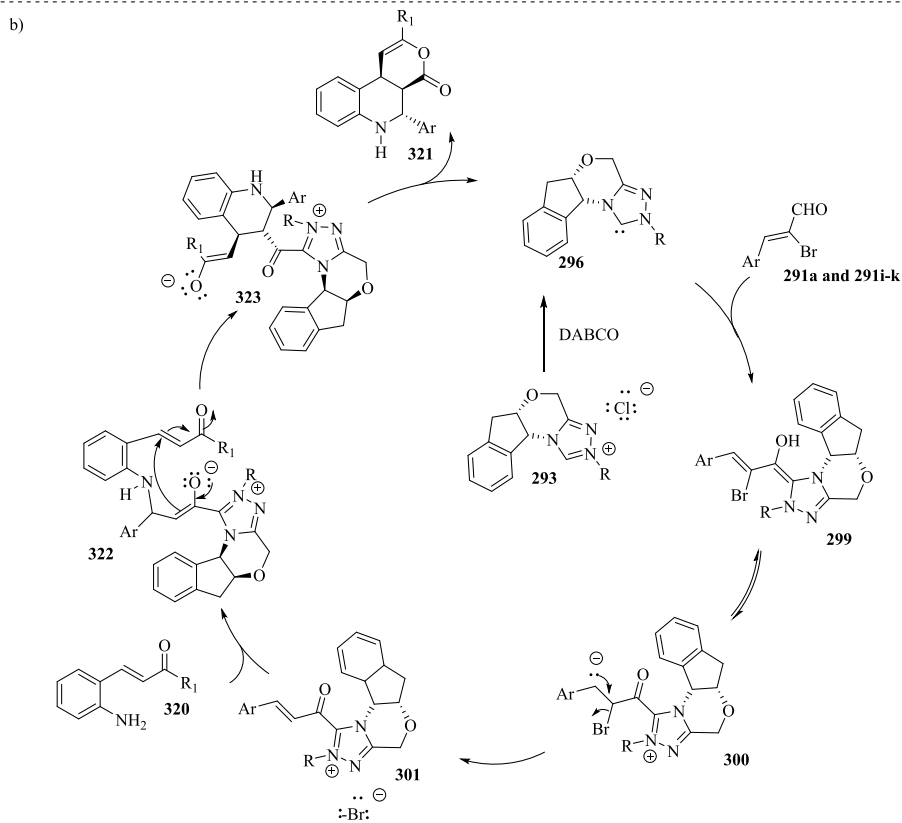
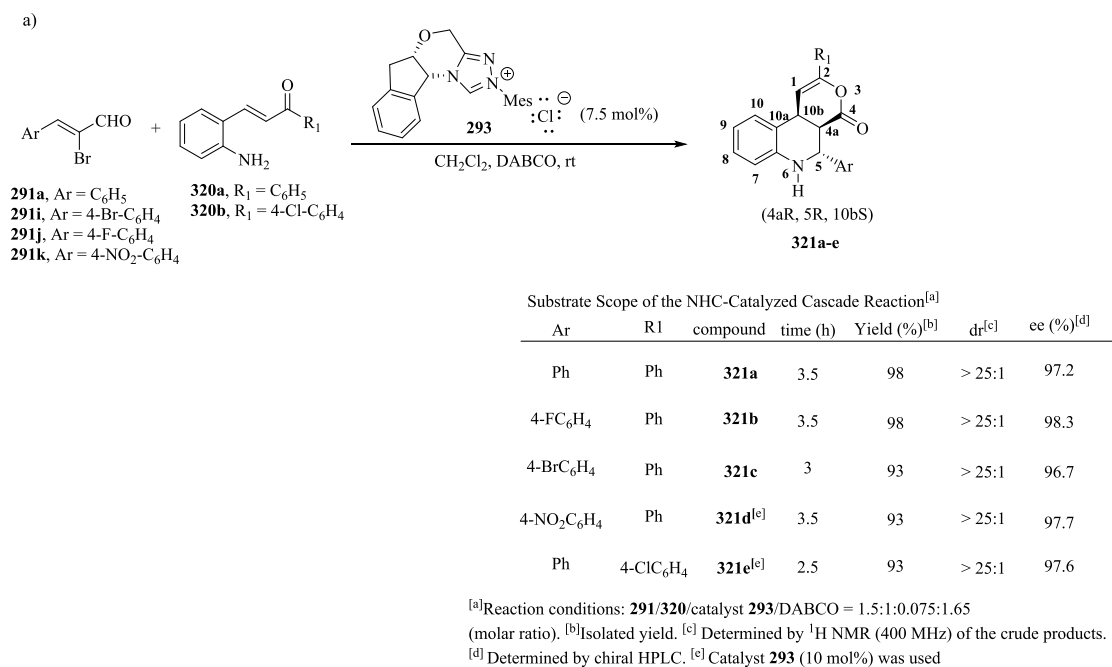
Zhang et al. (2013) (Zhang et al., 2013) reported the stereoselective aza-Michael-Michael-lactonization cascade synthesis for the construction of chiral functionalized tetrahydroquinolines **321a-e**, which contain three consecutive asymmetric centers, in high yields (up to 98%), with excellent diastereoselectivities (>25:1) and enantioselectivities (up to 98.3% ee) (Scheme 34a). The synthesis of these compounds involved the reaction between 2-bromoenal derivatives **291a** and **291i-k** and 2-aminophenylenones **320a-b** catalyzed by chiral Pre-NHC **293** (10 mol%). In the proposed mechanism (Scheme 34b), the Breslow intermediates **299** formed by the nucleophilic addition of NHC **296** to the carbonyl group of 2-bromoenal analogs **291a** and **291i-k** were transformed into compounds **300**, which undergo tautomerization and debromination, leading to the formation of compounds **301**. The aza-Michael addition of aminophenylenones **320a-b** to **301** provided the enolates **322**, which were later subjected to intramolecular Michael addition to provide compounds **323**. These latter substances were subjected to intramolecular lactonization, transforming into the desired products **321a-e** and regenerating the NHC catalyst. The spatial arrangement of atoms in chiral molecules (4aR, 5R, 10bS) was determined through the X-ray crystal analysis of compound **321b**.

#### 1.8.8. Enantioselective synthesis of functionalized cyclopentenes through NHC-catalyzed reaction

The NHC-catalyzed synthesis of functionalized cyclopentenes **325** generated from 2-bromo-enals **291a**, **291j** and **291 l-n** and malonic ester **324a-d** (Scheme 35a), which has a  $\gamma$ -aroyl group, proceeds via a Michael-intramolecular aldol- $\beta$ -lactonization-decarboxylation sequence to provide the cyclopentene derivatives **325a-g** in moderate to good yields (57–85% yield) and with high enantioselectivities (up to > 99%) (Scheme 35a) (Mondal et al., 2019). The addition of NHC to 2-bromo-enal derivatives **291a**, **291j** and **291 l-n**, followed by proton transfer, results in the formation of the corresponding Breslow intermediates



**Scheme 33.** a) NHC-catalyzed enantioselective addition of benzylic carbon to unsaturated acyl azolium; b) Proposed mechanism.

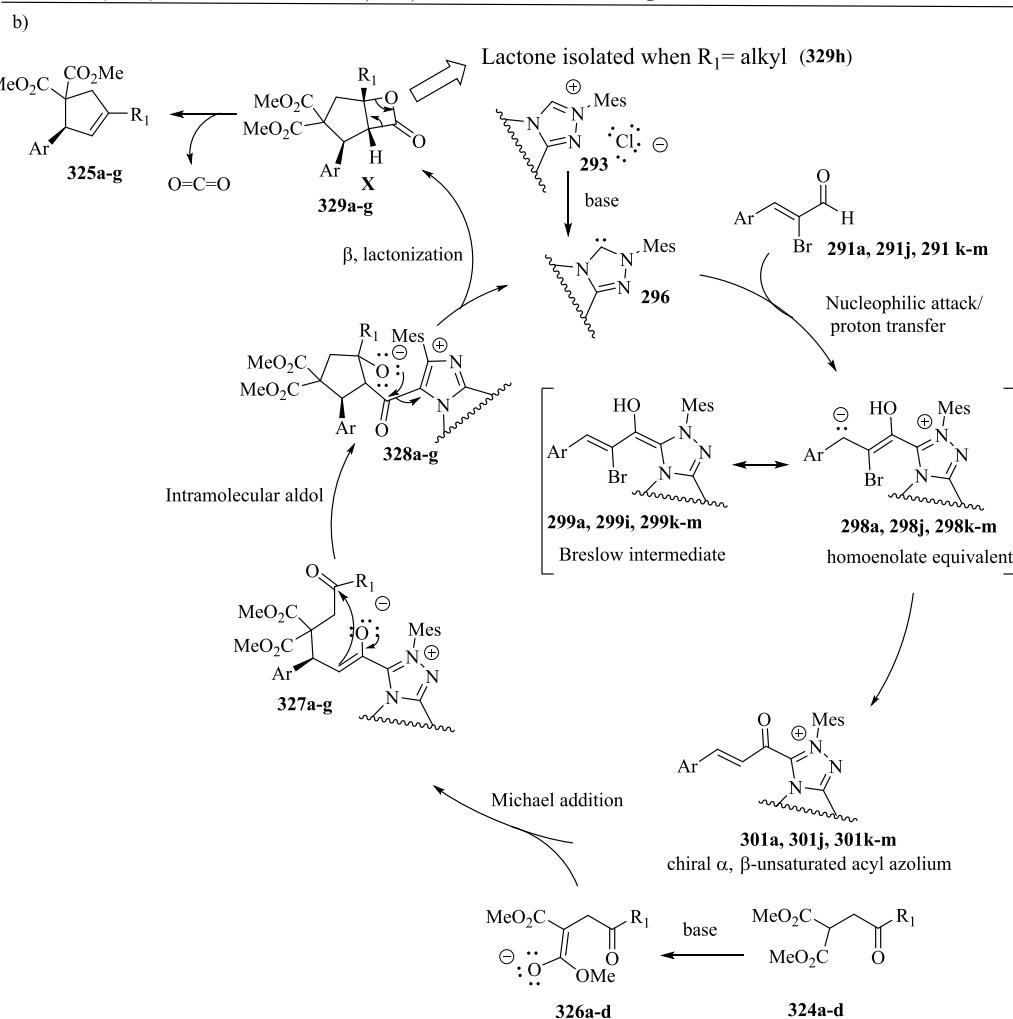
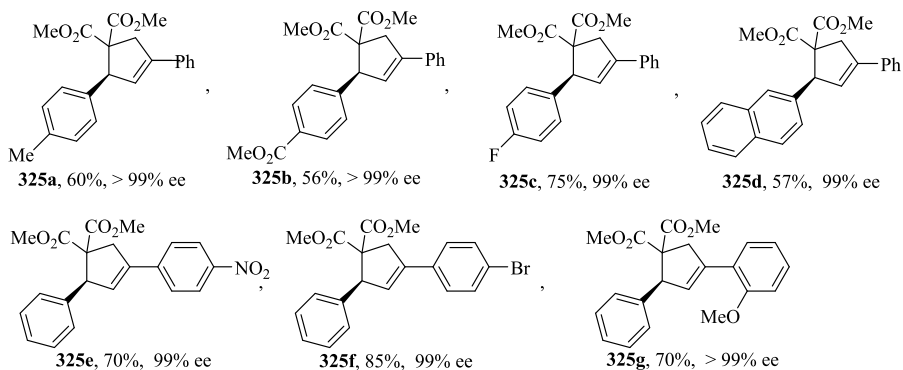
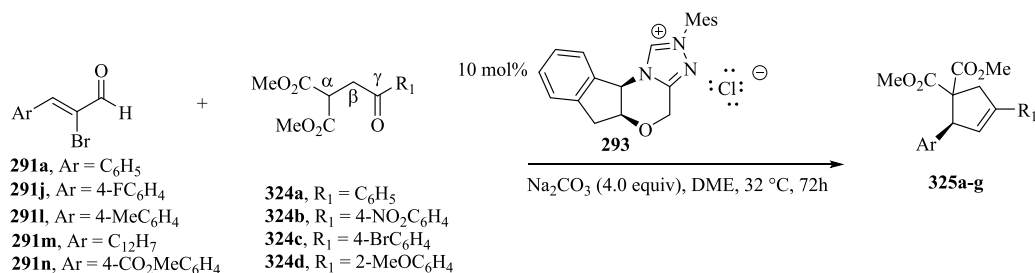


**Scheme 34.** a) Synthesis of tetrahydroquinolines through the aza-Michael-Michael-lactonization cascade reaction of 2'-aminophenylenones and 2-bromoaldehydes; b) Proposed mechanism.

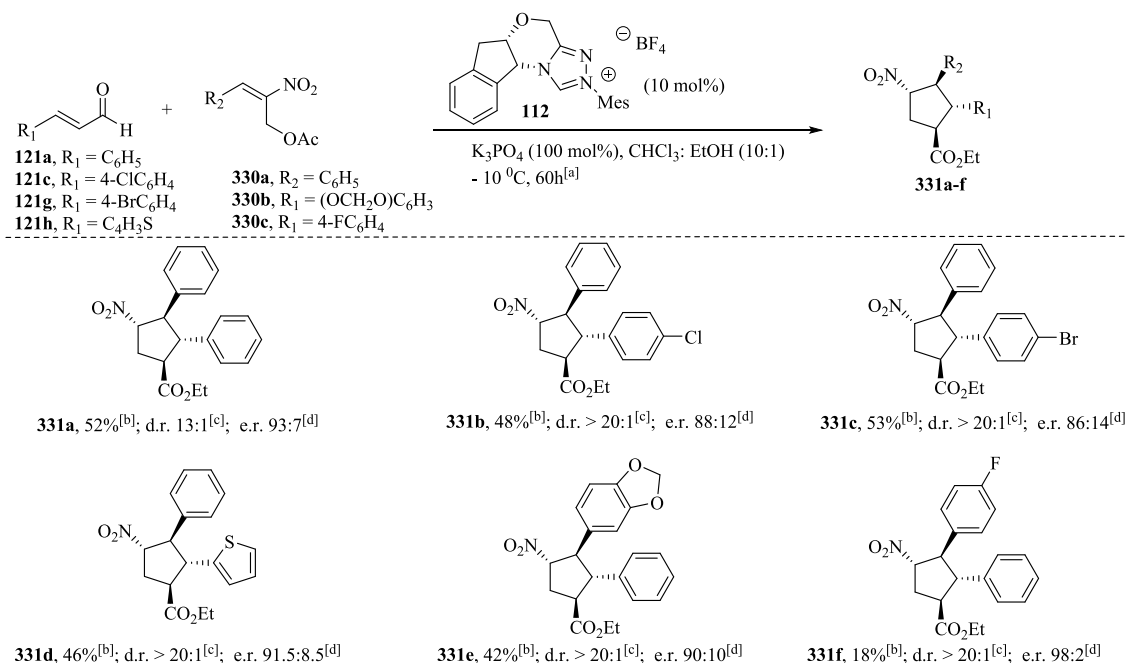
**299a**, **299j** and **299 l-n**, shown also as the mesomeric structures **298a**, **298j** and **298 l-n**, which then undergo debromination to generate the corresponding chiral  $\alpha,\beta$ -unsaturated acyl azoliums **301a**, **301j** and **301 l-n** (Flanigan et al., 2015; Mondal et al., 2019, 2014). The nucleophilic attack of 4-oxoenones **326a-d** to the species **301a**, **301j** and **301 l-n** leads to the formation of the enolate intermediates **327a-g**, which subsequently undergo a highly selective intramolecular aldol reaction, providing cyclopentenes **328a-g**. The  $\beta$ -lactonization reaction of

**328a-g**, followed by the elimination of the catalyst, delivers the expected cyclopentane-fused  $\beta$ -lactones **329a-g**. The decarboxylation reaction of these last compounds provides the desired cyclopentenes **325a-g** (Scheme 35b). In the same scheme, when this reaction was performed with malonate derivatives containing an alkyl group at the  $\gamma$ -position, it led to the formation of highly substituted  $\beta$ -lactone **329 h** (Flanigan et al., 2015; Mondal et al., 2019, 2014; Zhao et al., 2021).

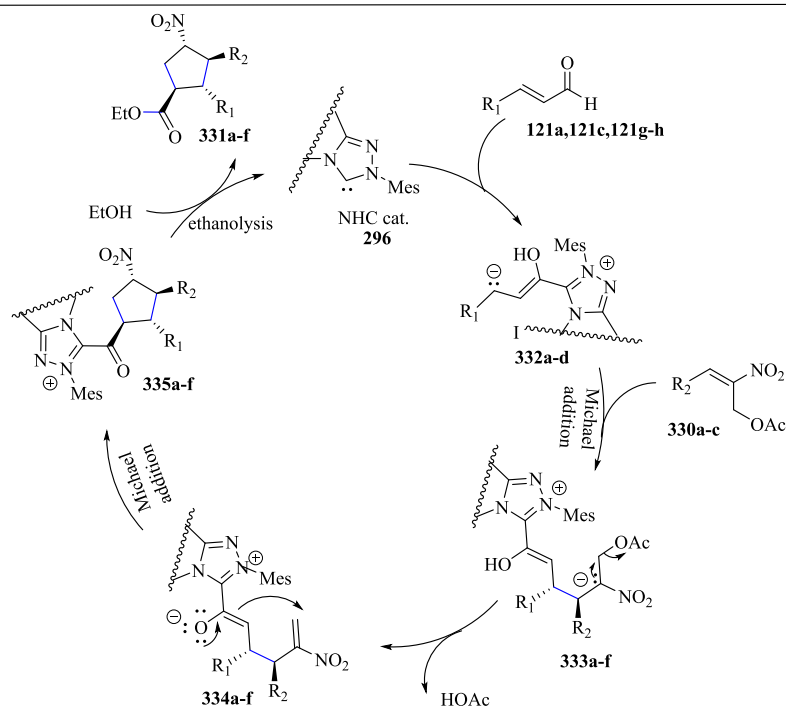
Scheme 36 shows the NHC-catalyzed Michael/Michael/esterification



Scheme 35. a) NHC-catalyzed enantioselective synthesis of cyclopentene derivatives; b) Proposed mechanism.



<sup>[a]</sup> Reaction conditions: **112** (0.3 mmol), **330** (0.2 mmol), Pre-NHC catalyst (10 mol%), base (1.0 equiv.), 24 h at rt. <sup>[b]</sup> Yield of isolated compound **331**. <sup>[c]</sup> d.r. determined by <sup>1</sup>H NMR. <sup>[d]</sup> The e.r. values were determined by HPLC on a chiral stationary phase.

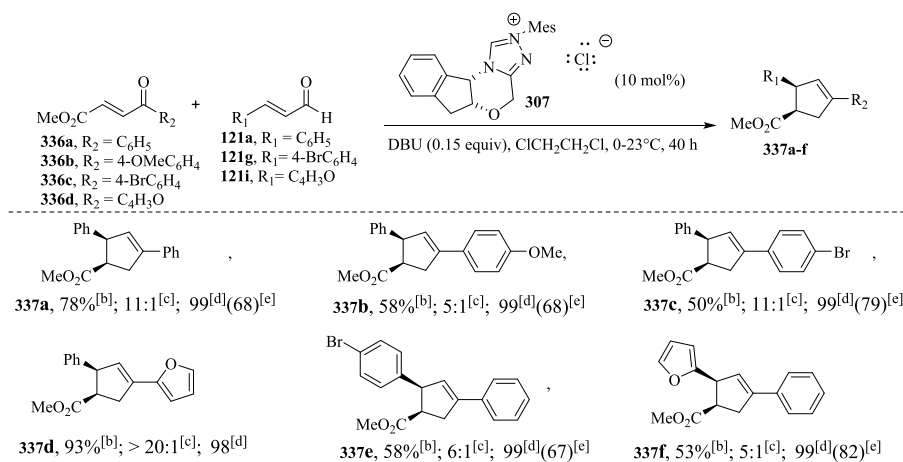


**Scheme 36.** a) Asymmetric synthesis of cyclopentanes through nhc-catalyzed Michael/Michael/esterification domino reaction; b) Proposed mechanism.

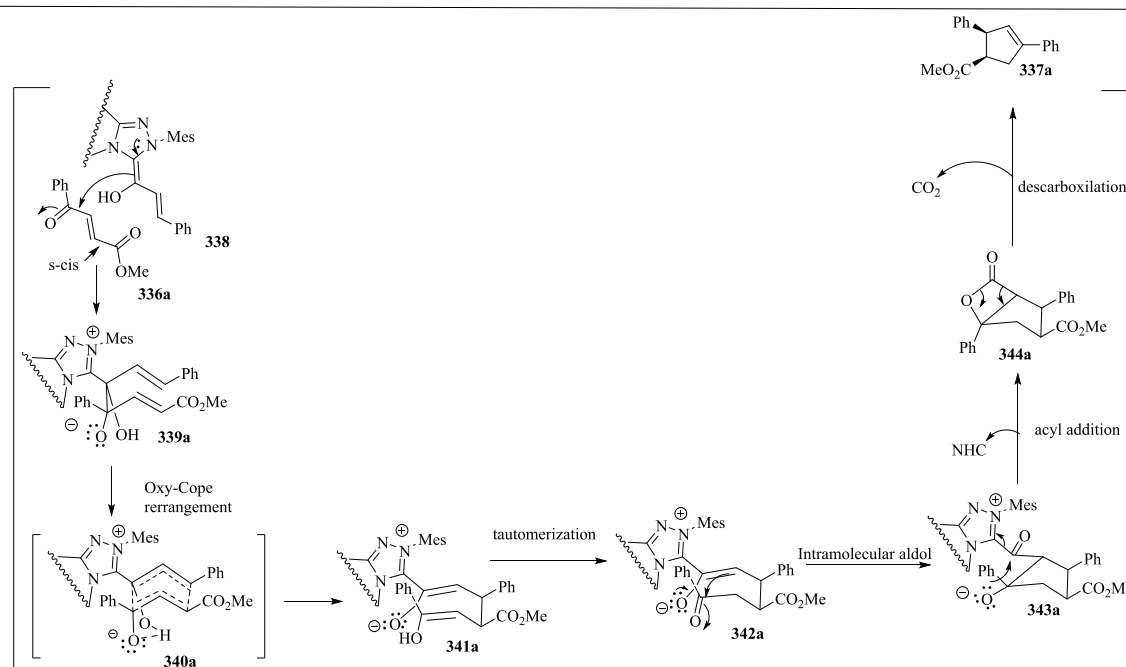
domino reaction for the construction of cyclopentanes **331a–f**, which have four contiguous stereocenters (Shu et al., 2016). The NHC-catalyzed reaction between a variety of  $\alpha$ ,  $\beta$ -unsaturated aldehydes **121a**, **121c**, **121 g–h** and 2-nitroallylic acetates **330a–c** produced cyclopentane derivatives **331a–f** in low to moderate yields (18–53 %) and with enantiomeric ratios from 86:14–98:2 (Scheme 36a). In the NHC-catalyzed [3 + 2] Michael/Michael/esterification cascade (Scheme 36b), the addition of carbanions **332a–d** to unsaturated compounds **329a–c**, which contain an electron-withdrawing group, followed by the elimination of the acetyl group from the intermediates **333a–f**, provided Michael acceptors **334a–f**. The Michael addition-ring closure reaction of

**334a–f**, followed by ethanolysis through nucleophilic acyl substitution on **335a–f**, converted these compounds into the corresponding cyclopentane derivatives **331a–f**.

Chiang et al. (2007) reported the synthesis of cyclopentene derivatives **337a–f** with good enantioselectivity for the *cis*-1,3,4-trisubstituted diastereomers via an NHC-catalyzed benzoin-oxy-Cope reaction of aldehydes **121a**, **121 g** and **121i** with ketones **336a–d** (Scheme 37a) (Chen et al., 2018a; Chiang et al., 2007; Jones et al., 2014). In the mechanism, 4-oxoenone **336a** adopts preferably an *s-cis* conformation in the conjugate addition of homoenolate **336a** to the enone providing the species **339a**, which undergoes oxy-Cope rearrangement through a



<sup>[a]</sup> Reactional condition: **336** (1 equiv), **121** (1.1 equiv), DBU (0.15 equiv), 5.0 mL, ClCH<sub>2</sub>CH<sub>2</sub>Cl, 0-23 °C, 40 h; <sup>[b]</sup> Isolated yield after chromatography; <sup>[c]</sup> Approximate ratio of *cis*:*trans* cyclopentene diastereomers determined by HPLC analyses; <sup>[d]</sup> % ee determined by HPLC analysis; <sup>[e]</sup> % ee of the minor diastereomer.



**Scheme 37.** a) Synthesis of cyclopentene derivatives via NHC-catalyzed benzoin-oxy-Cope reactions; b) Proposed mechanism.

boat transition state conformation that leads to the formation of the *cis*-stereochemistry observed in the cyclopentene product **337a-f** (Scheme 37b). The intermediate **341a** undergoes tautomerization and subsequent intramolecular aldol addition to generate alkoxide derivative **343a**. The intramolecular acylation of **343a**, followed by the elimination of the NHC catalyst, provides  $\beta$ -lactone **344a**. The [2 + 2] cycloreversion reaction of **344a** to form the desired product **337a** was carried out with the extrusion of CO<sub>2</sub>.

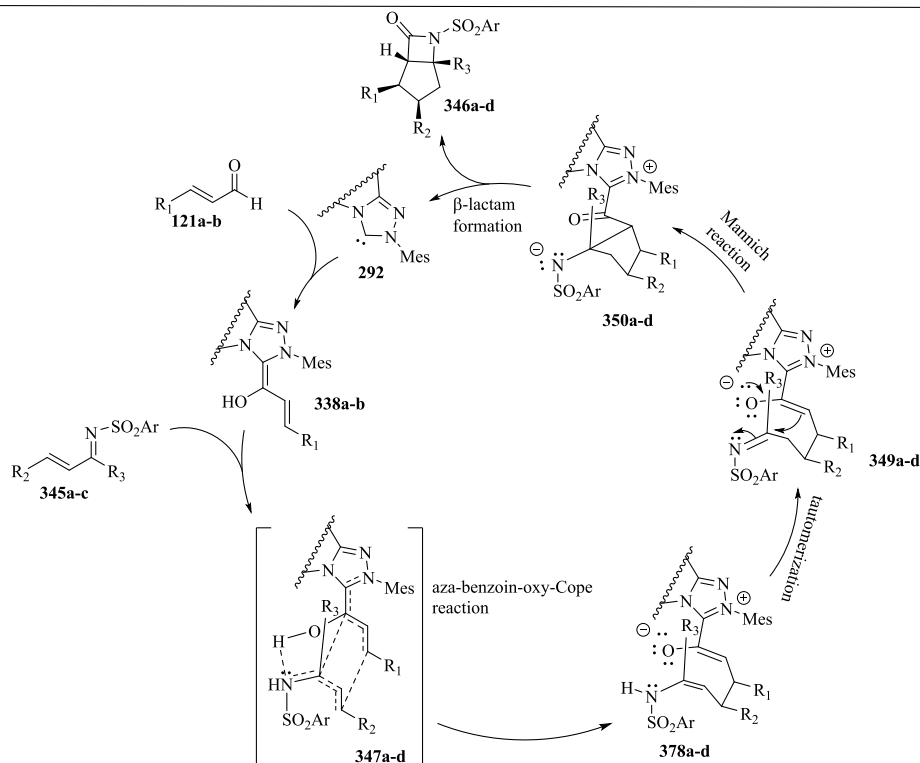
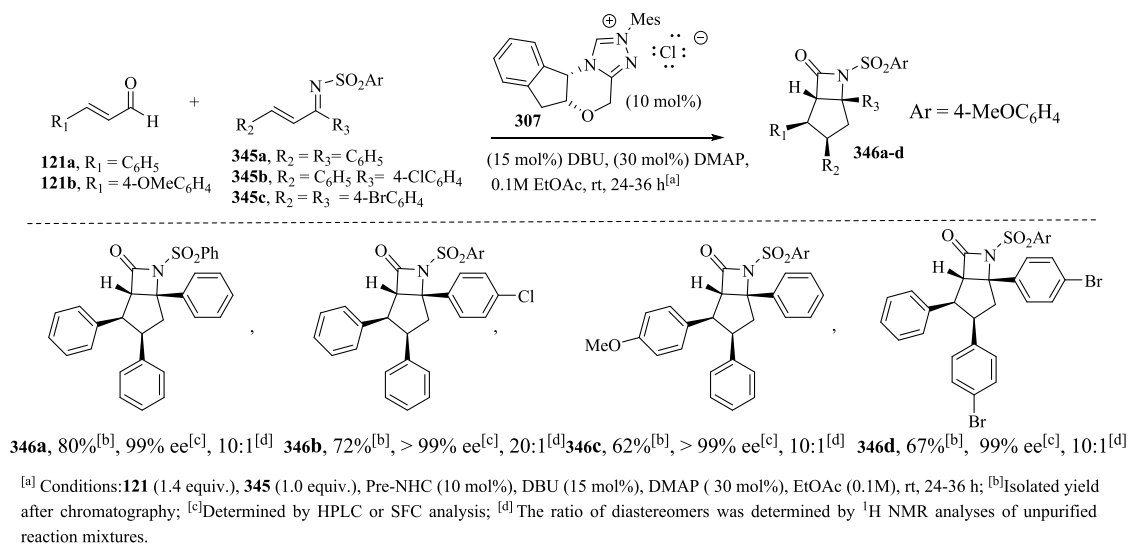
#### 1.8.9. Synthesis of cyclopentane-fused $\beta$ -lactams through NHC-catalyzed annulations of enals and unsaturated *N*-sulfonyl ketimines

He and Bode (2008) expanded NHC catalysis for the preparation of cyclopentane-fused  $\beta$ -lactams **346a-d** in good yields and with very good stereoselectivities from enals **121a-b** and unsaturated *N*-sulfonyl ketimines **345a-c** derived from chalcones (Scheme 38a) (He and Bode, 2008; Vora et al., 2012). These researchers suggest that the *cis*-relative configuration of the cyclopentane groups arises from the secondary orbital overlap considerations proceeding through a boat oxy-Cope transition state **347a-d** (Scheme 38b), followed by the

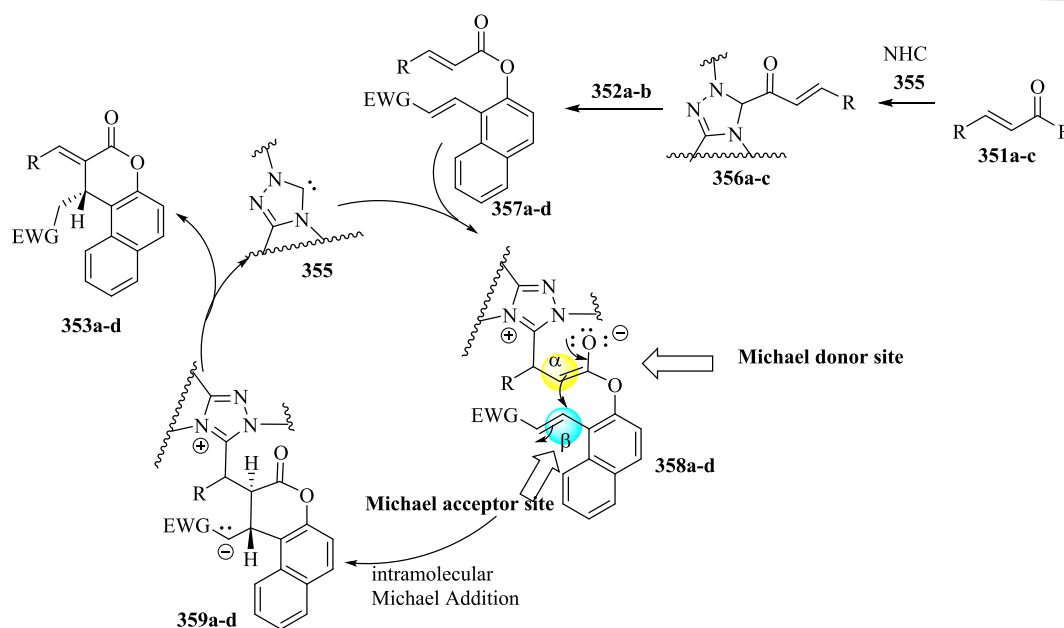
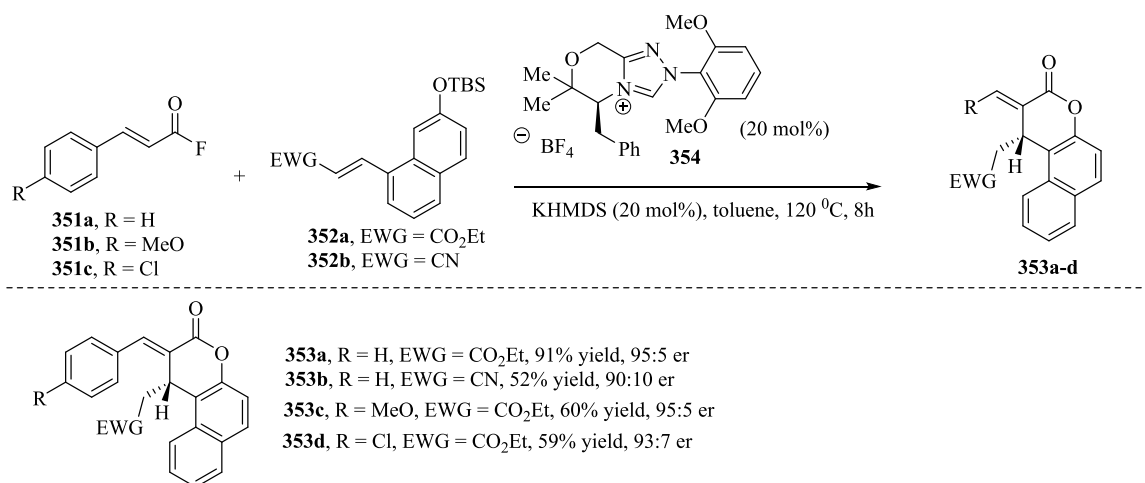
tautomerization reaction of **348a-d**. The remaining stereocenter is established via a reversible intramolecular Mannich reaction of the enolate and the azomethenic carbon–nitrogen double bond of sulfonylimine, whose adjacent C–C bond is freely rotated. Finally, the lactamization reaction of **350a-d** forms products **346a-d** and catalyst release occurs.

#### 1.8.10. NHC-catalyzed Rauhut-Currier reaction for the construction of naphthyl lactones

An example of NHC-promoted esterification/Rauhut-Currier (RC) reactions was explored by Bae et al. (2019) for the construction of naphthyl lactones (Bae et al., 2019; Dzieszowski et al., 2020). In Scheme 39a, the reaction of  $\alpha,\beta$ -unsaturated acid fluoride **351a-c** with NHC **355** produces anhydrous acyl azolium fluoride **356a-c**, which subsequently reacts with naphthol derivatives **352a-b** to provide *bis* (enoates) **357a-d**. In the process known as RC reaction, the *bis* (enoates) **357a-d** (Scheme 39b) participate as Michael donors after undergoing 1,2-addition with the NHC, providing the intermediate enolates **357a-d**, which undergo intramolecular Michael addition to provide lactones



**Scheme 38.** a) β-lactam synthesis through NHC catalysis; b) Proposed mechanism.



**Scheme 39.** a) Enantioselective NHC-catalyzed bis(enoate) Rauhut-Currier reaction; b) Plausible mechanism.

**359a-d**. In the RC method, also known as the vinylogous Morita-Baylis-Hillman reaction, the coupling of an active alkene / latent enolate (Michael donor) to a second Michael acceptor furnishes a new C-C bond between the  $\alpha$ -position of the activated alkene and the  $\beta$ -position of a second alkene under the influence of a nucleophilic catalyst. From intermediates **359a-d**, NHC diastereoselective elimination provides naphthyl lactones **252a-d** and returns the catalyst.

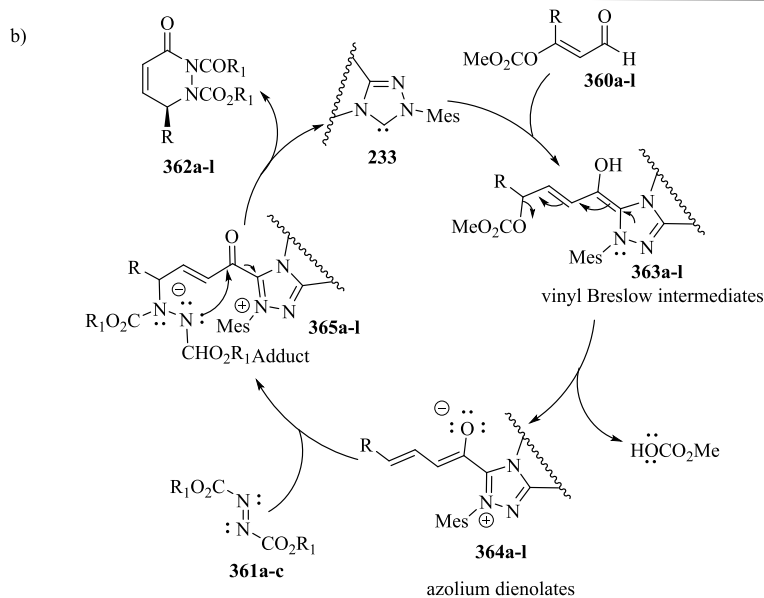
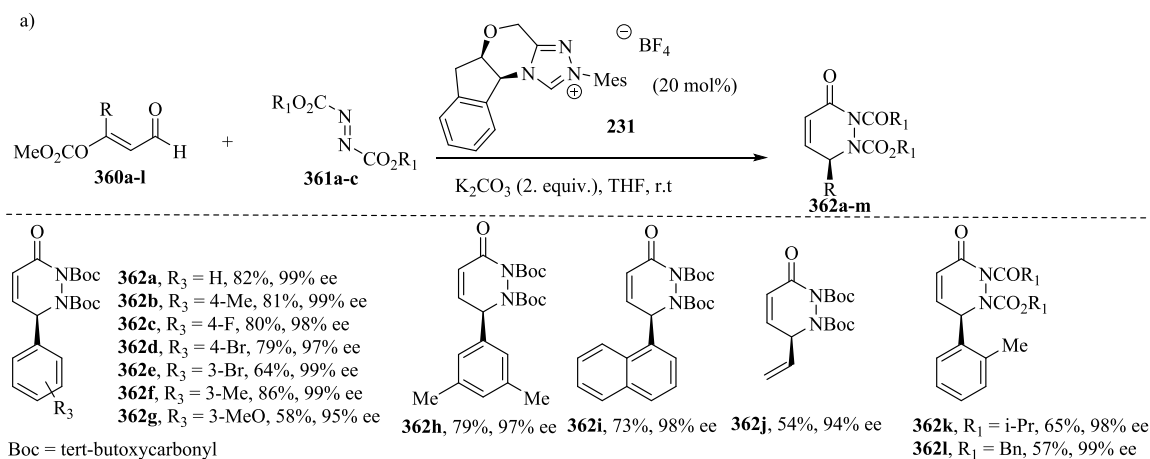
#### 1.8.11. NHC-catalyzed [4 + 2] cycloaddition of enals with azodicarboxylates

Chen et al. (2013) reported that azolium dienolates **364a-l** (Scheme 40b) could be synthesized by enals **360a-l**, which contain a leaving group (-OCO<sub>2</sub>Me) at the  $\gamma$ -position of their backbones (X. Y. Chen et al., 2013). In Scheme 29a, the NHC-catalyzed reaction between a variety of enals **360a-l** and azodicarboxylates **361a-c** provided dihydropyridazinone compounds **362a-l** with yields of 49–86 % and 94–99 % ee. In the proposed catalytic cycle, the addition of NHC catalyst **233** to enals **360a-l** leads to the formation of vinyl Breslow intermediates **363a-l**,

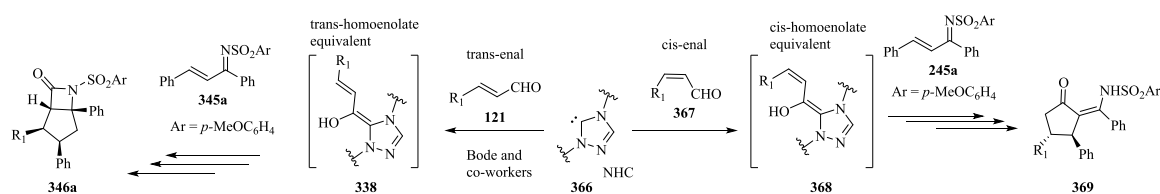
which subsequently undergo the elimination of the leaving group to provide the corresponding azolium dienolates **364a-l**. These latter compounds react with azodicarboxylates **361a-c** to provide acyl azolium intermediates **365a-l**, which undergo intramolecular cyclization to form the corresponding products **362a-l** and release the NHC catalyst (Scheme 40b).

#### 1.8.12. Synthesis of chiral cyclic ketones via NHC-catalyzed annulation of cis-homoenolate equivalents with unsaturated imines

Although the *cis*-enals are attractive raw materials for the development of catalytic reactions, their easy isomerization to the *trans* isomers under catalytic conditions often limits their use. Fortunately, the asymmetric reaction of  $\alpha$ ,  $\beta$ -unsaturated imines with *cis*-enals catalyzed by chiral NHCs in the presence of *N,N'*-diisopropylethylamine (DIEA) and benzene-1,2,3-triol acting as additives (Dirocco and Rovis, 2011) has been developed by Chen et al. (2013) (X. Chen et al., 2013a). The use of an additive and an NHC catalyst makes it possible to enhance the reaction performance in terms of both yield and stereoselectivity (Curti



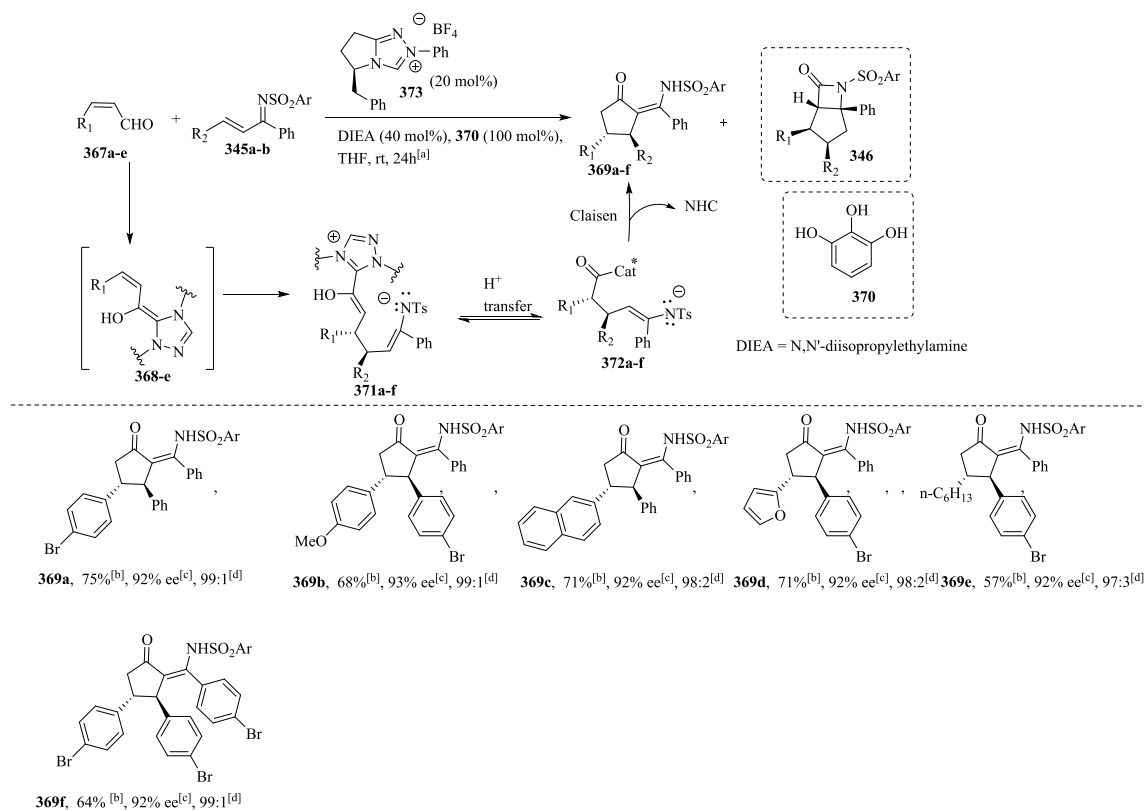
Scheme 40. a) NHC-catalyzed [4 + 2] cycloaddition reaction of enals with azodicarboxylates; b) Plausible mechanism.



Scheme 41. NHC-catalyzed reaction of a *trans*-enal and *cis*-enal with  $\alpha,\beta$ -unsaturated imine.

et al., 2020; Wang and Scheidt, 2016). Using this methodology, a variety of chiral cyclic ketones were obtained in good yields and with excellent enantioselectivities (Schemes 41 and 42). It should be emphasized that *trans*-enals (Schemes 40 and 41) and *cis*-enals (Schemes 41 and 42) show different stereoselectivities and reactivity patterns. The NHC-catalyzed reaction of *cis*-homoenolate intermediates from *cis*-enals with  $\beta$ -unsaturated imines preferentially leads to the formation of cyclic ketones **369**, whereas *trans*-homoenolate intermediates provide bicyclic  $\beta$ -lactam compounds **346**.

According to Chen et al. (2013) the reaction between *cis*- $\alpha, \beta$ -unsaturated aldehydes **367a–e** (Scheme 42) and unsaturated imines **345a–b** occurs via a concerted benzoin/Cope rearrangement process or a direct Michael addition pathway, resulting in the formation of intermediates **371a–f**, which subsequently undergo reversible proton transfer to produce the intermediate **372a–f**. The cyclic ketones **369a–f** were formed due to the intramolecular nucleophilic attack of the enamide carbon on the NHC-bound ester equivalent. Chen et al. (2013) report that the lactam derivative **346** can be detected under most



<sup>[a]</sup>Reaction conditions: **367** (0.2 mmol), **345** (0.1 mmol), rt, 12 h; <sup>[b]</sup>Isolated yield based on **345a**; <sup>[c]</sup>Enantiomeric excess of **369a**, determined via chiral-phase HPLC; absolute configuration was determined by X-ray of **369f**; <sup>[d]</sup>Ratio of ketone product **369** to lactam adduct **346**

**Scheme 42.** Synthesis of cyclic ketones via the NHC-catalyzed reaction of  $\alpha,\beta$ -unsaturated imines.

conditions using different Pre-NHCs. They also suggest that this product can be formed by the reaction of the imine **345** with *trans*-enal **121** generated from the isomerization of the corresponding *cis*-enal **367** (X. Chen et al., 2013a).

### 1.8.13. NHC-catalyzed diastereoselective annulations of isatin with $\beta,\beta$ -disubstituted enals

The stereoselective annulation of isatins **374a–e** with  $\beta,\beta$ -disubstituted enals **375a–c** through NHC/Brønsted acid dual catalysis leads to the formation of spirocyclic oxindoles **377a–g**, which have two highly congested contiguous quaternary carbon centers (Scheme 43a). The reaction is highly dependent on the Brønsted acid cocatalyst, which is considered crucial to ensuring excellent reactivity and high stereoselectivity (Flanigan et al., 2015; Li et al., 2014). The absolute configuration of the products has been determined through the X-ray crystallographic analysis of **377a**. In the mechanism proposed by Li et al. (2014) (Scheme 43b), the azolium enolate intermediates **378a–d** generated from the NHC, such as 1,2,4-triazolidin-3-ylidene **86** and enals **375a–d**, in the presence of an acid cocatalyst, preferentially react with isatin derivatives **374a–e** via a pre-transition state **379** favored by the presence of two stabilizing hydrogen bonds; one of these bonds decreases the electron density on the carbonyl carbon of isatin, making it more electron-deficient and facilitating the attack by the nucleophile. From the diastereoselective synthesis of intermediates **381a–g**, the intramolecular attack of the alkoxide on the carbonyl group occurs, leading to the formation of spirooxindoles **377a–g** and the regeneration of the catalyst **86** (Li et al., 2014).

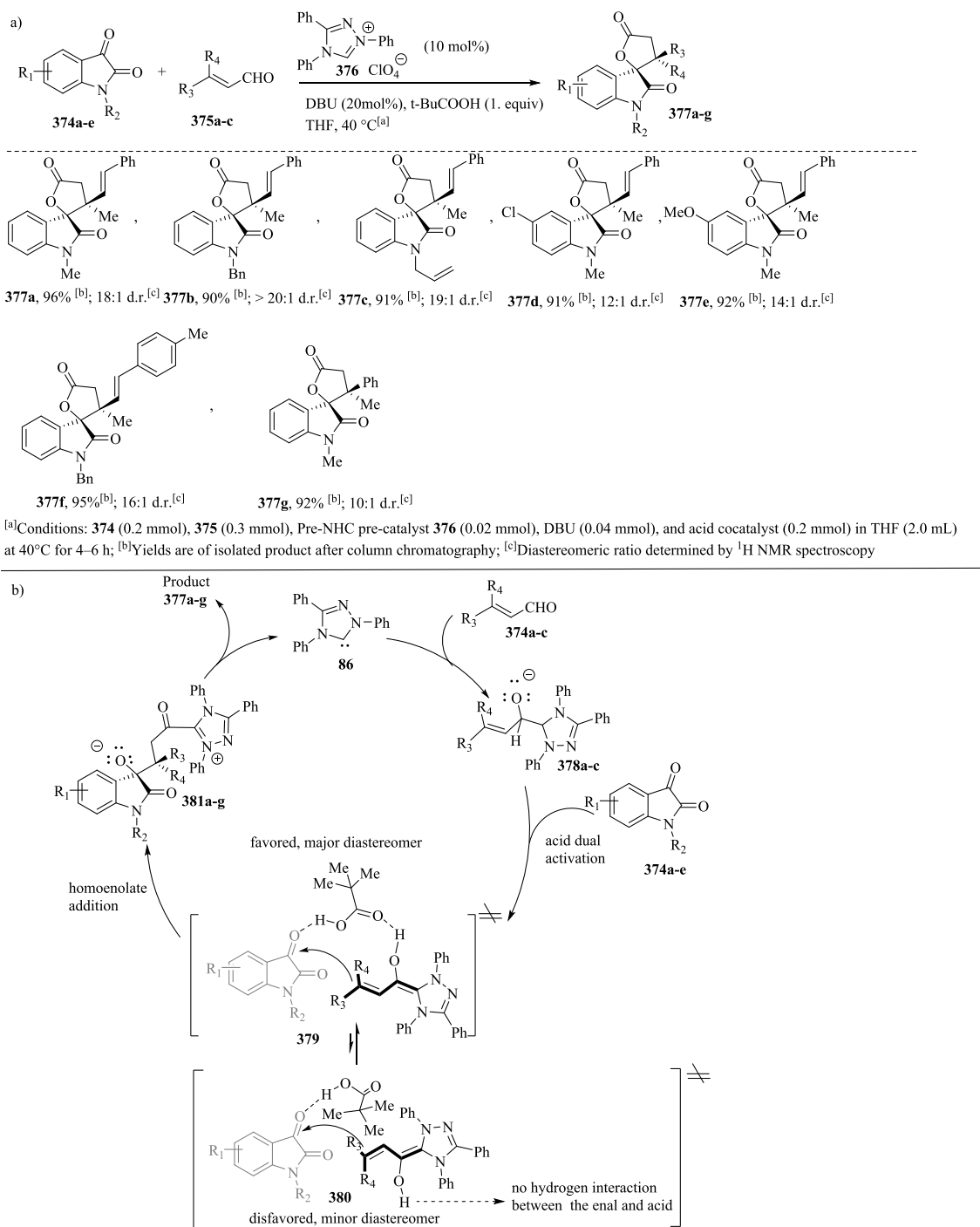
The central objective of this review is to document the NHC-catalyzed reactions, anchoring the discussion within the scope of experimental data. However, NHC-catalyzed transformation reactions have also been studied using theoretical methods based on density functional theory. Examples of theoretical studies involving reactions

catalyzed by NHC have been very well explored in the literature by Lan and Wei and other groups of researchers. (Alam, 2022; S. Li et al., 2019; Li et al., 2018b, 2018a; X. Li et al., 2019; Li et al., 2020; C. Liu et al., 2022; Liu et al., 2020; Yang Wang et al., 2016; Wang et al., 2017, 2019a, 2019c, 2019b, 2020a, 2020b, 2021, 2018a, 2018b; Yanyan Wang et al., 2016; Wei et al., 2011; Wu et al., 2020; Zhang et al., 2018, 2014; W. Zhang et al., 2016; X. Zhang et al., 2016).

## 2. Conclusion

N-Heterocyclic carbenes have multiple uses in many areas of organic and inorganic chemistry. Most NHC applications require coordination to transition metals, including applications in the areas of organometallic materials, coordination to surfaces, metallopharmaceuticals and homogenous catalysis. This review summarized the properties of NHC and metal-free triazolium carbene-catalyzed reactions involving the formation of C–C and C-heteroatom bonds with regioselectivity and stereoselectivity through umpolung and non-umpolung processes for unconventional access to various target molecules. The polarity inversion allows exploring new synthetic possibilities that cannot be realized from the normal reactivity of functional groups. NHC-catalyzed polarity reversal (umpolung) strategies have been explored in the generation of homoenolate, acyl anion and enolate equivalents, which are reactive species for a multitude of reactions, including annulation, benzoin, Stetter, Claisen rearrangement, cycloaddition and C–C bond functionalization reactions, among others. This review has provided examples of aerobic oxidative/oxygenative carbene catalysis, specifically highlighting NHC-catalyzed reactions involving oxygen and strategies employed for activation of oxygen in NHC-catalytic processes.

The future of NHCs looks highly promising, given the significant advances achieved thus far. In this sense, NHC chemistry can be used for the construction of molecules with great economic potential.



**Scheme 43.** a) NHC-catalyzed diastereoselective annulations of isatin **374a–e** with  $\beta,\beta$ -disubstituted enal **375a–c** for the synthesis of oxindoles **377a–g**; b) Proposed mechanism.

## Declaration of competing interest

The authors declare that they have no known competing financial interests or personal relationships that could have appeared to influence the work reported in this paper.

## Acknowledgments

This work was supported by the Brazilian agency FAPERJ. Fellowships granted to UFF, by CAPES, CNPq, CNPq-PIBIC and FAPERJ are gratefully acknowledged.

## References

- Alam, M.M., 2022. 1,2,3-Triazole hybrids as anticancer agents: A review. *Arch. Pharm. (Weinheim)* 355, 2100158. <https://doi.org/10.1002/ardp.202100158>.
- Alpers, T., Muesmann, T.W.T., Temme, O., Christoffers, J., 2018. Perfluorinated 1,2,3- and 1,2,4-Triazolium Ionic Liquids. *Eur. J. Org. Chem.* 2018, 4331–4337. <https://doi.org/10.1002/ejoc.201800582>.
- Ando, S., Otsuka, M., Ishizuka, T., 2020. Analyses of the Structural and Electronic Properties of NHCs with Bicyclic Architectures. *Organometallics* 39, 3839–3848. <https://doi.org/10.1021/acs.organomet.0c00564>.
- Arduengo, A.J., Harlow, R.L., Kline, M., 1991. A stable crystalline carbene. *J. Am. Chem. Soc.* 113, 361. <https://doi.org/10.1021/ja00001a054>.
- A. Axelsson, E. Hammarvid, L.T., H. Sundén, 2016. Asymmetric aerobic oxidative NHC-catalysed synthesis of dihydropyranones utilising a system of electron transfer mediators. *Chem. Commun.* 52, 11571–11574. <https://doi.org/10.1039/c6cc06060a>.
- Bae, S., Zhang, C., Gillard, R.M., Lupton, D.W., 2019. Enantioselective N-heterocyclic carbene catalyzed bis(enoate) Rauhut-Currier reaction. *Angew. Chem. Int. Ed.* 58, 13370–13374. <https://doi.org/10.1002/anie.201907111>.
- Benhamou, L., Chardon, E., Lavigne, G., Bellemín-Laponnaz, S., César, V., 2011. Synthetic routes to N-heterocyclic carbene precursors. *Chem. Rev.* 111, 2705–2733. <https://doi.org/10.1021/cr100328e>.
- Bhatia, R., Gaur, J., Jain, S., Lal, A., Tripathi, B., Attri, P., Kaushik, N., 2013. Synthetic strategies for free & stable N-heterocyclic carbenes and their precursors. *Mini. Rev. Org. Chem.* 10, 180–197. <https://doi.org/10.2174/1570193x11310020007>.
- Biju, A.T., Kuhl, N., Glorius, F., 2011. Extending NHC-catalysis: Coupling aldehydes with unconventional reaction partners. *Acc. Chem. Res.* 44, 1182–1195. <https://doi.org/10.1021/ar2000716>.
- Biswas, A., Neudörfl, J., Schlörer, N.E., Berkessel, A., 2021. Acyl donor intermediates in N-heterocyclic carbene catalysis: Acyl azolium or azolium enolate? *Angew. Chem.* 133, 4557–4561. <https://doi.org/10.1002/ange.202010348>.
- Bortolini, O., Chiappe, C., Fogagnolo, M., Giovannini, P.P., Massi, A., Pomelli, C.S., Ragnoa, D., 2014. An insight into the mechanism of the aerobic oxidation of aldehydes catalyzed by N-heterocyclic carbenes. *Chem. Commun.* 50, 2008–2011. <https://doi.org/10.1039/c3cc48929a>.
- Bortolini, O., Chiappe, C., Fogagnolo, M., Massi, A., Pomelli, C.S., 2017. Formation, oxidation, and fate of the Breslow intermediate in the N-heterocyclic carbene-catalyzed aerobic oxidation of aldehydes. *J. Org. Chem.* 82, 302–312. <https://doi.org/10.1021/acs.joc.6b02414>.
- Bugaut, X., Glorius, F., 2012. Organocatalytic umpolung: N-heterocyclic carbenes and beyond. *Chem. Soc. Rev.* 41, 3511–3522. <https://doi.org/10.1039/c2cs15333e>.
- Cavallo, L., Cazin, C.S.J., 2010. N-Heterocyclic carbenes: An introductory overview. In: Cazin, C.S.J. (Ed.), *N-Heterocyclic Carbenes in Transition Metal Catalysis and Organocatalysis*. Springer, Dordrecht, Dordrecht, pp. 1–22. <https://doi.org/10.1007/978-90-481-2866-2>.
- J. Chen, Y. Huang, 2019. N-heterocyclic carbenes as brønsted base catalysts, in: Biju, A.T. (Ed.), *N-Heterocyclic Carbenes in Organocatalysis*. Wiley-VCH, Weinheim, pp. 261–286. <https://doi.org/10.1002/9783527809042.ch9>.
- Chen, X., Fang, X., Chi, Y.R., 2013a. cis-Enals in N-heterocyclic carbene-catalyzed reactions: distinct stereoselectivity and reactivity. *Chem. Sci.* 4, 2613–2618. <https://doi.org/10.1039/c3sc50666e>.
- Chen, X.Y., Li, S., Vetica, F., Kumar, M., Enders, D., 2018a. N-heterocyclic-carbene-catalyzed domino reactions via two or more activation modes. *iScience* 2, 1–26. <https://doi.org/10.1016/j.isci.2018.03.006>.
- Chen, X.Y., Liu, Q., Chauhan, P., Enders, D., 2018b. N-heterocyclic carbene catalysis via azolium dienolates: An efficient strategy for remote enantioselective functionalizations. *Angew. Chem. - Int. Ed.* 57, 3862–3873. <https://doi.org/10.1002/anie.201709684>.
- Chen, X., Yang, S., Song, B., Chi, Y.R., 2013b. Functionalization of benzylic C(sp<sup>3</sup>) - H bonds of heteroaryl aldehydes through N-heterocyclic carbene organocatalysis. *Angew. Chem. Int. Ed.* 52, 11134–11137. <https://doi.org/10.1002/anie.201305861>.
- Chen, X., Wang, H., Jin, Z., Chi, Y.R., 2020. N-Heterocyclic Carbene Organocatalysis: Activation Modes and Typical Reactive Intermediates. *Chin. J. Chem* 38, 1167–1202. <https://doi.org/10.1002/cjoc.202000107>.
- Chen, X.Y., Xia, F., Cheng, J.T., Ye, S., 2013. Highly enantioselective  $\gamma$ -amination by N-heterocyclic carbene catalyzed [4+2] annulation of oxidized enals and azodicarboxylates. *Angew. Chem. Int. Ed.* 52, 10644–10647. <https://doi.org/10.1002/anie.201305571>.
- Chiang, P., Kaeobamrung, J., Bode, J.W., 2007. Enantioselective, cyclopentene-forming annulations via NHC-catalyzed benzoin-oxy-cope reactions. *J. Am. Chem. Soc.* 129, 3520–3521. <https://doi.org/10.1021/ja0705543>.
- Curti, C., Battistini, L., Sartori, A., Zanardi, F., 2020. New developments of the principle of vinylogy as applied to  $\pi$ -extended enolate-type donor systems. *Chem. Rev.* 120, 2448–2612. <https://doi.org/10.1021/acs.chemrev.9b00481>.
- Dai, L., Ye, S., 2021. Recent advances in N-heterocyclic carbene-catalyzed radical reactions. *Chinese Chem. Lett.* 32, 660–667. <https://doi.org/10.1016/j.ccl.2020.08.027>.
- De Risi, C., Brandolese, A., Di Carmine, G., Ragno, D., Massi, A., Bortolini, O., 2023. Oxidative N-heterocyclic carbene catalysis. *Chem. - Eur. J.* 29, e202202467.
- Delany, E.G., Fagan, C.L., Gundala, S., Mari, A., Broja, T., Zeitler, K., Connon, S.J., 2013. NHC-catalysed aerobic aldehyde-esterifications with alcohols: No additives or cocatalysts required. *Chem. Commun.* 49, 6510–6512. <https://doi.org/10.1039/c3cc42596g>.
- Di Carmine, G., Ragno, D., Massi, A., D'agostino, C., 2020. Oxidative coupling of aldehydes with alcohol for the synthesis of esters promoted by polystyrene-supported N-heterocyclic carbene: Unraveling the solvent effect on the catalyst behavior using NMR relaxation. *Org. Lett.* 22, 4927–4931. <https://doi.org/10.1021/acs.orglett.0c01188>.
- Dirocco, D.A., Rovis, T., 2011. Catalytic asymmetric intermolecular stetter reaction of enals bifunctional additives. *J. Am. Chem. Soc.* 133, 10402–10405. <https://doi.org/10.1021/ja203810b>.
- Dong, Z., Pezzato, C., Sienkiewicz, A., Scopelliti, R., Fadaei-Tirani, F., Severin, K., 2020. SET processes in Lewis acid-base reactions: The tritylation of N-heterocyclic carbenes. *Chem. Sci.* 11, 7615–7618. <https://doi.org/10.1039/d0sc01278e>.
- Dong, Z., Jiang, C., Zhao, C., 2022. A review on generation and reactivity of the N-heterocyclic carbene-bound alkynyl acyl azolium intermediates. *Molecules* 27, 7990. <https://doi.org/10.3390/molecules27227990>.
- Dröge, T., Glorius, F., 2010. The measure of all rings — N-heterocyclic carbenes. *Angew. Chem. Int. Ed.* 49, 6940–6952. <https://doi.org/10.1002/anie.201001865>.
- Dudding, T., Houk, K.N., 2004. Computational predictions of stereochemistry in asymmetric thiazolium- and triazolium-catalyzed benzoin condensations. *Proc. Natl. Acad. Sci. U. S. A.* 101, 5770–5775. <https://doi.org/10.1073/pnas.0307256101>.
- Dzieszkowski, K., Baranska, I., Mroczynska, K., Stotwinski, M., Rafinski, Z., 2020. Organocatalytic name reactions enabled by NHCs. *Materials (Basel)* 13, 3574. <https://doi.org/10.3390/MA13163574>.
- Enders, D., Grossmann, A., Fronert, J., Raabe, G., 2010. N-heterocyclic carbene catalysed asymmetric cross-benzoin reactions of heteroaromatic aldehydes with trifluoromethyl ketones. *Chem. Commun.* 46, 6282–6284. <https://doi.org/10.1039/c0cc02013c>.
- Enders, D., Kallfass, U., 2002. An efficient nucleophilic carbene catalyst for the asymmetric benzoin condensation. *Angew. Chem. Int. Ed.* 41, 1743–1745. [https://doi.org/10.1002/1521-3773\(20020517\)41:10<1743::AID-ANIE1743>3.0.CO;2-Q](https://doi.org/10.1002/1521-3773(20020517)41:10<1743::AID-ANIE1743>3.0.CO;2-Q).
- Falivene, L., Cavallo, L., 2017. Theoretical NMR spectroscopy of N-heterocyclic carbenes and their metal complexes. *Coord. Chem. Rev.* 344, 101–114. <https://doi.org/10.1016/j.ccr.2016.12.015>.
- Feroci, M., Chiarotto, I., D'Anna, F., Gala, F., Noto, R., Ornano, L., Zollo, G., Inesi, A., 2016a. N-heterocyclic carbenes and parent cations: Acidity, nucleophilicity, stability, and hydrogen bonding—Electrochemical study and ab initio calculations. *ChemElectroChem* 3, 1133. <https://doi.org/10.1002/celec.201600187>.
- Feroci, M., Chiarotto, I., Inesi, A., 2016b. Advances in the knowledge of N-heterocyclic carbenes properties. The backing of the electrochemical investigation. *Catalysts* 6, 178. <https://doi.org/10.3390/catal6110178>.
- Fèvre, M., Pinaud, J., Gnanou, Y., Vignolle, J., Taton, D., 2013. N-heterocyclic carbenes (NHCs) as organocatalysts and structural components in metal-free polymer synthesis. *Chem. Soc. Rev.* 42, 2142–2172. <https://doi.org/10.1039/c2cs35383k>.
- Finney, E.E., Ogawa, K.A., Boydston, A.J., 2012. Organocatalyzed anodic oxidation of aldehydes. *J. Am. Chem. Soc.* 134, 12374–12377. <https://doi.org/10.1021/ja304716r>.
- Flanigan, D.M., Romanov-michailidis, F., White, N.A., Rovis, T., 2015. Organocatalytic reactions enabled by N-heterocyclic carbenes. *Chem. Rev.* 115, 9307–9387. <https://doi.org/10.1021/acs.chemrev.5b00060>.
- Ghosh, A., Patra, A., Mukherjee, S., Biju, A.T., 2019. Synthesis of 2-aryl naphthoquinones by the cross-dehydrogenative coupling involving an NHC-catalyzed endo-Stetter reaction. *J. Org. Chem.* 84, 1103–1110. <https://doi.org/10.1021/acs.joc.8b02931>.
- Gilmore, K., Alabugin, I.V., 2011. Cyclizations of alkynes: Revisiting Baldwin's rules for ring closure. *Chem. Rev.* 111, 6513–6556. <https://doi.org/10.1021/cr200164y>.
- Gómez-Suárez, A., Nelson, D.J., Nolan, S.P., 2017. Quantifying and understanding the steric properties of N-heterocyclic carbenes. *Chem. Commun.* 53, 2650–2660. <https://doi.org/10.1039/c7cc00255f>.
- Green, R.A., Pletcher, D., Leach, S.G., Brown, R.C.D., 2015. N-heterocyclic carbene-mediated oxidative electrocatalysis of esters in a microflow cell. *Org. Lett.* 17, 3290–3293. <https://doi.org/10.1021/acs.orglett.5b01459>.
- Grieco, G., Blacque, O., Berke, H., 2015. A facile synthetic route to benzimidazolium salts bearing bulky aromatic N-substituents. *Beilstein J. Org. Chem.* 11, 1656–1666. <https://doi.org/10.3762/bjoc.11.182>.
- V.B. Gudimetla, B.P. Joy, S. Paul, 2022. Imidazolium-Based N-Heterocyclic Carbenes (NHCs) and Metal-Mediated Catalysis, in: Satyen Saha, Arunava Manna (Eds.), *Carbene*. IntechOpen. <https://doi.org/10.5772/INTECHOPEN.102561>.
- Guin, J., De Sarkar, S., Grimme, S., Studer, A., 2008. Biomimetic carbene-catalyzed oxidations of aldehydes using TEMPO. *Angew. Chem. - Int. Ed.* 47, 8727–8730. <https://doi.org/10.1002/anie.200802735>.
- Harnying, W., Sudkaow, P., Biswas, A., Berkessel, A., 2021. N-heterocyclic carbene/carboxylic acid co-catalysis enables oxidative esterification of demanding

- aldehydes/enals, at low catalyst loading. *Angew. Chem. - Int. Ed.* 60, 19631–19636. <https://doi.org/10.1002/anie.202104712>.
- Hawkes, K.J., Yates, B.F., 2008. The mechanism of the Stetter reaction - A DFT study. *Eur. J. Org. Chem.* 5563–5570. <https://doi.org/10.1002/ejoc.200800506>.
- He, M., Bode, J.W., 2008. Enantioselective, NHC-catalyzed bicyclo-lactam formation via direct annulations of enals and unsaturated N-sulfonyl ketimines. *J. Am. Chem. Soc.* 130, 418–419. <https://doi.org/10.1021/ja0778592>.
- He, Y., Xue, Y., 2011. Theoretical investigations on the mechanism of benzoin condensation catalyzed by pyrido[1,2-a]-[1,2,4]triazolo-3-ylidene. *J. Phys. Chem. A* 115, 1408–1417. <https://doi.org/10.1021/jp110352e>.
- Heravi, M.M., Zadsirjan, V., Kafshardzadeh, K., Amiri, Z., 2020. Recent advances in Stetter reaction and related chemistry: An update. *Asian J. Org. Chem.* 9, 1999–2034. <https://doi.org/10.1002/ajoc.202000378>.
- Higgins, E.M., Sherwood, J.A., Lindsay, A.G., Armstrong, J., Massey, R.S., Alder, W., Donoghue, A.C.O., 2011. *pK<sub>a</sub>*s of the conjugate acids of N-heterocyclic carbenes in water. *Chem. Commun.* 47, 1559–1561. <https://doi.org/10.1039/c0cc03367g>.
- Hopkinson, M.N., Richter, C., Schedler, M., Glorius, F., 2014. An overview of N-heterocyclic carbenes. *Nature* 510, 485. <https://doi.org/10.1038/nature13384>.
- Huang, G.T., Hsieh, M.H., Yu, J.S.K., 2022. Formation of Breslow intermediates under aprotic conditions: A computational study. *J. Org. Chem.* 87, 2501–2507. <https://doi.org/10.1021/acs.joc.1c02408>.
- Hutchinson, S.M., Ardónardón-Muñ Oz, L.G., Ratliff, M.L., Bolliger, J.L., 2019. Catalytic preparation of 1-aryl-substituted 1,2,4-triazolium salts. *ACS Omega* 18, 17923. <https://doi.org/10.1021/acsomega.9b03109>.
- Huynh, H.V., 2018. Electronic properties of N-heterocyclic carbenes and their experimental determination. *Chem. Rev.* 118, 9457. <https://doi.org/10.1021/acs.chemrev.8b00067>.
- Ishii, T., Kakeno, Y., Nagao, K., Ohmiya, H., 2019a. N-heterocyclic carbene-catalyzed decarboxylative alkylation of aldehydes. *J. Am. Chem. Soc.* 141, 3854–3858. <https://doi.org/10.1021/jacs.9b00880>.
- Ishii, T., Ota, K., Nagao, K., Ohmiya, H., 2019b. N-heterocyclic carbene-catalyzed radical relay enabling vicinal alkylation of alkenes. *J. Am. Chem. Soc.* 141, 14073–14077. <https://doi.org/10.1021/jacs.9b07194>.
- Ishii, T., Nagao, K., Ohmiya, H., 2020. Recent advances in N-heterocyclic carbene-based radical catalysis. *Chem. Sci.* 11, 5630–5636. <https://doi.org/10.1039/d0sc01538e>.
- M.C. Jahnke, F.E. Hahn, 2017. Introduction to N-Heterocyclic Carbenes: Synthesis and Stereoelectronic Parameters, in: *Laboratory Curiosities to Efficient Synthetic Tools*. The Royal Society of Chemistry, Münster, pp. 1–45. <https://doi.org/10.1039/9781782626817-00001>.
- Janssen-muller, D., Singha, S., Olyschlager, T., Daniliuc, C.G., Glorius, F., 2016. Annulation of o-quinodimethanes through N-heterocyclic carbene catalysis for the synthesis of 1-isochromanones. *Org. Lett.* 18, 4444–4447. <https://doi.org/10.1021/acs.orglett.6b02335>.
- Jones, A.C., May, J.A., Sarpong, R., Stoltz, B.M., 2014. Toward a symphony of reactivity: Cascades involving catalysis and sigmatropic rearrangements angewandte. *Angew. Chem. Int. Ed.* 53, 2556–2591. <https://doi.org/10.1002/anie.201302572>.
- Jousseume, T., Wurz, N.E., Glorius, F., 2011. Highly enantioselective synthesis of  $\alpha$ -amino acid derivatives by an NHC-catalyzed intermolecular stetter reaction. *Angew. Chem. - Int. Ed.* 50, 1410–1414. <https://doi.org/10.1002/anie.201006548>.
- Kaeobamrung, J., Mahatthanachai, J., Zheng, P., Bode, J.W., 2010. An enantioselective claisen rearrangement catalyzed by N-heterocyclic carbenes. *J. Am. Chem. Soc.* 132, 8810–8812. <https://doi.org/10.1021/ja103631u>.
- Kohsaka, Y., Mori, I., Homma, K., Akai, Y., Matsuura, D., Kimura, Y., 2021. Synthesis of polyarylates and aliphatic polyesters by divalent acyl-1,2,4-triazole: a route to metal-free synthesis at low temperature. *Polym. J.* 53, 887–893. <https://doi.org/10.1038/s41428-021-00484-0>.
- Konstandaras, N., Dunn, M.H., Guerry, M.S., Barnett, C.D., Cole, M.L., Harper, J.B., 2020. The impact of cation structure upon the acidity of triazolium salts in dimethyl sulfoxide. *Org. Biomol. Chem.* 18, 66–75. <https://doi.org/10.1039/c9ob02258a>.
- Lai, C.L., Lee, H.M., Hu, C.H., 2005. Theoretical study on the mechanism of N-heterocyclic carbene catalyzed transesterification reactions. *Tetrahedron Lett.* 46, 6265–6270. <https://doi.org/10.1016/j.tetlet.2005.07.046>.
- Levens, A., An, F., Breugst, M., Mayr, H., Lupton, D.W., 2016. In fl uence of the N-substituents on the nucleophilicity and Lewis basicity of N-heterocyclic carbenes. *Org. Lett.* 18, 3566–3569. <https://doi.org/10.1021/acs.orglett.6b01525>.
- Li, Z., Li, X., Cheng, J., 2017. An acidity scale of triazolium-based NHC precursors in DMSO. *J. Org. Chem.* 82, 9675–9681. <https://doi.org/10.1021/acs.joc.7b01755>.
- Li, X., Li, S.J., Wang, Y., Wang, Y., Qu, L.B., Li, Z., Wei, D., 2019. Insights into NHC-catalyzed oxidative  $\alpha$ -C(sp<sup>3</sup>)-H activation of aliphatic aldehydes and cascade [2 + 3] cycloaddition with azomethine imines. *Catal. Sci. Technol.* 9, 2514–2522. <https://doi.org/10.1039/c9cy00526a>.
- Li, Q.Z., Liu, Y.Q., Kou, X.X., Zou, W.L., Qi, T., Xiang, P., Xing, J.D., Zhang, X., Li, J.L., 2022. Oxidative radical NHC catalysis: Divergent difunctionalization of olefins through intermolecular hydrogen atom transfer. *Angew. Chem. - Int. Ed.* 61 <https://doi.org/10.1002/anie.202207824>.
- Li, J., Sahoo, B., Daniliuc, C., Glorius, F., 2014. Conjugate umpolung of  $\beta$ ,  $\beta$ -disubstituted enals by dual catalysis with an N-heterocyclic carbene and a Brønsted acid: Facile construction of contiguous quaternary stereocenters. *Angew. Chem. Int. Ed.* 53, 10515–10519. <https://doi.org/10.1002/anie.201405178>.
- Li, X., Tang, M., Wang, Y., Wang, Y., Li, Z., Qu, L.B., Wei, D., 2018a. Insights into the N-Heterocyclic Carbene (NHC)-catalyzed intramolecular cyclization of aldimines: General mechanism and role of catalyst. *Chem. - an Asian J.* 13, 1710–1718. <https://doi.org/10.1002/asia.201800313>.
- Li, S., Tang, Z., Wang, Y., Wang, D., Wang, Z., Yu, C., Li, T., Wei, D., Yao, C., 2019. NHC-catalyzed aldol-like reactions of allenates with isatins: Regiospecific syntheses of  $\gamma$ -functionalized allenates. *Org. Lett.* 21, 1306–1310. <https://doi.org/10.1021/acs.orglett.8b04082>.
- Li, X., Wang, Y., Wang, Y., Tang, M., Qu, L.B., Li, Z., Wei, D., 2018b. Insights into the N-Heterocyclic Carbene (NHC)-catalyzed oxidative  $\gamma$ -C(sp<sup>3</sup>)-H deprotonation of alkylaldehydes and cascade [4 + 2] cycloaddition with alkenylisoxazoles. *J. Org. Chem.* 83, 8543–8555. <https://doi.org/10.1021/acs.joc.8b01112>.
- Li, X., Xu, J., Li, S.J., Qu, L.B., Li, Z., Chi, Y.R., Wei, D., Lan, Y., 2020. Prediction of NHC-catalyzed chemoselective functionalizations of carbonyl compounds: A general mechanistic map. *Chem. Sci.* 11, 7214–7225. <https://doi.org/10.1039/d0sc01793k>.
- Li, Q.Z., Zeng, R., Han, B., Li, J.L., 2021. Single-electron transfer reactions enabled by N-heterocyclic carbene organocatalysis. *Chem. - Eur. J.* 27, 3238–3250. <https://doi.org/10.1002/chem.202004059>.
- Liu, Q., Chen, X.Y., 2020. Dual N-heterocyclic carbene/photocatalysis: A new strategy for radical processes. *Org. Chem. Front.* 7, 2082–2087. <https://doi.org/10.1039/d0qo00494d>.
- Liu, J., Gu, A., Jan-e, B., 2021. Efficient aerobic oxidation of organic molecules by multistep electron transfer. *Angew. Chem. Int.ed.* 60, 15686–15704. <https://doi.org/10.1002/anie.202012707>.
- Liu, C., Han, P., Zhang, X., Qiao, Y., Xu, Z., Zhang, Y., Li, D., Wei, D., Lan, Y., 2022. NHC-catalyzed transformation reactions of imines: Electrophilic versus nucleophilic attack. *J. Org. Chem.* 87, 7989–7994. <https://doi.org/10.1021/acs.joc.2c00621>.
- Liu, K., Schwenzer, M., Studer, A., 2022. Radical NHC catalysis. *ACS Catal.* 12, 11984–11999. <https://doi.org/10.1021/acscatal.2c03996>.
- Liu, Q., Wang, Y., Wang, Y., Li, X., Qu, L.B., Lan, Y., Wei, D., 2020. Computational study on N-heterocyclic carbene (NHC)-catalyzed intramolecular hydroacylation-Stetter reaction cascade. *Mol. Catal.* 484, 110723 <https://doi.org/10.1016/j.mcat.2019.110723>.
- Lyngvi, E., Bode, J.W., Schoenebeck, F., 2012. A computational study of the origin of stereoselection in NHC-catalyzed annulation reactions of  $\alpha$ ,  $\beta$ -unsaturated acyl azoliums. *Chem. Sci.* 3, 2346–2350. <https://doi.org/10.1039/c2sc20331f>.
- Mahatthanachai, J., Bode, J.W., 2014. On the mechanism of N-heterocyclic carbene-catalyzed reactions involving acyl azoliums. *Acc. Chem. Res.* 47, 696–707. <https://doi.org/10.1021/ar400239v>.
- Mahatthanachai, J., Kaeobamrung, J., Bode, J.W., 2012. Chiral N-heterocyclic carbene catalyzed annulations of enals and ynals with stable enols: A highly enantioselective coates–Claisen rearrangement. *ACS Catal.* 2, 494–503. <https://doi.org/10.1021/cs300020t>.
- Maji, B., Breugst, M., Mayr, H., 2011. N-heterocyclic carbenes: Organocatalysts with moderate nucleophilicity but extraordinarily high Lewis basicity. *Angew. Chem. Int. Ed.* 50, 6915–6919. <https://doi.org/10.1002/anie.201102435>.
- Maji, B., Horn, M., Mayr, H., 2012. Nucleophilic reactivities of deoxy breslow intermediates: How does aromaticity affect the catalytic activities of N-heterocyclic carbenes? *Angew. Chem. Int. Ed.* 51, 6231–6235. <https://doi.org/10.1002/anie.201202327>.
- Man, Y., Zeng, X., Xu, B., 2023. Synthesis of thioesters from aldehydes via N-Heterocyclic Carbene (NHC) catalyzed radical relay. *Chem. - Eur. J.* 29 <https://doi.org/10.1002/chem.202303716>.
- Massey, R.S., Collett, C.J., Lindsay, A.G., Smith, A.D., Donoghue, A.C.O., 2012. Proton transfer reactions of triazol-3-ylidenes: Kinetic acidities and carbon acid *pK<sub>a</sub>*. *J. Am. Chem. Soc.* 134, 20421–20432. <https://doi.org/10.1021/ja308420c>.
- Matsuki, Y., Ohnishi, N., Kakeno, Y., Takemoto, S., Ishii, T., Nagao, K., Ohmiya, H., 2021. Aryl radical-mediated N-heterocyclic carbene catalysis. *Nat. Commun.* 12, 1–8. <https://doi.org/10.1038/s41467-021-24144-2>.
- Mayr, H., Lakhdar, S., Maji, B., Ofial, A.R., 2012. A quantitative approach to nucleophilic organocatalysis. *Beilstein J. Org. Chem.* 8, 1458–1478. <https://doi.org/10.3762/bjoc.8.166>.
- Menon, R.S., Biju, A.T., Nair, V., 2016. Recent advances in N-heterocyclic carbene (NHC)-catalyzed benzoin reactions. *Beilstein J. Org. Chem.* 12, 444–461. <https://doi.org/10.3762/bjoc.12.47>.
- Mo, J., Chen, X., Chi, Y.R., 2012. Oxidative  $\gamma$ -addition of enals to trifluoromethyl ketones: enantioselectivity control via lewis acid/N-heterocyclic carbene cooperative catalysis. *J. Am. Chem. Soc.* 134, 8810–8813. <https://doi.org/10.1021/ja303618z>.
- Mondal, S., Yetra, S.R., Patra, A., Kunte, S.S., Gonnade, R.G., Biju, A.T., 2014. N-Heterocyclic carbene-catalyzed enantioselective synthesis of functionalized cyclopentenes via  $\alpha$ ,  $\beta$ -unsaturated acyl azoliums. *Chem. Commun.* 50, 14539–14542. <https://doi.org/10.1039/c4cc07433e>.
- Mondal, S., Yetra, S.R., Mukherjee, S., Biju, A.T., 2019. NHC-catalyzed generation of  $\alpha$ ,  $\beta$ -unsaturated acylazoliums for the enantioselective synthesis of heterocycles and carbocycles. *Acc. Chem. Res.* 52, 425–436. <https://doi.org/10.1021/acs.accounts.8b00550>.
- Movassaghi, M., Schmidt, M.A., 2005. N-heterocyclic carbene-catalyzed amidation of unactivated esters with amino alcohols. *Org. Lett.* 7, 2453–2456. <https://doi.org/10.1021/ol050773y>.
- Mulks, F.F., Melaimi, M., Yan, X., Baik, M.H., Bertrand, G., 2023. How to enhance the efficiency of breslow intermediates for SET catalysis. *J. Org. Chem.* 88, 2535–2542. <https://doi.org/10.1021/acs.joc.2c02978>.
- Naik, P.U., Refes, K., Sadaka, F., Brachais, C.-H., Boni, G., Couvercelle, J.-P., Picquet, M., Plasseraud, L., 2012. Polymer Chemistry Organo-catalyzed synthesis of aliphatic polycarbonates in solvent-free conditions. *Polym. Chem.* 3, 1475–1480. <https://doi.org/10.1039/c2py20056b>.
- Nandi, A., Al Assad, Z., Milo, A., Kozuch, S., 2021. Quantum tunneling on carbene organocatalysis: Breslow intermediate formation via water-bridges. *ACS Catal.* 11, 14836–14841. <https://doi.org/10.1021/acscatal.1c04475>.
- Naumann, S., Buchmeiser, M.R., 2014. Liberation of N-heterocyclic carbenes (NHCs) from thermally labile progenitors: Protected NHCs as versatile tools in organo- and

- polymerization catalysis. *Catal. Sci. Technol.* 4, 2466–2479. <https://doi.org/10.1039/c4cy00344f>.
- Naumann, S., Dove, A.P., 2016. N-Heterocyclic carbenes for metal-free polymerization catalysis: An update. *Polym. Int.* 65, 16–27. <https://doi.org/10.1002/pi.5034>.
- Nelson, D.J., Nolan, S.P., Nelson, D.J., Nolan, S.P., 2013. Quantifying and understanding the electronic properties of N-heterocyclic carbenes. *Chem. Soc. Rev.* 42, 6723–6753. <https://doi.org/10.1039/c3cs60146c>.
- Nesterov, V., Reiter, D., Bag, P., Frisch, P., Holzner, R., Porzelt, A., Inoue, S., 2018. NHCs in main group chemistry. *Chem. Rev.* 118, 9678–9842. <https://doi.org/10.1021/acs.chemrev.8b00079>.
- Ni, Q., Xiong, J., Song, X., Raabe, G., Enders, D., 2015. NHC-catalyzed activation of  $\alpha$ ,  $\beta$ -unsaturated N-acyltriazoles: An easy access to dihydropyranones. *Chem. Commun.* 51, 14628–14631. <https://doi.org/10.1039/c5cc06044c>.
- Niu, Y., Wang, N., Mun, A., Xu, J., Zeng, H., Rovis, T., 2017. Experimental and computational gas phase acidities of conjugate acids of triazolylidene carbenes: Rationalizing subtle electronic effects. *J. Am. Chem. Soc.* 139, 14917–14930. <https://doi.org/10.1021/jacs.7b05229>.
- Ogawa, K.A., Boydston, A.J., 2014. Electrochemical characterization of azolium salts. *Chem. Lett.* 43, 907–909. <https://doi.org/10.1246/cl.140162>.
- Okano, T., 2013. Heterocyclic synthesis via catalysis of N-heterocyclic carbenes: Very classical and very modern chemical species. *Heterocycl. Commun.* 19, 311–326. <https://doi.org/10.1515/hc-2013-0075>.
- Ou, C., Pan, Y., Tang, H., 2022. Electrochemically promoted N-heterocyclic carbene polymer-catalyzed cycloaddition of aldehyde with isocyanide acetate. *Sci. China Chem.* 65, 1873–1878. <https://doi.org/10.1007/s11426-022-1360-3>.
- Pareek, M., Reddi, Y., Sunoj, R.B., 2021. Tale of the Breslow intermediate, a central player in N-heterocyclic carbene organocatalysis: then and now. *Chem. Sci.* 12, 7973–7992. <https://doi.org/10.1039/d1sc01910d>.
- Petersen, H.A., Taylor, A., Chloe, G., Charles, B., Luca, R., 2022. Predictive energetic tuning of C-Nucleophiles for the electrochemical capture of carbon dioxide. *ISCIENCE* 25, 103997. <https://doi.org/10.1016/j.isci.2022.103997>.
- Que, Y., He, H., 2020. Advances in N-heterocyclic carbene catalysis for natural product synthesis. *Eur. J. Org. Chem.* 5917–5925. <https://doi.org/10.1002/ejoc.202000305>.
- Quinn, M.S., Smith, J., Zhu, D.R.W., Hodgson, A.C., O'donoghue, 2021. Triazolium salt organocatalysis: Mechanistic evaluation of unusual ortho-substituent effects on deprotonation. *Catalysts* 11, 1055. <https://doi.org/10.3390/catal11091055>.
- Ragno, D., Brandolese, A., Carmine, D., Buoso, S., Belletti, G., Leonardi, C., Bortolini, O., Bertoldo, M., Massi, A., 2021. Exploring oxidative NHC-catalysis as organocatalytic polymerization strategy towards polyamide oligomers. *Chem. Eur. J.* 27, 1839–1848. <https://doi.org/10.1002/chem.202004296>.
- Reddi, Y., Sunoj, R.B., 2017. Origin of stereoselectivity in cooperative asymmetric catalysis involving N-heterocyclic carbenes and Lewis acids toward the synthesis of spiroindole lactone. *ACS Catal.* 7, 530–537. <https://doi.org/10.1021/acscatal.6b03026>.
- Rezayee, N.M., Lamhauge, J.N., Jørgensen, K.A., 2022. Organocatalyzed cross-nucleophile couplings: Umpolung of catalytic enamines. *Acc. Chem. Res.* 55, 1703–1717. <https://doi.org/10.1021/acs.accounts.2c00149>.
- Riederer, S.K.U., Bechlers, B., Herrmann, W.A., Kühn, F.E., 2011. Chiral N-heterocyclic carbenes based on 1,2,4-triazole as ligands for metal-catalyzed asymmetric synthesis. *Dalt. Trans.* 40, 41–43. <https://doi.org/10.1039/c0dt00724b>.
- Rocco, D., Folgueiras-amador, A.A., Brown, R.C.D., Feroci, M., 2022. First example of organocatalysis by cathodic N-heterocyclic carbene generation and accumulation using a divided electrochemical flow cell. *J. Org. Chem.* 18, 979–990. <https://doi.org/10.3762/bjoc.18.98>.
- Ryan, S.J., Candish, L., Lupton, D.W., 2013. Acyl anion free N-heterocyclic carbene organocatalysis. *Chem. Soc. Rev.* 42, 4906–4917. <https://doi.org/10.1039/c3cs35522e>.
- Samanta, R.C., Maji, B., De Sarkar, S., Bergander, K., Fröhlich, R., Mück-Lichtenfeld, C., Mayr, H., Studer, A., 2012. Nucleophilic addition of enols and enamines to  $\alpha$ ,  $\beta$ -unsaturated acyl azoliums: Mechanistic studies. *Angew. Chem. Int. Ed.* 51, 5234–5238. <https://doi.org/10.1002/anie.201109042>.
- Santra, S., Porey, A., Jana, B., Guin, J., 2018. N-Heterocyclic carbenes as chiral Brønsted base catalysts: a highly diastereo- and enantioselective 1,6-addition reaction. *Chem. Sci.* 9, 6446–6450. <https://doi.org/10.1039/c8sc02138d>.
- Schotten, C., Bourne, R.A., Kapur, N., Nguyen, B.N., Willans, C.E., 2021a. Electrochemical generation of N-heterocyclic carbenes for use in synthesis and catalysis. *Adv. Synth. Catal.* 363, 3189–3200. <https://doi.org/10.1002/adsc.2021100264>.
- Schotten, C., Taylor, C.J., Bourne, R.A., Chamberlain, T.W., Nguyen, B.N., Kapur, N., Willans, C.E., 2021b. Alternating polarity for enhanced electrochemical synthesis. *React. Chem. Eng.* 6, 147–151. <https://doi.org/10.1039/d0re00399a>.
- Shen, L., Shao, P., Ye, S., 2011. N-heterocyclic carbene-catalyzed cyclization of unsaturated acyl chlorides and ketones. *Adv. Synth. Catal.* 353, 1943–1948. <https://doi.org/10.1002/adsc.201100178>.
- Shen, H., Tian, G., Xu, Z., Wang, L., Wu, Q., Zhang, Y., Teo, B.K., Zheng, N., 2022. N-heterocyclic carbene coordinated metal nanoparticles and nanoclusters. *Coord. Chem. Rev.* 458, 214425. <https://doi.org/10.1016/j.ccr.2022.214425>.
- Shu, T., Ni, Q., Song, X., Zhao, K., Wu, T., Puttreddy, R., Rissanen, K., Enders, D., 2016. Asymmetric synthesis of cyclopentanes bearing four contiguous stereocenters via an NHC-catalyzed Michael/Michael/esterification domino reaction. *Chem. Commun.* 52, 2609–2611. <https://doi.org/10.1039/c5cc09581f>.
- Song, R., Chi, Y.R., 2019. N-heterocyclic carbene catalyzed radical coupling of aldehydes with redox-active esters. *Angew. Chem. - Int. Ed.* 58, 8628–8630. <https://doi.org/10.1002/anie.201902792>.
- Stenkvis, S., Bacaicoa, S., Goossens, E., Sundén, H., 2023. Aerobic oxidative N-heterocyclic carbene catalysis. *Chem. Rec.* 23, 1–24. <https://doi.org/10.1002/tcr.202300091>.
- Ta, L., Axelsson, A., Sundén, H., 2016. Attractive aerobic access to the  $\alpha$ ,  $\beta$ -unsaturated acyl azolium intermediate: oxidative NHC catalysis via multistep electron transfer. *Green Chem.* 18, 686–690. <https://doi.org/10.1039/c5gc01965f>.
- Tan, H., Wang, S., Yan, Z., Liu, J., Wei, J., Song, S., Jiao, N., 2011. N-heterocyclic carbene catalyzed ester synthesis from organic halides through incorporation of oxygen atoms from air. *Angew. Chem.* 60, 2140–2144. <https://doi.org/10.1002/anie.202011039>.
- T. Ukai, R. Tanaka, T. Dokawa, 1943. A new catalyst for acyloin condensation. *J. Pharm. Soc. Jpn* 63, 296–300. <https://doi.org/DOI:10.1248/yakushi1881.63.6.296>.
- Vellé, A., Cebollada, A., Macías, R., Iglesias, M., Gil-Moles, M., Sanz Miguel, P.J., 2017. From imidazole toward imidazolium salts and N-heterocyclic carbene ligands: Electronic and geometrical redistribution. *ACS Omega* 2, 1392–1399. <https://doi.org/10.1021/acsomega.7b00138>.
- Vetica, F., Bortolami, M., Petrucci, R., Rocco, D., Feroci, M., 2021. Electrogenerated NHCs in organic synthesis: Ionic liquids vs organic solvents effects. *Chem. Rec.* 21, 2130–2147. <https://doi.org/10.1002/tcr.202000178>.
- Vora, H.U., Wheeler, P., Rovis, T., 2012. Exploiting acyl and enol azolium intermediates via N-heterocyclic carbene catalyzed reactions of  $\alpha$ -reducible aldehydes. *Adv. Synth. Catal.* 354, 1617–1639. <https://doi.org/10.1002/adsc.201200031>.
- Wang, J., Li, Y., Sun, J., Wang, H., Jin, Z., Chi, Y.R., 2018. Carbene-catalyzed enantioselective addition of benzylic carbonyl to unsaturated acyl azolium for rapid synthesis of pyrrolo[3,2-c]quinolines. *ACS Catal.* 8, 9859–9864. <https://doi.org/10.1021/acscatal.8b02651>.
- Wang, Y., Wu, B., Zheng, L., Wei, D., Tang, M., 2016. DFT perspective toward [3 + 2] annulation reaction of enals with  $\alpha$ -ketoamides through NHC and Brønsted acid cooperative catalysis: Mechanism, stereoselectivity, and role of NHC. *Org. Chem. Front.* 3, 190–203. <https://doi.org/10.1039/c5qo00338e>.
- Wang, Y., Wei, D., Wang, Y., Zhang, W., Tang, M., 2016. N-Heterocyclic Carbene (NHC)-catalyzed sp<sup>3</sup>  $\beta$ -C-H activation of saturated carbonyl compounds: Mechanism, role of NHC, and origin of stereoselectivity. *ACS Catal.* 6, 279–289. <https://doi.org/10.1021/acscatal.5b01710>.
- Wang, Y., Qiao, Y., Wei, D., Tang, M., 2017. Computational study on NHC-catalyzed enantioselective and chemoselective fluorination of aliphatic aldehydes. *Org. Chem. Front.* 4, 1987–1998. <https://doi.org/10.1039/c7qo00436b>.
- Wang, Y., Qu, L.B., Lan, Y., Wei, D., 2019a. Unravelling the mechanism and selectivity of the NHC-catalyzed three-membered ring-opening/fluorination of epoxy enals: A DFT study. *ChemCatChem* 11, 2919–2925. <https://doi.org/10.1002/cctc.201900424>.
- Wang, Y., Qu, L.B., Lan, Y., Wei, D., 2020a. Origin of regio- and stereoselectivity in the NHC-catalyzed reaction of alkyl pyridinium with aliphatic enal. *ChemCatChem* 12, 1068–1074. <https://doi.org/10.1002/cctc.201901965>.
- Wang, Y., Qu, L.B., Wei, D., Lan, Y., 2020b. Unveiling the chemo- and stereoselectivities of NHC-catalyzed reactions of an aliphatic ester with aminoaldehyde. *J. Org. Chem.* 85, 8437–8446. <https://doi.org/10.1021/acs.joc.0c00769>.
- Wang, Y., Qiao, Y., Lan, Y., Wei, D., 2021. Predicting the origin of selectivity in NHC-catalyzed ring opening of formylcyclopropane: A theoretical investigation. *Catal. Sci. Technol.* 11, 332–337. <https://doi.org/10.1039/d0cy01768j>.
- Wang, M.H., Scheidt, K.A., 2016. Cooperative catalysis and activation with N-heterocyclic carbenes. *Angew. Chem. Int. Ed.* 55, 14912–14922. <https://doi.org/10.1002/anie.201605319>.
- Wang, Y., Wang, Y., Wang, X., Li, X., Qu, L.B., Wei, D., 2018a. Competing mechanisms and origins of chemo- and stereo-selectivities of NHC-catalyzed reactions of enals with 2-aminoacrylates. *Catal. Sci. Technol.* 8, 4229–4240. <https://doi.org/10.1039/c8cy01272e>.
- Wang, Y., Qu, L.B., Wei, D., 2019b. Prediction on the origin of selectivities in base-controlled switchable NHC-catalyzed transformations. *Chem. - Asian J.* 14, 293–300. <https://doi.org/10.1002/asia.201801583>.
- Wang, Y., Wu, Q.Y., Lai, T.H., Zheng, K.J., Qu, L.B., Wei, D., 2019c. Prediction on the origin of selectivities of NHC-catalyzed asymmetric dearomatization (CADA) reactions. *Catal. Sci. Technol.* 9, 465–476. <https://doi.org/10.1039/c8cy02238k>.
- Wang, N., Xu, J., Lee, J.K., 2018. The importance of N-heterocyclic carbene basicity in organocatalysis. *Org. Biomol. Chem.* 16, 6852–6866. <https://doi.org/10.1039/c8ob01667d>.
- Wang, Y., Zhang, S.R., Wang, Y., Qu, L.B., Wei, D., 2018b. Insights into the NHC-catalyzed cascade Michael/aldol/lactamization reaction: Mechanism and origin of stereoselectivity. *Org. Chem. Front.* 5, 2065–2072. <https://doi.org/10.1039/c8qo00398j>.
- Wei, Z., Mullaj, K., Price, A., Wei, K., Luo, Q., Thanneer, S., Sun, S., He, J., 2022. Polymer N-Heterocyclic Carbene (NHC) ligands for silver nanoparticles. *ACS Appl. Mater. Interfaces* 14, 55227–55237. <https://doi.org/10.1021/acsmi.2c17706>.
- Wei, Y., Sastry, G.N., Zipse, H., 2008. Methyl cation affinities of commonly used organocatalysts. *J. Am. Chem. Soc.* 130, 3473–3477. <https://doi.org/10.1021/ja0764409>.
- Wei, D., Zhu, Y., Zhang, C., Sun, D., Zhang, W., Tang, M., 2011. A DFT study on enantioselective synthesis of  $\alpha$ - $\beta$ -lactams via NHC-catalyzed [2 + 2] cycloaddition of ketenes with diazenedicarboxylates. *J. Mol. Catal. A Chem.* 334, 108–115. <https://doi.org/10.1016/j.molcata.2010.11.004>.
- Wessels, A., Klusmann, M., Breugst, M., Schlöter, N.E., Berkessel, A., 2022. Formation of Breslow intermediates from N-heterocyclic carbenes and aldehydes involves autocatalysis by the Breslow intermediate, and a hemiacetal. *Angew. Chem. - Int. Ed.* 61 <https://doi.org/10.1002/anie.202117682>.

- Wu, Z., Jiang, D., Wang, J., 2019. Carbene-catalyzed oxidative acylation promoted by an unprecedented oxidant CCl<sub>3</sub>CN. *Org. Chem. Front.* 6, 688–693. <https://doi.org/10.1039/c8qo01420e>.
- Wu, W., Xu, S., Zhang, Y., Wang, X., Li, R., Sun, F., Yu, C., Li, T., Wei, D., Yao, C., 2020. NHC-catalyzed  $\beta$ -specific addition of N-based nucleophiles to allenates. *Org. Chem. Front.* 7, 1593–1599. <https://doi.org/10.1039/d0qo00189a>.
- Wu, X., Zhang, Y., Wang, Y., Ke, J., Jeret, M., Reddi, R.N., Yang, S., Song, B.A., Chi, Y.R., 2017. Polyhalides as efficient and mild oxidants for oxidative carbene organocatalysis by radical processes. *Angew. Chem. - Int. Ed.* 56, 2942–2946. <https://doi.org/10.1002/anie.201611692>.
- Yao, C., Wang, D., Lu, J., Li, T., Jiao, W., Yu, C., 2012. N-heterocyclic carbene catalyzed reactions of  $\alpha$ -bromo- $\alpha$ ,  $\beta$ -unsaturated aldehydes/ $\alpha$ ,  $\beta$ -dibromoaldehydes with 1,3-dinucleophilic reagents. *Chem. Eur. J.* 18, 1914–1917. <https://doi.org/10.1002/chem.201103358>.
- Yetra, S.R., Bhunia, A., Patra, A., Mane, M.V., Vanka, K., Biju, A.T., 2013. Enantioselective N-heterocyclic carbene-catalyzed annulations of 2-bromoaldehydes with 1,3-dicarbonyl compounds and enamines via chiral  $\alpha$ ,  $\beta$ -unsaturated acylazoliums. *Adv. Synth. Catal.* 355, 1089–1097. <https://doi.org/10.1002/adsc.201300219>.
- Zeitler, K., 2006. Stereoselective synthesis of (E) -  $\alpha$ ,  $\beta$ -unsaturated esters via carbene-catalyzed redox esterification. *Org. Lett.* 8, 637–640. <https://doi.org/10.1021/ol052826h>.
- Zhang, H., Dong, Z., Yang, Y., Wang, P., Hui, X., 2013. N-heterocyclic carbene-catalyzed stereoselective cascade reaction: Synthesis of functionalized tetrahydroquinolines. *Org. Lett.* 15, 4750–4753. <https://doi.org/10.1021/ol4024985>.
- Zhang, X., Tang, M., Wang, Y., Ran, Y., Wei, D., Zhu, Y., Zhang, W., 2016. DFT study on the mechanism and stereoselectivity of NHC-catalyzed synthesis of substituted trifluoromethyl dihydropyranones with contiguous stereocenters. *J. Org. Chem.* 81, 868–877. <https://doi.org/10.1021/acs.joc.5b02439>.
- Zhang, W., Wang, Y., Wei, D., Tang, M., Zhu, X., 2016. A DFT study on NHC-catalyzed intramolecular aldehyde-ketone crossed-benzoin reaction: Mechanism, regioselectivity, stereoselectivity, and role of NHC. *Org. Biomol. Chem.* 14, 6577–6590. <https://doi.org/10.1039/c6ob00791k>.
- Zhang, M., Wei, D., Wang, Y., Li, S., Liu, J., Zhu, Y., Tang, M., 2014. DFT study on the reaction mechanisms and stereoselectivities of NHC-catalyzed [2 + 2] cycloaddition between arylalkylketenes and electron-deficient benzaldehydes. *Org. Biomol. Chem.* 12, 6374–6383. <https://doi.org/10.1039/c4ob00606b>.
- Zhang, H., Xu, H., Bai, H., Wei, D., Zhu, Y., Zhang, W., 2018. Theoretical study on the mechanism and enantioselectivity of NHC-catalyzed intramolecular SN<sup>2</sup>/nucleophilic substitution: What are the roles of NHC and DBU? *Org. Chem. Front.* 5, 1493–1501. <https://doi.org/10.1039/c8qo00129d>.
- Zhao, C., Blaszczyk, S.A., Wang, J., 2021. Asymmetric reactions of N-heterocyclic carbene (NHC)-based chiral acylazoliums and azolium enolates. *Green Synth. Catal.* 2, 198–215. <https://doi.org/10.1016/j.gresc.2021.03.003>.
- Zhao, Q., Meng, G., Nolan, S.P., Szostak, M., 2020. N-heterocyclic carbene complexes in C-H activation reactions. *Chem. Rev.* 120, 1981–2048. <https://doi.org/10.1021/acs.chemrev.9b00634>.
- Zhao, J., Mück-Lichtenfeld, C., Studer, A., 2013. Cooperative N-Heterocyclic Carbene (NHC) and ruthenium redox catalysis: Oxidative esterification of aldehydes with air as the terminal oxidant. *Adv. Synth. Catal.* 355, 1098–1106. <https://doi.org/10.1002/adsc.201300034>.
- Zhou, P., Li, W., Lan, J., Zhu, T., 2022. Electroredox carbene organocatalysis with iodide as promoter. *Nat. Commun.* 13, 3827. <https://doi.org/10.1038/s41467-022-31453-7>.
- Zhu, J., Moreno, I., Quinn, P., Yufit, D.S., Song, L., Young, C.M., Duan, Z., Tyler, A.R., Waddell, P.G., Hall, M.J., Probert, M.R., Smith, A.D., O'Donoghue, A.C., 2022. The role of the fused ring in bicyclic triazolium organocatalysts: Kinetic, X-ray, and DFT insights. *J. Org. Chem.* 87, 4241–4253. <https://doi.org/10.1021/acs.joc.1c03073>.
- Zhu, Z.Q., Xiao, J.C., 2010. N-heterocyclic carbene-catalyzed reaction of alkynyl aldehydes with 1,3-keto esters or 1,3-diketones. *Adv. Synth. Catal.* 352, 2455–2458. <https://doi.org/10.1002/adsc.201000240>.
- Zhu, Z.Q., Zheng, X.L., Jiang, N.F., Wan, X., Xiao, J.C., 2011. Chiral N-heterocyclic carbene catalyzed annulation of  $\alpha$ ,  $\beta$ -unsaturated aldehydes with 1,3-dicarbonyls. *Chem. Commun.* 47, 8670–8672. <https://doi.org/10.1039/c1cc12778k>.